Bioinformatic and molecular study of the regulation of SIRT3 expression

Bioinformatic and molecular study of the regulation of SIRT3 expression

A dissertation presented

by

Frederick Kyle Satterstrom

to

The School of Engineering and Applied Sciences

in partial fulfillment of the requirements
for the degree of
Doctor of Philosophy
in the subject of

Engineering Sciences

Harvard University
Cambridge, Massachusetts

November, 2014

Dissertation Advisor: Dr. Marcia Haigis Frederick Kyle Satterstrom

Bioinformatic and molecular study of the regulation of SIRT3 expression

Abstract

Calorie restriction (CR) is a dietary intervention that extends lifespan, delays the onset of age-related diseases, and induces a wide-ranging metabolic adaptation in multiple model organisms. One of its primary effectors is the mitochondrial NAD^+-dependent deacetylase sirtuin 3 (SIRT3). SIRT3 expression is upregulated by CR in multiple tissues, yet the mechanism of this induction is unclear. We therefore pursued multiple avenues in the study of the regulation of SIRT3 expression. To study *SIRT3* transcriptional activity, we developed a plasmid with the *SIRT3* promoter driving expression of the reporter gene luciferase, and we used it to demonstrate that SIRT3 expression in human 293T cells is upregulated by rapamycin, an inhibitor of the nutrient-sensing Target of Rapamycin pathway. Because SIRT3 expression level is a predictor of clinical outcome in breast cancer, this construct could be applied as a diagnostic and prognostic tool. We next conducted a bioinformatic analysis to identify transcription factors that may induce SIRT3 expression and identified nuclear respiratory factor 2 (NRF-2) as a top candidate. We showed that SIRT3 levels respond to NRF-2 overexpression or knockdown and that NRF-2 binds the *SIRT3* promoter. Notably, NRF-2 and estrogen-related receptor α – the only other transcription factor previously identified as binding the *SIRT3* promoter directly – are both co-activated by peroxisome proliferator-activated receptor γ coactivator 1-α (PGC-1α), a major regulator of the expression of mitochondrial and metabolic genes. Future study will be necessary to determine whether this pathway underlies the upregulation of SIRT3 expression in CR. Finally, we also used high-throughput RNA sequencing to suggest that calorie restriction

was capable of reversing not just age-related changes in gene expression, but also age-related changes in the usage of different isoforms of the same gene. This may be a new mechanism by which CR controls the biological activity of certain genes. Together, these studies provide novel tools and insights in the study of the regulation of SIRT3 expression and the effects of CR.

TABLE OF CONTENTS

ACKNOWLEDGEMENTS

I owe many thanks to my advisor Marcia Haigis for her support, encouragement, and mentorship. She has offered discussion, provided resources, helped me find collaborations, and urged me forward at every step. I also thank current and former members of the Haigis lab for their input and support, particularly Lydia Finley, Gaëlle Laurent, Natalie German, Karina Gonzalez, and Daniel Santos.

I have followed a somewhat unconventional path in my graduate career: as a fourth-year student, after spending three years in a biomaterials lab, where I cultured human embryonic stem cells for tissue engineering purposes and synthesized nanoparticles for gene delivery, I moved to the Haigis lab to study the intersection of metabolism and aging. It is a move I am glad I made. I am grateful to Ellen Fox in the Harvard GSAS Student Services Office for meeting with me regularly to talk through the process of switching labs, and I am thankful for conversations with Amy Wagers and with Marcia as I identified prospective new labs.

I have learned and benefitted greatly from collaboration with several excellent scientists, particularly Martha Bulyk and Bill Swindell, from whom I have learned about bioinformatic DNA sequence analysis, and Jon Seidman and members of the Seidman lab, including Joshua Gorham and Danos Christodoulou, from whom I have learned about high-throughput RNA sequencing. I would also like to thank the members of my dissertation advisory committee, David Mooney, Daniel Needleman, and Zoltan Arany, for their support and guidance.

Finally, I am grateful to my wife, Patricia, for her unflagging encouragement and understanding.

CHAPTER I

Introduction

Portions of this chapter have been adapted from:

From sirtuin biology to human diseases: an update

Carlos Sebastián[1,*], F. Kyle Satterstrom[2,3,*], Marcia C. Haigis[3], and Raul Mostoslavsky[1]

The Journal of Biological Chemistry (2012) **287**, 42444-42452

[1] Massachusetts General Hospital Cancer Center, Harvard Medical School, Boston, Massachusetts 02114

[2] Harvard School of Engineering and Applied Sciences, Cambridge, Massachusetts 02138

[3] Department of Cell Biology, Harvard Medical School, Boston, Massachusetts 02115

[*] Both authors contributed equally to this work

Over three-quarters of a century ago, Clive McCay and colleagues first noted that rats kept on a calorie-restricted diet lived longer than freely fed controls (McCay et al., 1935). Since then, calorie restriction (CR), defined as undernutrition without malnutrition, has been shown to increase lifespan in several model organisms, including yeast, worms, flies, and mice (Weindruch et al., 1986). Yet despite the length of time that has elapsed since its initial discovery, the molecular mechanisms that drive this lifespan extension have remained elusive. In 1999, it was discovered that a *Saccharomyces cerevisiae* gene named silent information regulator 2 (Sir2), which controls transcriptional silencing by deacetylating histones (Ivy et al., 1986; Dang et al., 2009), shortened lifespan in yeast when deleted and extended it when overexpressed (Kaeberlein et al., 1999). Moreover, Sir2 was required for the lifespan of yeast to be extended by calorie restriction (Lin et al., 2000). These discoveries launched a new field in biology – the study of Sir2 and its homologs, called sirtuins.

The sirtuins

Following the discovery that Sir2 promoted longevity in yeast, sirtuins were shown to regulate lifespan in other organisms (Haigis and Guarente, 2006). In *Caenorhabditis elegans*, lifespan was extended by increased levels of the Sir2 homolog sir-2.1 (Tissenbaum and Guarente, 2001). In flies, an increase in levels of the *Drosophila melanogaster* gene dSir2 extended lifespan, while a decrease blocked the lifespan-extending effects of calorie restriction (Rogina and Helfand, 2004). Both of these results were later called into question (Burnett et al., 2011), but subsequent studies verified the essential findings. The initial study in *C. elegans* overestimated lifespan extension by sir-2.1 because of an unlinked mutation that was not controlled for, but a significant effect still remained with proper controls (Viswanathan and

Guarente, 2011), and other studies also found that sir-2.1 overexpression in worms extended lifespan (Rizki et al., 2011; Mouchiroud et al., 2013). In flies, meanwhile, follow-up studies determined that expression of dSir2 specifically in the fat body was crucial to lifespan regulation. Levels of dSir2 were normally increased during yeast restriction, a CR-like intervention, and deletion of dSir2 in the fat body abrogated the lifespan-extending effects of yeast restriction (Banerjee et al., 2012). Overexpression of dSir2 in the fat body also extended lifespan (Banerjee et al., 2012; Hoffman et al., 2013). This body of work reinforced the idea that sirtuins were important for the regulation of lifespan through pathways activated during calorie restriction.

In mammals, and in most vertebrates, there are seven sirtuins (SIRT1-7), and they possess NAD^+-dependent deacetylase, deacylase, and ADP-ribosyltransferase activities (Vaziri et al., 2001; Blander and Guarente, 2004; Liszt et al., 2005; Haigis et al., 2006; Du et al., 2011). The seven sirtuins arose early during animal evolution (Greiss and Gartner, 2009) and are found in different subcellular locations, with the primary localizations of each being the nucleus (SIRT1, SIRT6, SIRT7), cytosol (SIRT2), and mitochondria (SIRT3, SIRT4, SIRT5). SIRT1 is the closest mammalian homolog to yeast Sir2, and SIRT3 is the closest of the mitochondrial sirtuins (Frye, 2000). In fact, so close is the homology between SIRT1 and SIRT3 that they deacetylate homologous substrates (Hirschey et al., 2011a). Together, the sirtuins have important functions in a diverse yet interrelated set of physiological processes, including aging, metabolism, and several age-related pathologies.

Though the data suggests that the effect may be context-dependent, sirtuins have been shown to regulate lifespan in mice. Importantly, one study suggests that loss of SIRT1 removes the ability of CR to extend lifespan (Boily et al., 2008). Lifespan is also extended by brain-specific overexpression of SIRT1 (Satoh et al., 2013), although not by whole-body

overexpression (Herranz et al., 2010), perhaps due to increased cancer incidence (Guarente, 2013). Nor is SIRT1 alone in its impact – evidence for a positive effect of sirtuins on longevity also comes from the recent discovery that SIRT6 overexpression extends lifespan (Kanfi et al., 2012). Early experiments using SIRT6 knockout mice suggested that it could be involved in aging (Mostoslavsky et al., 2006), and although the effects of its transgenic overexpression are modest (the median lifespan increases between 10 and 15%) and gender-specific (affecting males only), they are significant. The role of all seven sirtuins in longevity is still being investigated, but at least a subset of them has a positive influence on lifespan.

Sirtuins are also central mediators of the metabolic effects of calorie restriction. CR induces a metabolic reprogramming at the cellular level that includes an enhancement of mitochondrial function and a preference for fat over glucose as a source of fuel (Anderson and Weindruch, 2010). In multiple tissues, the relative energy deficit wrought by CR also increases intracellular levels of NAD^+, the metabolite which is reduced to NADH during energy-generating processes such as glycolysis (Chen et al., 2008). Because sirtuin enzymatic activity is dependent upon the presence of NAD^+, their activity is directly linked to the metabolic state of the cell. This is a very suggestive link, and indeed nearly every sirtuin has been shown to play a role in regulating metabolism and energy homeostasis, often in roles that help the cell adapt to periods of low energy input. SIRT1, for example, promotes the oxidation of fatty acids (Gerhart-Hines et al., 2007), helping the body to draw energy from its fat reserves. SIRT5 activates the urea cycle during fasting (Nakagawa et al., 2009), helping to reduce levels of ammonia in the blood when amino acids are used as a source of energy. Additionally, administration of resveratrol, a small-molecule activator of SIRT1 (Howitz et al., 2003; Hubbard et al., 2013), mimics the transcriptional (Barger et al., 2008; Pearson et al., 2008) and physiological effects of

CR (Lam et al., 2013). It is the mitochondrial SIRT3, however, that is the major sirtuin player in the metabolic adaptation to CR.

SIRT3 in metabolism

SIRT3 is upregulated by calorie restriction in liver and brown adipose tissue (Shi et al., 2005; Hallows et al., 2011). It in turn upregulates several metabolic functions that promote adaptation to periods of low energy input (Figure 1.1), including activation of the urea cycle via ornithine transcarbamoylase (Hallows et al., 2011), ketone body synthesis via mitochondrial 3-hydroxy-3-methylglutaryl-CoA synthase 2 (Shimazu et al., 2010), and the electron transport chain via subunit A of the succinate dehydrogenase complex (Finley et al., 2011a). SIRT3 also promotes mitochondrial oxidative metabolism via deacetylation of long-chain acyl coenzyme A dehydrogenase, an enzyme involved in fatty acid catabolism (Hirschey et al., 2010). This activity has been linked to the phenotype of SIRT3 knockout mice, which exhibit an abnormal accumulation of fatty acid oxidation intermediates and, when fasted, show reduced ATP production and intolerance to cold. SIRT3 knockout mice are also unable to cope with a high-fat diet and gain more weight than their wildtype counterparts, developing hepatic steatosis and exhibiting signs of inflammation (Hirschey et al., 2011b). On a proteomic scale, loss of SIRT3 leads to a loss of the widespread reprogramming of mitochondrial protein acetylation patterns normally seen with CR (Hebert et al., 2013), showing that SIRT3 is deeply involved in the cellular adaptation to CR. Conversely, wildtype mice on a high-fat diet have reduced SIRT3 levels, reduced hepatic SIRT3 activity, and increased protein acetylation relative to those on a control diet (Hirschey et al., 2011b, Kendrick et al., 2011), highlighting the dynamic nature of the interplay between SIRT3, diet, and metabolism.

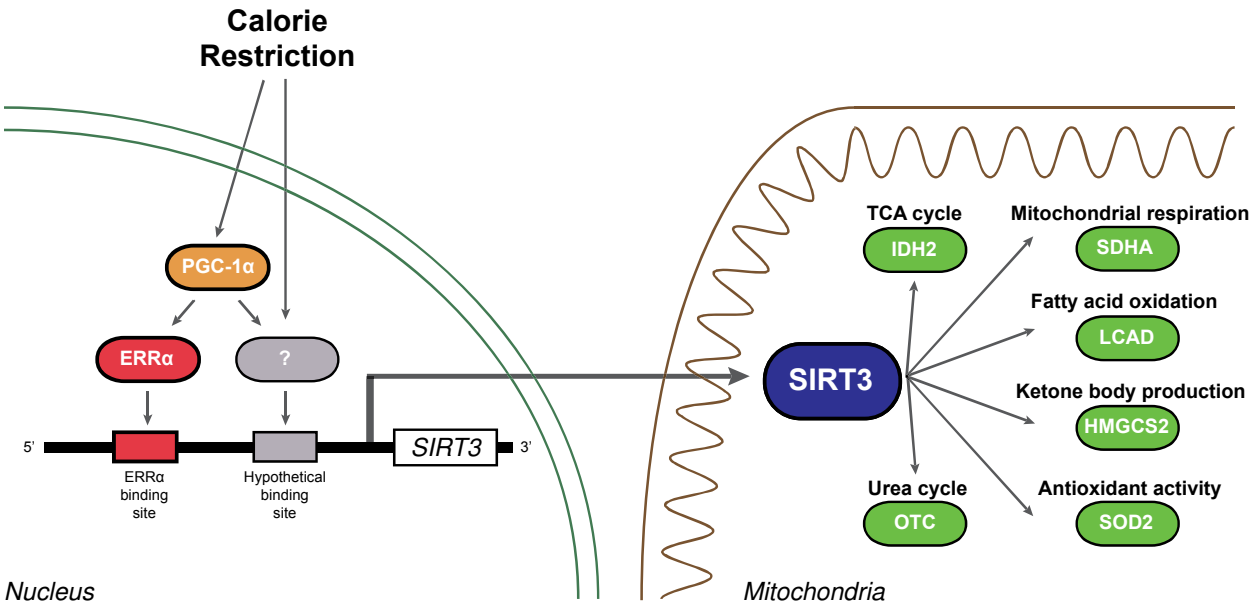

Figure 1.1. Overview of SIRT3 expression and function. Calorie restriction induces activity of the transcriptional coactivator PGC-1α and expression of SIRT3. The PGC-1α effector ERRα regulates SIRT3 in certain contexts, but this connection has not been studied in CR. Other transcription factors may play a role. Once expressed and translated into protein, SIRT3 localizes to the mitochondria and activates several pathways that are adaptive during periods of nutrient scarcity, such as the tricarboxylic acid cycle, mitochondrial respiration, fatty acid oxidation, ketone body production, antioxidant activity, and the urea cycle. Example SIRT3 enzymatic targets (green ovals) are given for each pathway.

SIRT3 also mediates the prevention of age-related hearing loss by CR (Someya et al., 2010), providing perhaps the strongest link between mammalian sirtuins and a specific anti-aging effect of calorie restriction. Hearing loss is a hallmark of mammalian aging and is characterized by a gradual loss of spiral ganglion neurons and sensory hair cells in the cochlea of the inner ear, which is triggered by oxidative damage in these cells (Liu and Yan, 2007). Remarkably, CR prevents hearing loss and oxidative damage in wild-type mice, whereas SIRT3-deficient mice remain subject to hearing loss with age. In addition, the same study demonstrated that SIRT3 is required for the CR-mediated reduction of oxidative damage in multiple tissues via regulation of the glutathione antioxidant system (Someya et al., 2010). This evidence suggested that SIRT3 may play a broader role in raising the cell's defenses against inflammation and cellular damage resulting from superoxide and peroxide byproducts of the electron transport chain, collectively termed reactive oxygen species (ROS).

SIRT3 in inflammation and disease

Inflammation driven by ROS plays a central role in the pathogenesis of many age-related diseases, and current research points to an anti-inflammatory role for sirtuins, especially SIRT1 and SIRT3 (e.g. Gillum et al., 2011; Wu et al., 2012). Inflammation typically increases with age (e.g. Li et al., 2010), and sirtuins counteract the effects of ROS-induced inflammatory factors such as nuclear factor NF-κB (Schug et al., 2010) and tumor necrosis factor (Yoshizaki et al., 2010) and also fight ROS directly. For example, in primary cultures of cardiomyocytes, SIRT3 reduced ROS by activating mitochondrial superoxide dismutase (SOD2), a mitochondrial matrix protein which transforms toxic superoxide into hydrogen peroxide and oxygen, and catalase, which decomposes hydrogen peroxide into oxygen and water (Sundaresan et al., 2009). The

presence of functional SIRT3 was also necessary for the reduction of oxidative damage seen in mouse liver during calorie restriction (Qiu et al., 2010). These signs pointed to SIRT3-mediated activation of SOD2 as key for fighting inflammation, and several groups have shown that SIRT3 directly deacetylates and activates SOD2, though the studies do not all agree on which residue is most important (Qiu et al., 2010; Chen et al., 2011; Tao et al., 2010). SIRT3 also deacetylates and activates mitochondrial isocitrate dehydrogenase, a tricarboxylic acid cycle enzyme which generates the NADPH necessary for regenerating the cell's reserves of reduced glutathione, and this may contribute to its ability to protect cells from oxidative stress and stress-induced inflammation (Yu et al., 2012). In support of SIRT3's anti-inflammatory role, SIRT3 mRNA levels were reduced in a cellular mouse model of kidney inflammation, while SIRT3 overexpression reduced markers of inflammation (Koyama et al., 2011).

One inflammation-driven pathology in which SIRT3 plays a protective role is cardiovascular disease. Cardiovascular disease involves the deterioration of heart and blood vessel function and is the leading cause of death worldwide. Inflammation and increased oxidative damage are two of the major contributors to its pathogenesis (Malik et al., 2004). Remarkably, calorie restriction protects from cardiovascular disease by improving both endothelial and heart function (Weiss et al., 2011). Given the role of sirtuins in mediating the effects of CR, multiple studies have explored their function in cardiovascular disease. SIRT1, for example, plays a role in endothelial function, vessel inflammation, vascularization, and cholesterol metabolism (Haigis and Sinclair, 2010; Borradaile and Pickering, 2009). SIRT3 has also emerged as a critical regulator of cardiac function (Pillai et al., 2010a; Sack, 2011). SIRT3-deficient mice develop cardiac hypertrophy, while transgenic animals overexpressing SIRT3 in the heart are protected against agonist-mediated cardiac hypertrophy (Sundaresan et al., 2009).

In addition to its induction of SOD2 and catalase, SIRT3 also deacetylates and activates LKB1, leading to active AMPK. This suppresses AKT phosphorylation, which in turn leads to downregulation of mTOR-driven growth (Pillai et al., 2010b). Both increased ROS levels and AKT activation play a crucial role in the development of cardiac hypertrophy (Lang, 2002; Condorelli et al., 2002). Thus, by downregulating these two pathways, SIRT3 exerts a key anti-hypertrophic function in cardiomyocytes.

SIRT3 also plays a protective role in cancer. Tumorigenesis is a multi-step process that involves the acquisition of several mutations leading to cell transformation and cancer initiation (Hanahan and Weinberg, 2000). Among the hallmarks of cancer cells, metabolic reprogramming is an important regulator of tumor growth, allowing tumor cells to meet their energetic and anabolic demands (Vander Heiden et al., 2009). While differentiated cells under normal conditions obtain energy by oxidizing fuels such as glucose through mitochondrial oxidative phosphorylation, rapidly proliferating cancer cells often upregulate glycolysis, allowing them to generate the macromolecules needed for cellular proliferation. This metabolic switch is known as the Warburg effect, and SIRT3 normally counteracts it by destabilizing hypoxia inducible factor 1-α via downregulation of ROS (Finley et al., 2011b). Additionally, overexpression of SIRT3 slowed tumorigenesis in xenograft models (Bell et al., 2011), suggesting that SIRT3 may be a tumor suppressor. Consistent with this role, SIRT3 expression is downregulated in human breast cancers, and SIRT3 knockout mice have a higher incidence of spontaneous mammary tumors (Kim et al., 2010).

Regulation of SIRT3 and mitochondrial gene expression

Because of the enormous importance of the diseases in which active SIRT3 plays a protective role, it is of major therapeutic significance to better understand the conditions under which SIRT3 is expressed and is active. Surprisingly little about this is actually known. Only one transcription factor, estrogen-related receptor α (ERRα), has been identified which binds the SIRT3 promoter directly (Figure 1.1) (Kong et al., 2010; Giralt et al., 2011). ERRα is a transcription factor with an important role in mitochondrial metabolism. Among its targets are medium-chain acyl coenzyme A dehydrogenase, an enzyme which is central to the mitochondrial β-oxidation of fatty acids (Sladek et al., 1997), and several components of the tricarboxylic acid cycle and mitochondrial electron transport chain (Giguère, 2008). ERRα is co-activated by peroxisome proliferator-activated receptor γ coactivator 1-α (PGC-1α) and carries out part of the PGC-1α transcriptional program (Schreiber et al., 2003; Scarpulla, 2011). Overexpressing ERRα in cardiac myocytes, for example, upregulates PGC-1α target genes involved in mitochondrial respiration and fatty acid oxidation (Huss et al., 2004). In at least mouse adipocytes and hepatocytes, this includes inducing SIRT3 expression upon co-activation by PGC-1α (Kong et al., 2010; Giralt et al., 2011).

PGC-1α itself drives a wider transcriptional program controlling mitochondrial biogenesis, mitochondrial metabolism, and other processes. PGC-1α was originally identified for its key role in upregulating thermogenesis in response to cold exposure (Puigserver et al., 1998). It is upregulated in several tissues in response to nutrient stress in order to increase mitochondrial function and cellular capacity for energy production. It is induced in skeletal muscle by exercise (Baar et al., 2002), and it is important for exercise capacity and fatigue resistance (Leone et al., 2005). It is induced in mouse heart by short-term fasting, where it

stimulates mitochondrial biogenesis and respiration (Lehman et al., 2000), and it is induced by fasting in the liver, where it activates gluconeogenesis (Yoon et al., 2001). Calorie restriction also induces PGC-1α in skeletal muscle, where it underlies the upregulation of many mitochondrial genes in CR (Finley et al., 2012). In skeletal muscle, PGC-1α activity also increases fatty acid oxidative capacity (Hoeks et al., 2012) and lessens age-related pathologies such as inflammation (Wenz et al., 2009).

Another important effector of PGC-1α is nuclear respiratory factor 2 (NRF-2). NRF-2 is an E26 transformation specific-family transcription factor that is important for the expression of many mitochondrial genes (Scarpulla, 2002). NRF-2 functions as a heterodimer composed of α and β subunits, with the NRF-2α subunit binding DNA and the NRF-2β subunit facilitating binding between heterodimers (Batchelor et al, 1998). Like ERRα, NRF-2 is bound and co-activated by PGC-1α and is central to mitochondrial biogenesis and metabolism (Mootha et al., 2004; Baldelli et al., 2013; Yang et al., 2014). Among its targets are all ten nuclear-encoded cytochrome c oxidase subunits (Ongwijitwat and Wong-Riley, 2005; Ongwijitwat et al., 2006), ATP synthase subunit β, and succinate dehydrogenase subunits B, C, and D (Scarpulla, 2002). Noteably, both NRF-2 and ERRα drive the expression not only of oxidative genes but also each other (Mootha et al., 2004). However, it is not known whether one is more active than another in different tissues or different physiological contexts such as calorie restriction. NRF-2 has received comparatively less study than ERRα and is sometimes confused in the literature with the transcription factor nuclear factor erythroid 2-related factor 2 (often abbreviated NRF2), which induces antioxidant pathway genes (Baldelli et al., 2013).

Study overview

Do PGC-1α and its effectors represent the pathway responsible for upregulating SIRT3 expression during CR? What are the transcription factors controlling SIRT3 expression? With so much being discovered about the downstream effects of SIRT3 and other sirtuins, we focused our efforts on uncovering upstream factors that control SIRT3 expression. Chapter II describes the development of a luciferase-based plasmid reporter to assay SIRT3 expression. SIRT3 shares a short bidirectional promoter with the 26S proteasome non-ATPase regulatory subunit 13 (PSMD13), and we cloned the PSMD13-SIRT3 promoter into a reporter plasmid, with activation of the promoter driving expression of the luciferase reporter gene. We validate that it functions as expected in control situations, and we use it to demonstrate that SIRT3 expression is induced by rapamycin, a small molecule inhibitor of the nutrient-sensing target of rapamycin (TOR) pathway.

One of the studies which originally detailed the interplay between PGC-1α, ERRα, and NRF-2 was driven by bioinformatic analysis (Mootha et al., 2004). To identify transcription factors involved in activating oxidative phosphorylation, either PGC-1α or a control vector were overexpressed in cultured mouse C2C12 myotubes, followed by microarray analysis of gene expression. Genes were then ranked based on induction by PGC-1α and the genes' DNA sequences were analyzed for transcription factor binding motifs which were enriched in the promoters of genes ranked near the top of the list. ERRα and NRF-2 were the two top-scoring motifs identified. In chapter III, we use a similar approach developed by Warner et al. (2008) to identify transcription factors which may control SIRT3 induction. Using publicly available microarray data, we identify datasets in which SIRT3 is upregulated by fasting or CR. We then analyze enrichment of transcription factor binding motifs in the DNA sequences of not only

SIRT3, but also the genes whose expression profiles are most highly correlated with SIRT3, under the hypothesis that genes which are co-expressed may be controlled by the same transcription factor(s). Using a set of several genes increases the statistical power over an analysis of one gene alone. With this method, we identify NRF-2 as a top candidate regulator of SIRT3. We then experimentally verify that NRF-2 overexpression and knockdown affect SIRT3 mRNA levels in human 293T cells and that NRF-2α binds the SIRT3 promoter. We thus establish that SIRT3 expression is controlled by both arms of the PGC-1α – ERRα and PGC-1α – NRF-2 pathway.

In chapter IV, we take a different view of regulation during CR using a high-throughput RNA sequencing (RNA-seq) approach. RNA-seq enables analysis of not just raw gene expression level but also of relative isoform expression levels and start site usage for a particular gene. Using liver and heart tissue from young control, aged control, and aged CR mice, we examine both gene expression and isoform usage changes that occur with age and with calorie restriction. We note that calorie restriction opposes the effects of aging for a large proportion of the gene expression changes we observed in the liver, and we also identify genes whose age-related changes in isoform usage are reversed by CR. We examine SIRT3 specifically and observe that a particular 8 bp insert is incorporated into SIRT3 transcripts twice as often in liver as in heart, suggesting a previously unappreciated role for the regulation of isoform expression in SIRT3 biology.

Finally, we also include an appendix from a "targeted screen" looking at the effect of six small molecule CR mimetics on SIRT3 expression in 293T cells. This series of experiments initially identifies rapamycin's effect on SIRT3 levels, and we subsequently investigate the effect

of rapamycin on expression levels of the mitochondrial sirtuins – SIRT3, SIRT4, and SIRT5 – in multiple cell lines and with multiple methods of inhibiting the TOR pathway.

Together, these chapters provide an important step in elucidating the pathways which induce SIRT3. SIRT3 is induced during calorie restriction and mediates some of its benefits. SIRT3 also plays an important role in the suppression of inflammation and the delayed onset of age-related disease. A fuller knowledge of the mechanisms by which it is expressed may in the future lead to therapeutic strategies for the mimicry of calorie restriction and the treatment or prevention of age-related disease.

References

Anderson RM, Weindruch R (2010) Metabolic reprogramming, caloric restriction and aging. *Trends Endocrinol. Metab.* **21**, 134-141.

Baar K, Wende AR, Jones TE, Marison M, Nolte LA, Chen M, Kelly DP, Holloszy JO (2002) Adaptations of skeletal muscle to exercise: rapid increase in the transcriptional coactivator PGC-1. *FASEB J*. **16**, 1879-1886.

Baldelli S, Aquilano K, Ciriolo MR (2013) Punctum on two different transcription factors regulated by PGC-1α: nuclear factor erythroid-derived 2-like 2 and nuclear respiratory factor 2. *Biochim. Biophys. Acta* **1830**, 4137-4146.

Banerjee KK, Ayyub C, Ali SZ, Mandot V, Prasad NG, Kolthur-Seetharam U (2012) dSir2 in the adult fat body, but not in muscles, regulates life span in a diet-dependent manner. *Cell Rep.* **2**, 1485-1491.

Barger JL, Kayo T, Vann JM, Arias EB, Wang J, Hacker TA, Wang Y, Raederstorff D, Morrow JD, Leeuwenburgh C, Allison DB, Saupe KW, Cartee GD, Weindruch R, Prolla TA (2008) A low dose of dietary resveratrol partially mimics caloric restriction and retards aging parameters in mice. *PLoS One* **3**, e2264.

Batchelor AH, Piper DE, de la Brousse FC, McKnight SL, Wolberger C (1998) The structure of GABPalpha/beta: an ETS domain- ankyrin repeat heterodimer bound to DNA. *Science* **279**, 1037-1041.

Bell EL, Emerling BM, Ricoult SJ, Guarente L (2011) SirT3 suppresses hypoxia inducible factor 1alpha and tumor growth by inhibiting mitochondrial ROS production. *Oncogene* **30**, 2986-2996.

Blander G, Guarente L (2004) The sir2 family of protein deacetylases. *Annu. Rev. Biochem.* **73**, 417-435.

Boily G, Seifert EL, Bevilacqua L, He XH, Sabourin G, Estey C, Moffat C, Crawford S, Saliba S, Jardine K, Xuan J, Evans M, Harper ME, McBurney MW (2008) SirT1 regulates energy metabolism and response to caloric restriction in mice. *PLoS One* **3**, e1759.

Borradaile NM, Pickering JG (2009) NAD(+), sirtuins, and cardiovascular disease. *Curr. Pharm. Des.* **15**, 110-117.

Burnett C, Valentini S, Cabreiro F, Goss M, Somogyvári M, Piper MD, Hoddinott M, Sutphin GL, Leko V, McElwee JJ, Vazquez-Manrique RP, Orfila AM, Ackerman D, Au C, Vinti G, Riesen M, Howard K, Neri C, Bedalov A, Kaeberlein M, Soti C, Partridge L, Gems D (2011) Absence of effects of Sir2 overexpression on lifespan in C. elegans and Drosophila. *Nature* **477**, 482-485.

Chen D, Bruno J, Easlon E, Lin SJ, Cheng HL, Alt FW, Guarente L (2008) Tissue-specific regulation of SIRT1 by calorie restriction. *Genes Dev*. 22, 1753-1757.

Chen Y, Zhang J, Lin Y, Lei Q, Guan KL, Zhao S, Xiong Y (2011) Tumour suppressor SIRT3 deacetylates and activates manganese superoxide dismutase to scavenge ROS. *EMBO Rep.* **12**, 534-541.

Condorelli G, Drusco A, Stassi G, Bellacosa A, Roncarati R, Iaccarino G, Russo MA, Gu Y, Dalton N, Chung C, Latronico MV, Napoli C, Sadoshima J, Croce CM, Ross J Jr. (2002) Akt induces enhanced myocardial contractility and cell size in vivo in transgenic mice. *Proc. Natl. Acad. Sci. U. S. A.* **99**, 12333-12338.

Dang W, Steffen KK, Perry R, Dorsey JA, Johnson FB, Shilatifard A, Kaeberlein M, Kennedy BK, Berger SL (2009) Histone H4 lysine 16 acetylation regulates cellular lifespan. *Nature* **459**, 802-807.

Du J, Zhou Y, Su X, Yu JJ, Khan S, Jiang H, Kim J, Woo J, Kim JH, Choi BH, He B, Chen W, Zhang S, Cerione RA, Auwerx J, Hao Q, Lin H (2011) Sirt5 is a NAD-dependent protein lysine demalonylase and desuccinylase. *Science* **334**, 806-809.

Finley LW, Haas W, Desquiret-Dumas V, Wallace DC, Procaccio V, Gygi SP, Haigis MC (2011a) Succinate dehydrogenase is a direct target of sirtuin 3 deacetylase activity. *PLoS One* **6**, e23295.

Finley LW, Carracedo A, Lee J, Souza A, Egia A, Zhang J, Teruya-Feldstein J, Moreira PI, Cardoso SM, Clish CB, Pandolfi PP, Haigis MC (2011b) SIRT3 opposes reprogramming of cancer cell metabolism through HIF1alpha destabilization. *Cancer Cell* **19**, 416-428.

Finley LW, Lee J, Souza A, Desquiret-Dumas V, Bullock K, Rowe GC, Procaccio V, Clish CB, Arany Z, Haigis MC (2012) Skeletal muscle transcriptional coactivator PGC-1α mediates mitochondrial, but not metabolic, changes during calorie restriction. *Proc. Natl. Acad. Sci. U. S. A.* **109**, 2931-2936.

Frye RA (2000) Phylogenetic classification of prokaryotic and eukaryotic Sir2-like proteins. *Biochem. Biophys. Res. Commun.* **273**, 793-798.

Gerhart-Hines Z, Rodgers JT, Bare O, Lerin C, Kim SH, Mostoslavsky R, Alt FW, Wu Z, Puigserver P (2007) Metabolic control of muscle mitochondrial function and fatty acid oxidation through SIRT1/PGC-1alpha. *EMBO J*. *26*, 1913-1923.

Giguère V (2008) Transcriptional control of energy homeostasis by the estrogen-related receptors. *Endocr. Rev*. **29**, 677-696.

Gillum MP, Kotas ME, Erion DM, Kursawe R, Chatterjee P, Nead KT, Muise ES, Hsiao JJ, Frederick DW, Yonemitsu S, Banks AS, Qiang L, Bhanot S, Olefsky JM, Sears DD, Caprio S, Shulman GI (2011) SirT1 regulates adipose tissue inflammation. *Diabetes* **60**, 3235-3245.

Giralt A, Hondares E, Villena JA, Ribas F, Díaz-Delfín J, Giralt M, Iglesias R, Villarroya F (2011) Peroxisome proliferator-activated receptor-gamma coactivator-1alpha controls transcription of the Sirt3 gene, an essential component of the thermogenic brown adipocyte phenotype. *J. Biol. Chem*. **286**, 16958-16966.

Greiss S, Gartner A (2009) Sirtuin/Sir2 phylogeny, evolutionary considerations and structural conservation. *Mol. Cells* **28**, 407-415.

Guarente L (2013) Calorie restriction and sirtuins revisited. *Genes Dev*. **27**, 2072-2085.

Haigis MC, Guarente LP (2006) Mammalian sirtuins--emerging roles in physiology, aging, and calorie restriction. *Genes Dev.* **20**, 2913-2921.

Haigis MC, Mostoslavsky R, Haigis KM, Fahie K, Christodoulou DC, Murphy AJ, Valenzuela DM, Yancopoulos GD, Karow M, Blander G, Wolberger C, Prolla TA, Weindruch R, Alt FW, Guarente L (2006) SIRT4 inhibits glutamate dehydrogenase and opposes the effects of calorie restriction in pancreatic beta cells. *Cell* **126**, 941-954.

Haigis MC, Sinclair DA (2010) Mammalian sirtuins: biological insights and disease relevance. *Annu. Rev. Pathol.* **5**, 253-295.

Hallows WC, Yu W, Smith BC, Devries MK, Ellinger JJ, Someya S, Shortreed MR, Prolla T, Markley JL, Smith LM, Zhao S, Guan KL, Denu JM (2011) Sirt3 promotes the urea cycle and fatty acid oxidation during dietary restriction. *Mol. Cell* **41**, 139-149.

Hanahan D, Weinberg RA (2000) The hallmarks of cancer. *Cell* **100**, 57-70.

Hebert AS, Dittenhafer-Reed KE, Yu W, Bailey DJ, Selen ES, Boersma MD, Carson JJ, Tonelli M, Balloon AJ, Higbee AJ, Westphall MS, Pagliarini DJ, Prolla TA, Assadi-Porter F, Roy S, Denu JM, Coon JJ (2013) Calorie restriction and SIRT3 trigger global reprogramming of the mitochondrial protein acetylome. *Mol. Cell* **49**, 186-199.

Herranz D, Muñoz-Martin M, Cañamero M, Mulero F, Martinez-Pastor B, Fernandez-Capetillo O, Serrano M. (2010) Sirt1 improves healthy ageing and protects from metabolic syndrome-associated cancer. *Nat. Commun* **1**, 3.

Hirschey MD, Shimazu T, Goetzman E, Jing E, Schwer B, Lombard DB, Grueter CA, Harris C, Biddinger S, Ilkayeva OR, Stevens RD, Li Y, Saha AK, Ruderman NB, Bain JR, Newgard CB, Farese RV Jr, Alt FW, Kahn CR, Verdin E (2010) SIRT3 regulates mitochondrial fatty-acid oxidation by reversible enzyme deacetylation. *Nature* **464**, 121-125.

Hirschey MD, Shimazu T, Capra JA, Pollard KS, Verdin E (2011a) SIRT1 and SIRT3 deacetylate homologous substrates: AceCS1,2 and HMGCS1,2. *Aging (Albany NY)* **3**, 635-642.

Hirschey MD, Shimazu T, Jing E, Grueter CA, Collins AM, Aouizerat B, Stančáková A, Goetzman E, Lam MM, Schwer B, Stevens RD, Muehlbauer MJ, Kakar S, Bass NM, Kuusisto J, Laakso M, Alt FW, Newgard CB, Farese RV Jr, Kahn CR, Verdin E (2011b) SIRT3 deficiency and mitochondrial protein hyperacetylation accelerate the development of the metabolic syndrome. *Mol. Cell* **44**, 177-190.

Hoeks J, Arany Z, Phielix E, Moonen-Kornips E, Hesselink MK, Schrauwen P (2012) Enhanced lipid-but not carbohydrate-supported mitochondrial respiration in skeletal muscle of PGC-1α overexpressing mice. *J. Cell. Physiol*. **227**, 1026-1033.

Hoffmann J, Romey R, Fink C, Yong L, Roeder T (2013) Overexpression of Sir2 in the adult fat body is sufficient to extend lifespan of male and female Drosophila. *Aging (Albany NY)* **5**, 315-327.

Howitz KT, Bitterman KJ, Cohen HY, Lamming DW, Lavu S, Wood JG, Zipkin RE, Chung P, Kisielewski A, Zhang LL, Scherer B, Sinclair DA (2003) Small molecule activators of sirtuins extend Saccharomyces cerevisiae lifespan. *Nature* **425**, 191-196.

Hubbard BP, Gomes AP, Dai H, Li J, Case AW, Considine T, Riera TV, Lee JE, E SY, Lamming DW, Pentelute BL, Schuman ER, Stevens LA, Ling AJ, Armour SM, Michan S, Zhao H, Jiang Y, Sweitzer SM, Blum CA, Disch JS, Ng PY, Howitz KT, Rolo AP, Hamuro Y, Moss J, Perni RB, Ellis JL, Vlasuk GP, Sinclair DA (2013) Evidence for a common mechanism of SIRT1 regulation by allosteric activators. *Science* **339**, 1216-1219.

Huss JM, Torra IP, Staels B, Giguère V, Kelly DP (2004) Estrogen-related receptor alpha directs peroxisome proliferator-activated receptor alpha signaling in the transcriptional control of energy metabolism in cardiac and skeletal muscle. *Mol Cell Biol*. **24**, 9079-9091.

Ivy JM, Klar AJ, Hicks JB (1986) Cloning and characterization of four SIR genes of Saccharomyces cerevisiae. *Mol. Cell. Biol.* **6**, 688-702.

Kaeberlein M, McVey M, Guarente L (1999) The SIR2/3/4 complex and SIR2 alone promote longevity in Saccharomyces cerevisiae by two different mechanisms. *Genes Dev.* **13**, 2570-2580.

Kanfi Y, Naiman S, Amir G, Peshti V, Zinman G, Nahum L, Bar-Joseph Z, Cohen HY (2012) The sirtuin SIRT6 regulates lifespan in male mice. *Nature* **483**, 218-221.

Kendrick AA, Choudhury M, Rahman SM, McCurdy CE, Friederich M, Van Hove JL, Watson PA, Birdsey N, Bao J, Gius D, Sack MN, Jing E, Kahn CR, Friedman JE, Jonscher KR (2011) Fatty liver is associated with reduced SIRT3 activity and mitochondrial protein hyperacetylation. *Biochem. J.* **433**, 505-514.

Kim HS, Patel K, Muldoon-Jacobs K, Bisht KS, Aykin-Burns N, Pennington JD, van der Meer R, Nguyen P, Savage J, Owens KM, Vassilopoulos A, Ozden O, Park SH, Singh KK, Abdulkadir SA, Spitz DR, Deng CX, Gius D (2010) SIRT3 is a mitochondria-localized tumor suppressor

required for maintenance of mitochondrial integrity and metabolism during stress. *Cancer Cell* **17**, 41-52.

Kong X, Wang R, Xue Y, Liu X, Zhang H, Chen Y, Fang F, Chang Y (2010) Sirtuin 3, a new target of PGC-1alpha, plays an important role in the suppression of ROS and mitochondrial biogenesis. *PLoS One* **5**, e11707.

Koyama T, Kume S, Koya D, Araki S, Isshiki K, Chin-Kanasaki M, Sugimoto T, Haneda M, Sugaya T, Kashiwagi A, Maegawa H, Uzu T (2011) SIRT3 attenuates palmitate-induced ROS production and inflammation in proximal tubular cells. *Free Radic. Biol. Med.* **51**, 1258-1267.

Lam YY, Peterson CM, Ravussin E (2013) Resveratrol vs. calorie restriction: data from rodents to humans. *Exp. Gerontol*. **48**, 1018-1024.

Lang D (2002) Cardiac hypertrophy and oxidative stress: a leap of faith or stark reality? *Heart* **87**, 316-317.

Lehman JJ, Barger PM, Kovacs A, Saffitz JE, Medeiros DM, Kelly DP (2000) Peroxisome proliferator-activated receptor gamma coactivator-1 promotes cardiac mitochondrial biogenesis. *J. Clin. Invest.* **106**, 847-856.

Leone TC, Lehman JJ, Finck BN, Schaeffer PJ, Wende AR, Boudina S, Courtois M, Wozniak DF, Sambandam N, Bernal-Mizrachi C, Chen Z, Holloszy JO, Medeiros DM, Schmidt RE, Saffitz JE, Abel ED, Semenkovich CF, Kelly DP (2005) PGC-1alpha deficiency causes multi-system energy metabolic derangements: muscle dysfunction, abnormal weight control and hepatic steatosis. *PLoS Biol*. **3**, e101.

Li L, Smith A, Hagen TM, Frei B (2010) Vascular oxidative stress and inflammation increase with age: ameliorating effects of alpha-lipoic acid supplementation. *Ann. N. Y. Acad. Sci.* **1203**, 151-159.

Lin SJ, Defossez PA, Guarente, L (2000) Requirement of NAD and SIR2 for life-span extension by calorie restriction in Saccharomyces cerevisiae. *Science* **289**, 2126-2128.

Liszt G, Ford E, Kurtev M, Guarente L (2005) Mouse Sir2 homolog SIRT6 is a nuclear ADP-ribosyltransferase. *J. Biol. Chem.* **280**, 21313-21320.

Liu XZ, Yan D (2007) Ageing and hearing loss. *J. Pathol.* **211**, 188-197.

Malik S, Wong ND, Franklin SS, Kamath TV, L'Italien GJ, Pio JR, Williams GR (2004) Impact of the metabolic syndrome on mortality from coronary heart disease, cardiovascular disease, and all causes in United States adults. *Circulation* **110**, 1245-1250.

McCay CM, Crowell MF, Maynard LA (1935) The effect of retarded growth upon the length of life span and upon the ultimate body size. *J. Nutr.* **10**, 63-79.

Mootha VK, Handschin C, Arlow D, Xie X, St Pierre J, Sihag S, Yang W, Altshuler D, Puigserver P, Patterson N, Willy PJ, Schulman IG, Heyman RA, Lander ES, Spiegelman BM (2004) Errα and Gabpa/b specify PGC-1α-dependent oxidative phosphorylation gene expression that is altered in diabetic muscle. *Proc. Natl. Acad. Sci. U. S. A.* **101**, 6570-6575.

Mostoslavsky R, Chua KF, Lombard DB, Pang WW, Fischer MR, Gellon L, Liu P, Mostoslavsky G, Franco S, Murphy MM, Mills KD, Patel P, Hsu JT, Hong AL, Ford E, Cheng HL, Kennedy C, Nunez N, Bronson R, Frendewey D, Auerbach W, Valenzuela D, Karow M, Hottiger MO, Hursting S, Barrett JC, Guarente L, Mulligan R, Demple B, Yancopoulos GD, Alt FW. (2006) Genomic instability and aging-like phenotype in the absence of mammalian SIRT6. *Cell* **124**, 315-329.

Mouchiroud L, Houtkooper RH, Moullan N, Katsyuba E, Ryu D, Cantó C, Mottis A, Jo YS, Viswanathan M, Schoonjans K, Guarente L, Auwerx J (2013) The NAD(+)/Sirtuin Pathway Modulates Longevity through Activation of Mitochondrial UPR and FOXO Signaling. *Cell* **154**, 430-441.

Nakagawa T, Lomb DJ, Haigis MC, Guarente L (2009) SIRT5 Deacetylates carbamoyl phosphate synthetase 1 and regulates the urea cycle. *Cell* **137**, 560-570.

Ongwijitwat S, Wong-Riley MT (2005) Is nuclear respiratory factor 2 a master transcriptional coordinator for all ten nuclear-encoded cytochrome c oxidase subunits in neurons? *Gene* **360**, 65-77.

Ongwijitwat S, Liang HL, Graboyes EM, Wong-Riley MT (2006) Nuclear respiratory factor 2 senses changing cellular energy demands and its silencing down-regulates cytochrome oxidase and other target gene mRNAs. *Gene* **374**, 39-49.

Pearson KJ, Baur JA, Lewis KN, Peshkin L, Price NL, Labinskyy N, Swindell WR, Kamara D, Minor RK, Perez E, Jamieson HA, Zhang Y, Dunn SR, Sharma K, Pleshko N, Woollett LA, Csiszar A, Ikeno Y, Le Couteur D, Elliott PJ, Becker KG, Navas P, Ingram DK, Wolf NS, Ungvari Z, Sinclair DA, de Cabo R (2008) Resveratrol delays age-related deterioration and mimics transcriptional aspects of dietary restriction without extending life span. *Cell Metab*. **8**, 157-168.

Pillai VB, Sundaresan NR, Jeevanandam V, Gupta MP (2010a) Mitochondrial SIRT3 and heart disease. *Cardiovasc. Res.* **88**, 250-256.

Pillai VB, Sundaresan NR, Kim G, Gupta M, Rajamohan SB, Pillai JB, Samant S, Ravindra PV, Isbatan A, Gupta MP (2010b) Exogenous NAD blocks cardiac hypertrophic response via activation of the SIRT3-LKB1-AMP-activated kinase pathway. *J. Biol. Chem.* **285**, 3133-3144.

Puigserver P, Wu Z, Park CW, Graves R, Wright M, Spiegelman BM (1998) A cold-inducible coactivator of nuclear receptors linked to adaptive thermogenesis. *Cell* **92**, 829-839.

Qiu X, Brown K, Hirschey MD, Verdin E, Chen D (2010) Calorie restriction reduces oxidative stress by SIRT3-mediated SOD2 activation. *Cell Metab.* **12**, 662-667.

Rizki G, Iwata TN, Li J, Riedel CG, Picard CL, Jan M, Murphy CT, Lee SS (2011) The evolutionarily conserved longevity determinants HCF-1 and SIR-2.1/SIRT1 collaborate to regulate DAF-16/FOXO. *PLoS Genet*. **7**, e1002235.

Rogina B, Helfand SL (2004) Sir2 mediates longevity in the fly through a pathway related to calorie restriction. *Proc. Natl. Acad. Sci. U. S. A*. **101,** 15998-16003.

Sack MN (2011) Emerging characterization of the role of SIRT3-mediated mitochondrial protein deacetylation in the heart. *Am. J. Physiol. Heart Circ. Physiol.* **301**, H2191-2197.

Satoh A, Brace CS, Rensing N, Cliften P, Wozniak DF, Herzog ED, Yamada KA, Imai S (2013) Sirt1 extends life span and delays aging in mice through the regulation of Nk2 homeobox 1 in the DMH and LH. *Cell Metab*. **18**, 416-430.

Scarpulla RC (2002) Nuclear activators and coactivators in mammalian mitochondrial biogenesis. *Biochim. Biophys. Acta* **1576**, 1-14.

Scarpulla RC (2011) Metabolic control of mitochondrial biogenesis through the PGC-1 family regulatory network. *Biochim. Biophys. Acta* **1813**, 1269-1278.

Schreiber SN, Knutti D, Brogli K, Uhlmann T, Kralli A (2003) The transcriptional coactivator PGC-1 regulates the expression and activity of the orphan nuclear receptor estrogen-related receptor alpha (ERRalpha). *J. Biol. Chem.* **278**, 9013-9018.

Schug TT, Xu Q, Gao H, Peres-da-Silva A, Draper DW, Fessler MB, Purushotham A, Li, X (2010) Myeloid deletion of SIRT1 induces inflammatory signaling in response to environmental stress. *Mol. Cell. Biol.* **30**, 4712-4721.

Shi T, Wang F, Stieren E, Tong Q (2005) SIRT3, a mitochondrial sirtuin deacetylase, regulates mitochondrial function and thermogenesis in brown adipocytes. *J. Biol. Chem.* **280**, 13560-13567.

Shimazu T, Hirschey MD, Hua L, Dittenhafer-Reed KE, Schwer B, Lombard DB, Li Y, Bunkenborg J, Alt FW, Denu JM, Jacobson MP, Verdin E (2010) SIRT3 deacetylates mitochondrial 3-hydroxy-3-methylglutaryl CoA synthase 2 and regulates ketone body production. *Cell Metab* **12**, 654-661.

Sladek R, Bader JA, Giguère V (1997) The orphan nuclear receptor estrogen-related receptor alpha is a transcriptional regulator of the human medium-chain acyl coenzyme A dehydrogenase gene. *Mol. Cell. Biol.* **17**, 5400-5409.

Someya S, Yu W, Hallows WC, Xu J, Vann JM, Leeuwenburgh C, Tanokura M, Denu JM, Prolla TA (2010) Sirt3 mediates reduction of oxidative damage and prevention of age-related hearing loss under caloric restriction. *Cell* **143**, 802-812.

Sundaresan NR, Gupta M, Kim G, Rajamohan SB, Isbatan A, Gupta MP (2009) Sirt3 blocks the cardiac hypertrophic response by augmenting Foxo3a-dependent antioxidant defense mechanisms in mice. *J. Clin. Invest.* **119**, 2758-2771.

Tao R, Coleman MC, Pennington JD, Ozden O, Park SH, Jiang H, Kim HS, Flynn CR, Hill S, Hayes McDonald W, Olivier AK, Spitz DR, Gius D (2010) Sirt3-mediated deacetylation of evolutionarily conserved lysine 122 regulates MnSOD activity in response to stress. *Mol. Cell* **40**, 893-904.

Tissenbaum HA, Guarente L (2001) Increased dosage of a sir-2 gene extends lifespan in Caenorhabditis elegans. *Nature* **410**, 227-230.

Vander Heiden MG, Cantley LC, Thompson CB (2009) Understanding the Warburg effect: the metabolic requirements of cell proliferation. *Science* **324**, 1029-1033.

Vaziri H, Dessain SK, Ng Eaton E, Imai SI, Frye RA, Pandita TK, Guarente L, Weinberg RA (2001) hSIR2(SIRT1) functions as an NAD-dependent p53 deacetylase. *Cell* **107**, 149-159.

Viswanathan M, Guarente L (2011) Regulation of Caenorhabditis elegans lifespan by sir-2.1 transgenes. *Nature* **477**, E1-2.

Warner JB, Philippakis AA, Jaeger SA, He FS, Lin J, Bulyk ML (2008) Systematic identification of mammalian regulatory motifs' target genes and functions. *Nat. Methods* **5**, 347-353.

Weindruch R, Walford RL, Fligiel S, Guthrie D (1986) The retardation of aging in mice by dietary restriction: longevity, cancer, immunity and lifetime energy intake. *J. Nutr.* **116**, 641-654.

Weiss EP, Fontana L (2011) Caloric restriction: powerful protection for the aging heart and vasculature. *Am. J. Physiol. Heart Circ. Physiol.* **301**, H1205-1219.

Wenz T, Rossi SG, Rotundo RL, Spiegelman BM, Moraes CT (2009) Increased muscle PGC-1alpha expression protects from sarcopenia and metabolic disease during aging. *Proc. Natl. Acad. Sci. U. S. A.* **106**, 20405-20410.

Wu Z, Liu MC, Liang M, Fu J (2012) Sirt1 protects against thrombomodulin down-regulation and lung coagulation after particulate matter exposure. *Blood* **119**, 2422-2429.

Yang ZF, Drumea K, Mott S, Wang J, Rosmarin AG (2014) GABP transcription factor (nuclear respiratory factor 2) is required for mitochondrial biogenesis. *Mol. Cell. Biol.* **34**, 3194-3201.

Yoon JC, Puigserver P, Chen G, Donovan J, Wu Z, Rhee J, Adelmant G, Stafford J, Kahn CR, Granner DK, Newgard CB, Spiegelman BM (2001) Control of hepatic gluconeogenesis through the transcriptional coactivator PGC-1. *Nature* **413**, 131-138.

Yoshizaki T, Schenk S, Imamura T, Babendure JL, Sonoda N, Bae EJ, Oh DY, Lu M, Milne JC, Westphal C, Bandyopadhyay G, Olefsky JM (2010) SIRT1 inhibits inflammatory pathways in macrophages and modulates insulin sensitivity. *Am. J. Physiol. Endocrinol. Metab.* **298**, E419-428.

Yu W, Dittenhafer-Reed KE, Denu JM (2012) SIRT3 protein deacetylates isocitrate dehydrogenase 2 (IDH2) and regulates mitochondrial redox status. *J. Biol. Chem.* **287**, 14078-14086.

CHAPTER II

This chapter has been published as:

Luciferase-based reporter to monitor the transcriptional activity of the *SIRT3* promoter

F. Kyle Satterstrom[1,2] and Marcia C. Haigis[2]

Methods in Enzymology (2014) **543**, 141-163

[1] Harvard School of Engineering and Applied Sciences, Cambridge, Massachusetts 02138

[2] Department of Cell Biology, Harvard Medical School, Boston, Massachusetts 02115

Abstract

Sirtuin 3 (SIRT3) is a major regulator of oncometabolism. Its activity or lack thereof significantly affects cellular oxidative stress, glycolytic gene expression, and tumorigenic potential. Thus, a system to accurately measure the level of *SIRT3* transcriptional activation could lead to the identification of new cancer therapies and may have diagnostic applications. Here, we describe the development of a luciferase-based plasmid reporter system to measure activation of the human *SIRT3* promoter. We detail the steps involved in construction of the system, including primer design, promoter fragment amplification, cloning, bacterial transformation, and mutagenesis. We validate this system in human 293T cells using the known activation of the *SIRT3* promoter by the transcription factor estrogen-related receptor α, and we further show novel activation by the small molecule rapamycin, which has been used as a calorie restriction mimetic. Finally, we give an overview of the complementary molecular biology techniques that may be used to verify the results of this system.

Introduction

Sirtuins are mammalian homologs of the yeast enzyme silent information regulator 2 (Sir2), a regulator of chromatin packing and transcription which may also be involved in the regulation of replicative lifespan (Lin et al., 2000). The seven mammalian sirtuins possess NAD^+-dependent activities including deacetylation, deacylation, and ADP-ribosylation (as reviewed in Houtkooper et al., 2012). Their best-known biological functions involve helping the cell adapt to nutrient challenges and stress. For example, SIRT1 and SIRT3 levels are upregulated during calorie restriction to promote fatty acid oxidation (Cohen et al., 2004; Chakrabarti et al., 2011; Hallows et al., 2011; Hirschey et al., 2010). Recently, the sirtuins have

come under close study by cancer biologists because several of them – at least SIRT3, SIRT4, and SIRT6 – function as tumor suppressors through their regulation of cellular metabolism (e.g. Kim et al., 2010; Finley et al., 2011; Jeong et al., 2013; Sebastián et al., 2012).

SIRT3 in particular seems to lie at the nexus of metabolism and tumor suppression. In addition to promoting fatty acid metabolism, SIRT3 activates superoxide dismutase 2 (SOD2), one of the cell's main defenses against reactive oxygen species (ROS) (Tao et al., 2010). By fighting ROS, SIRT3 plays dual roles: first, it helps to promote genomic integrity (Kim et al., 2010), and second, it maintains hypoxia inducible factor 1α (HIF1α) in a destabilized state, preventing it from inducing the glycolytic gene expression and Warburg effect which are typical of cancer cells (Finley et al., 2011; Bell et al., 2011). When SIRT3 activity is low, tumor formation is more likely – in fact, one copy of *SIRT3* is deleted in approximately 20% of all human tumors (Finley et al., 2011). Because SIRT3 plays such an important role in metabolism and tumor suppression, it is important to develop quantitative and sensitive methods to monitor its expression.

This chapter details the construction of a luciferase-based reporter system for assaying the activity of the *SIRT3* promoter. The system was inspired by previous work (Bellizzi et al., 2007) but greatly expands and improves upon it. The first part of the protocol describes cloning the *SIRT3* promoter into an otherwise promoter-less luciferase reporter plasmid. The construct can then be mutagenized site-specifically to test the effects of ablating certain sequence elements. Assaying *SIRT3* promoter activation with the construct involves transfecting it into cells under different conditions and measuring the activity of the luciferase reporter gene; we present two example applications to illustrate validation and use of the system, including the novel upregulation of SIRT3 expression by rapamycin, a small molecule inhibitor of the nutrient-

responsive kinase mammalian target of rapamycin (mTOR) (Zoncu et al., 2011). The protocol concludes by describing verification of reporter results by quantitative PCR and western blot. Though tailored specifically for *SIRT3* in this chapter, these same methods could be applied to any target gene of interest.

Protocol for construction of reporter plasmid

Primer design

Perhaps the most crucial step in creating a reporter construct is to decide which DNA fragment to clone. Because this fragment will be bounded by the primers used to amplify it, the first step is therefore a decision about where to place the primers.

Place the reverse (downstream) primer. The reverse primer is more straightforward to place than the forward (upstream) primer. In most cases, place the reverse primer in the region after the transcriptional start site for the gene of interest but before the translation start codon. This will allow the construct to respond to the transcriptional machinery that normally controls the gene but instead produce the reporter enzyme after translation. The location of a gene's transcriptional and translational start sites can be read from DNA sequence information annotated by the National Center for Biotechnology Information (NCBI), displayed via the NCBI's own website (searchable by gene at http://www.ncbi.nlm.nih.gov/gene) or the University of California, Santa Cruz Genome Browser (http://genome.ucsc.edu/index.html).

We followed these guidelines and placed our downstream primer between the *SIRT3* transcription start site and translation start codon (Table 2.1).

Table 2.1. Location of salient features within the *SIRT3-PSMD13* promoter (using the NM_001017524.2 transcript annotation for *SIRT3* and NM_002817.3 transcript annotation for *PSMD13* from the National Center for Biotechnology Information).

Feature	**Location (DNA base) relative to *SIRT3* transcription start site**
PSMD13 start codon	-687 to -685
First homologous base of forward primer	-682
Last base of forward primer	-663
PSMD13 transcription start site	-446
First base of reverse primer	+8
Last homologous base of reverse primer	+29
SIRT3 start codon	+35 to +37
First base of Bellizzi reverse primer	+150
Last homologous base of Bellizzi reverse primer	+169

Place the forward (upstream) primer. Placement of the forward (upstream) primer depends on the size of the promoter and the locations of known upstream regulatory sequences. Use DNA sequence analysis algorithms such as MAPPER (http://genome.ufl.edu/mapper/) or TFSearch (http://www.cbrc.jp/research/db/TFSEARCH.html) to identify upstream regions containing potential transcription factor binding sites, and combine this information with any regulatory sequences already known to exist in the promoter. When possible, place the primer to include these regions in the amplified fragment. For genes with lengthy promoters or vague promoter boundaries, the number of kilobases between the forward and reverse primers may depend on how large a region you are able to amplify via PCR. Approximately one in ten human genes has a bidirectional promoter – that is, a short (generally less than 1 kb) stretch of non-coding DNA between the 5' ends of two genes on opposite strands that may be functionally related and co-regulated (Lin et al., 2007). This situation establishes more definite bounds for the promoter region.

SIRT3 shares a bidirectional promoter with the proteasome subunit gene *PSMD13*. The intergenic sequence is not prohibitively long (only 721bp between start codons for *PSMD13* and the "canonical" *SIRT3* isoform, using the NCBI NC_000011.9 human chromosome 11 sequence and UniProt.org for isoform information). We therefore placed the forward primer between the *PSMD13* translation start codon and transcription start site (Figure 2.1, Table 2.1). This symmetric design allowed for the amplified fragment to be used in assaying either *SIRT3* or *PSMD13* promoter activity depending on its orientation in the reporter vector.

Design the exact primer sequences. Having selected the rough locations, design the exact primer sequences using the NCBI Primer Blast tool (http://www.ncbi.nlm.nih.gov/tools/primer-

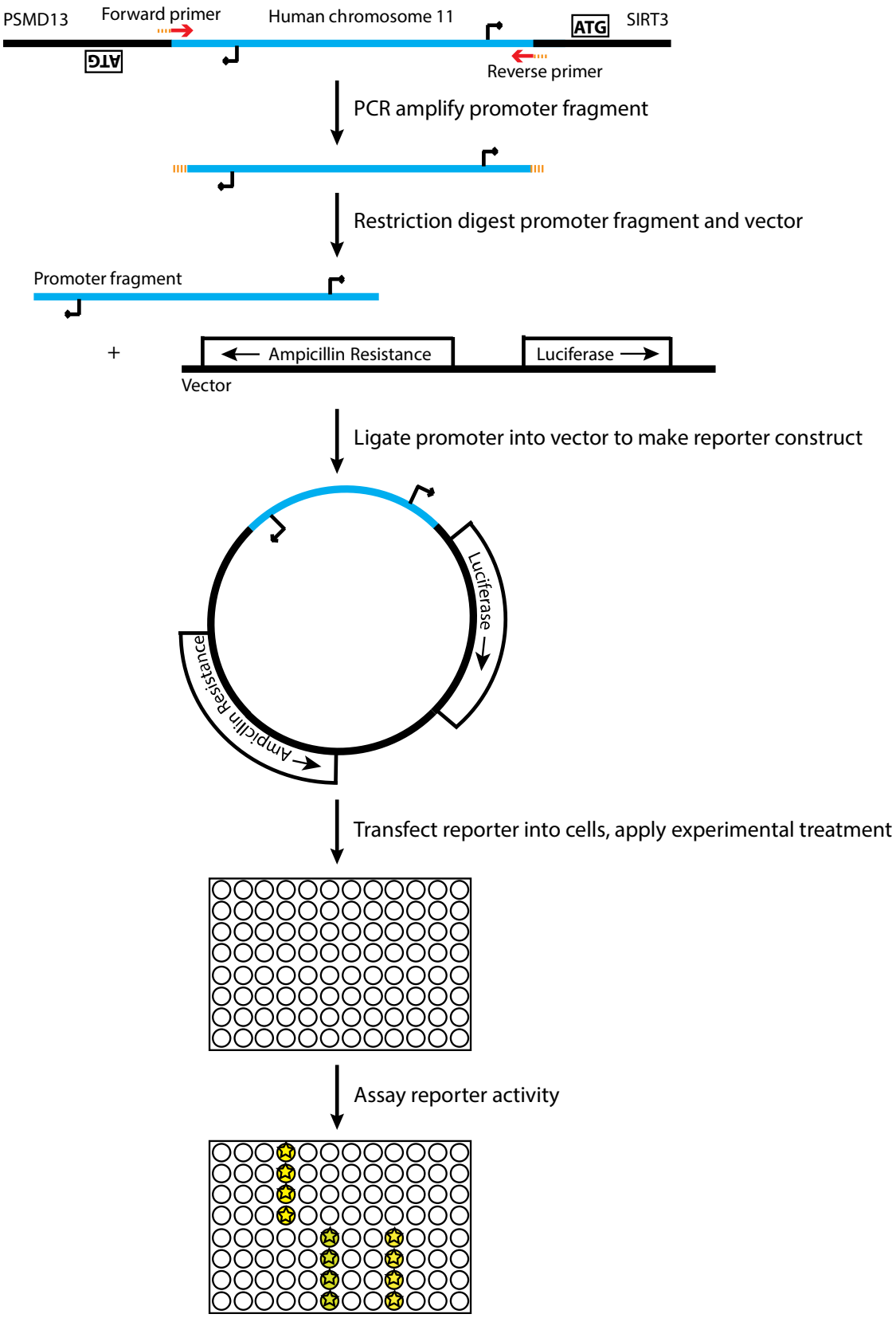

Figure 2.1. Overview of promoter fragment amplification, cloning, and experimental use.

blast/). This tool designs primer pairs that have minimal sequence similarity to other regions in the genome while maintaining desirable estimated hybridization properties to a given input sequence. To enable subsequent cloning, add the recognition site for a restriction enzyme to the 5' ends of the primers, as well as an overhang of three bases to allow the restriction enzyme to bind. The forward and reverse primers may optionally be designed to have recognition sites for different restriction enzymes, which will direct the insert to adopt a definite orientation during its later ligation into the vector (ensure that the order of recognition sites in the vector's multiple cloning site matches the planned directionality of the insert). Check that the recognition sequences do not occur in the region you plan to amplify.

For *SIRT3*, the NCBI Primer Blast algorithm identified a primer pair which fit the desired regions. We added a recognition site (ggtacc) for the restriction enzyme KpnI on the 5' end of each primer, as well as a three-base (ctc) overhang. The specific primers we used for the reversible insert were thus:

Forward: 5'-ctcggtaccCAGGAAGACCCCCGGCACAG-3'

Reverse: 5'-ctcggtaccGCGCAGTCCAAGGAGTCCTCCG-3'

Their positions within the *SIRT3-PSMD13* promoter are given in Table 2.1. (It should be noted that our construct does not contain bases -97 to -20, as we sequenced human DNA from multiple sources and none contained that fragment.)

We additionally made a *SIRT3* reporter using the reverse primer from Bellizzi et al. (2007), which is 5'-ctcggtaccATCGTCCCTGCCGCCAAGCA-3'. This primer falls after the *SIRT3* translation start codon. Transcription factor binding sites or other regulatory elements may in some instances overlap the start codon (Xi et al., 2007), necessitating its inclusion in the

amplified promoter fragment. In this scenario, it is important to design the reverse primer so that the reporter gene encoded by the construct remains in frame.

Promoter fragment amplification

Following primer design, the next step is to amplify the promoter fragment. This process involves generating a starting material to use as template, amplifying the promoter fragment via PCR, and verifying correct amplification.

Extract template genomic DNA. A single 10 cm dish or T75 flask of cultured cells that is near confluence will provide ample DNA for use as template. Collect the cells and proceed to DNA extraction. We extracted DNA from a pellet of human embryonic kidney 293T cells using a DNEasy kit (Qiagen, cat. # 69504), following manufacturer's instructions.

Amplify promoter fragment via PCR. Amplify the promoter fragment using the primers designed above and the template DNA extracted in the previous step. We used a FastStart PCR Master kit (Roche, cat. # 04710444001) with 50 ng template DNA in 20 µl total volume, following manufacturer's instructions. The recommended length of the elongation step is 1 minute for every 1 kb of DNA to be amplified (up to 3 minutes); because the *SIRT3-PSMD13* intergenic promoter sequence is slightly less than 1 kb, we used a 1 minute elongation step.

Verify amplification. Check for successful amplification by running a small amount of PCR product (2 µl of the reaction, plus 2 µl of DNA loading dye, New England Biolabs, cat. # B7021S) on a 2% agarose gel with SYBR Safe DNA Gel Stain (Life Technologies, cat. #

S33102) incorporated into the gel at a 1:10,000 dilution. Include control lanes (e.g. 5 µl of 100bp DNA ladder alongside 5 µl of 1kb DNA ladder, New England Biolabs, cat. #s N3231S and N3232S) for size comparison. Bands may be visualized by exciting the gel with blue or ultraviolet light (if using UV light, use proper shielding to limit personal UV exposure). If the PCR bands are clean and the expected size, proceed to cloning the promoter fragment into the vector.

Troubleshoot. If the PCR results are not clean, try one or more troubleshooting strategies. To optimize the reaction, use annealing temperatures 5°C warmer or cooler than recommended, or design entirely new primers. To control for template quality, include reactions with a pair of primers known to amplify well. If these steps do not lead to improved PCR results, then it may help to use as template a bacterial artificial chromosome (BAC) with the segment of the genome that includes the promoter of interest. BACs generally contain only a few hundred kilobases, greatly increasing the chances that primers will encounter the desired region for amplification rather than a different genomic location of similar sequence.

Though our PCR results with genomic template were usable, we found that our reactions were cleaner when using BACs as a template. We tested two BACs which contain *SIRT3*: CTD-2344F1 (a clone with human DNA from sperm, developed by the California Institute of Technology, available from Life Technologies) and RP11-652O18 (a clone with human male DNA from white blood cells, developed by the Roswell Park Cancer Institute, available from Life Technologies).

Inserting the promoter into the vector

After verifying that a band of the desired length is the major PCR product, insert it into the reporter vector. This process involves digesting both the PCR products and the vector plasmid with a restriction enzyme. The vector is additionally treated with alkaline phosphatase to prevent re-circularization prior to the ligation reaction, which inserts the amplified promoter fragment into the vector.

Purify PCR product. Remove excess primer from the PCR product by prepping the reactions with a PCR purification kit (Qiagen, cat. # 28104), eluting into 40 µl of water in the final step. This typically gives PCR products with concentrations of 100-200 ng/µl, of which only ~1% is residual template.

Digest PCR product with restriction enzyme. Cleave the PCR products with the restriction enzyme corresponding to the recognition sites that were added to the primers designed above. To digest the PCR products and create the insert for our *SIRT3* reporter construct, we used 35.5 µl of each product and 0.5 µl of the restriction enzyme KpnI-HF (New England Biolabs, cat. # R3142S) with 4 µl of NEBuffer 4. We then incubated in a 37°C water bath for 1.5 hours. The 0.5 µl of restriction enzyme was 10 units, which was sufficient to cut 10 µg of DNA in one hour at that temperature.

Similarly cleave the vector. As with the PCR products, cleave the vector. We used the vector pGL3 basic (Promega, cat. # E1751). A similar vector may also be used, provided it is a promoterless vector with a luciferase reporter gene immediately following the recognition site(s)

for the restriction enzyme(s) used in amplifying the promoter fragment. We cleaved with KpnI-HF, again using 10 units of enzyme with approximately 10 µg of DNA in a 37°C water bath for 1.5 hours.

Treat the vector with alkaline phosphatase. Treat the vector with alkaline phosphatase (from calf intestine, New England Biolabs, cat. # M0290S) to ensure that it does not self-ligate and re-circularize after digestion. An efficient way to do this is to prep the post-digest vector DNA using the same purification kit as above (Qiagen, cat. # 28104) and elute with 40 µl of water directly into a microtube containing 5 µl of the 10x buffer, 2 µl of water, and 3 µl of alkaline phosphatase (or approximately 0.5 units per µg of DNA). Then mix and incubate in a 37°C water bath for 1 hour.

Gel extract the PCR products and vector. To prepare pure DNA samples for ligation, run the cleaved fragments (PCR product and vector alike) on a 2% agarose gel with 1:10,000 SYBR Safe. Under blue or UV light, carefully excise the desired DNA bands (if using UV light, work quickly to avoid excessive DNA crosslinking). Extract the DNA from the bands with a gel extraction kit (Qiagen, cat. # 28704), eluting into 40 µl of water. Yields are typically ~20 ng/µl for the PCR products.

Perform ligation. Ligate the fragment into the vector using T4 DNA ligase (New England Biolabs, cat. # M0202S). Each reaction is 20 µl total volume and should contain 1 µl of a 1:10 dilution of the ligase and 2 µl of the 10x buffer. Use 50 ng of vector DNA with a 5-to-1 molar ratio of insert to vector and incubate at 16°C in a thermal cycler for 30 minutes. Include

two control ligation reactions: one with no DNA, and one with vector DNA but no ligase. These will be important for troubleshooting in the next section. (Note that molarity of DNA need not be calculated explicitly. To calculate the ng of insert to use per ng of vector, multiply the desired 5-to-1 molar ratio by the insert/vector length ratio. In our case, the promoter fragment was only 0.13 times the length of the vector, so we used approximately 0.65 ng insert per ng vector DNA.)

Transforming the bacteria with the reporter construct

At this point, the reporter construct may be finished, but usable quantities of it must be produced in order to verify proper incorporation of the insert. This is accomplished by electroporating and growing bacteria, followed by extracting DNA from individual colonies. This section follows standard biological procedures with bacteria.

Electroporate. Transform electrocompetent bacteria with the reporter construct by electroporation. To do this, add 1 µl of ligation product to 60 µl of DH5α *E. coli* bacteria, place into an electroporation cuvette (Bio-Rad, cat. #165-2089), and electroporate with a Gene Pulser (Bio-Rad) or similar instrument. Resuspend the bacteria in 600 µl LB medium (Sigma, cat. # L7275) and incubate for one hour at 37°C. Next, spread 200 µl of each onto a 10 cm dish containing LB-agar (Sigma, cat. # L2897) and 100 µg/mL ampicillin (EMD Millipore, cat. # 171254) and at grow overnight at 37°C. Include control plates which contain bacteria treated with the no-DNA and the no-ligase control reactions from the previous step.

Pick and grow colonies. The next day, pick colonies from the plates to seed mini (~7 mL) LB-ampicillin cultures (final concentration of ampicillin 100 µg/mL, as in the agar plates).

The control plate with no DNA should not grow colonies unless the ampicillin selection is faulty, and the control with no ligase should not grow more than a few colonies unless the vector was able to re-circularize itself efficiently, which would indicate a problem with alkaline phosphatase treatment. After seeding the cultures, grow them overnight (with shaking) at 37°C.

Extract DNA. After growing overnight, set aside ~500 µl of each culture at 4°C for later use. Prep the rest using a Wizard Plus SV Miniprep DNA Purification kit (Promega, cat. # A1460). Eluting each sample into 50 µl of water typically gives a yield of about 5 µg DNA, which is sufficient to test for incorporation of the insert into the clone.

Verify incorporation of insert by restriction digest. First, test for incorporation of the insert by cleaving 1 µg of each clone with restriction enzyme, following manufacturer's instructions as above. Run on a 2% agarose gel (with SYBR Safe, adding loading dye to the DNA and running ladder lanes as above) and visualize. If the insert has been incorporated, the lane will have one band for the insert and one band for the vector. If the insert is not present in the clone, the vector will be the only visible band.

Verify proper insert sequence and orientation by sequencing. For the clones which contain an insert, verify proper sequence and proper insert orientation by sequencing. The forward and reverse cloning primers may be used as sequencing primers; additional internal primers may also be designed to obtain better read coverage of the entire insert. Because the construct will be used as template, primers can be designed with tools such as Primer3

(http://bioinfo.ut.ee/primer3/) without worrying about potential homology to other locations in the genome.

We designed and used multiple internal primers to verify the sequence of our *SIRT3* constructs:

5'-GTGGGCGCCTGTGGTCGAAC-3' (starts at position -441)

5'-TCACCGCCATCCGGGTTGAA-3' (starts at position -277)

5'-AGGTTTGACCTCCGGGGCGA-3' (starts at position -221)

Our sequencing runs were performed by the Dana-Farber / Harvard Cancer Center DNA Sequencing Facility and required 1 µg of template per reaction.

Grow larger amounts of correct construct(s). After identifying which constructs contain the correct insert in the desired orientation, take 50 µl of the saved aliquot from these samples and seed larger (~50 mL) LB-ampicillin cultures. Grow them overnight (with shaking) at 37°C, then prep the DNA from each. We used Plasmid Plus Midi Kits (Qiagen, cat. # 12945) because the vacuum manifold allowed for quick sample preparation (although it was necessary to clear the bacterial lysate by centrifugation prior to the syringe filtering step in order to prevent the DNA-binding column from becoming overloaded with debris). We then eluted into 200 µl of elution buffer. Yields were on the order of 100 µg DNA.

Mutagenesis

To disrupt specific sequence elements by introducing site-specific mutations into the promoter construct, use the QuikChange II Site-Directed Mutagenesis Kit (Agilent, cat. # 200523). This kit uses mutagenized primers to amplify a new version of the construct in a PCR

reaction followed by cleaving methylated template DNA with the restriction enzyme DpnI, leaving behind only the newly synthesized mutagenized strands which can then be used to transform bacteria.

Design primers. As with the original construct design, primer design is important. This depends on identifying the specific sequence element to alter and deciding upon the specific mutation(s) to introduce. Once these decisions are made, use the Agilent mutagenesis primer design tool (http://www.genomics.agilent.com/primerDesignProgram.jsp) to design primer pairs which introduce the desired mutations while adhering to the parameters of the kit.

The *SIRT3* promoter contains a binding site for the transcription factor estrogen-related receptor α (ERRα), and this site plays a role in mediating induction of SIRT3 expression by the transcription factor peroxisome proliferator-activated receptor gamma coactivator 1-α (PGC-1α) (Kong et al., 2010). We created a version of our plasmid with an abrogated ERRα element by mutating the native binding site (TGCCATTG) to TGTAATTG (as Kong et al. did with murine *SIRT3*). We used the following mutagenic primers (with the binding site underlined):

Forward ERRα mutagenic primer: 5'-ccgcgcacttggctgtgtaattgaggcgttaaagag-3'

Reverse ERRα mutagenic primer: 5'-ctctttaacgcctcaattacacagccaagtgcgcgg-3'

Amplify mutagenized construct. Create a mutagenized construct by using the mutagenic primers in a PCR reaction. The manufacturer's instructions can largely be followed, though we slightly modified the PCR protocol to better handle a large amplification product. In our mutagenesis reactions, we used a 7-minute elongation step and repeated the denaturation-annealing-elongation cycle 18 times. We then added 1 µl of DpnI restriction enzyme directly to

each amplification reaction and incubated at 37°C for 1 hour to degrade the original template, and we subsequently checked for presence of amplified plasmid by running 5 µl of each reaction (mixed with 5 µl of DNA sample buffer) on a 2% agarose gel (with SYBR Safe). We ran an equal volume of a 1:50 template dilution to use as comparison.

Transform bacteria. To introduce the mutagenized vector into bacteria, we found that electroporation of DH5α electrocompetent cells worked more efficiently than the heat shock system described in the manufacturer's protocol. We electroporated and then grew these bacteria in the same manner as described above for cloning the construct. We also verified introduction of the correct mutation by sequencing. Note that the internal sequencing primers designed above are especially important when high-quality sequences are needed to examine a few specific base pairs.

Assaying *SIRT3* promoter activity with the construct

Assay protocol

The completed constructs may be used to assay promoter activity when transfected into cells growing in an opaque tissue culture plate. The assay involves transfecting the cells with the construct along with a second, constitutively expressed plasmid (to control for transfection efficiency), applying one or more treatments to the cells, waiting 24-48 hours, and measuring luciferase activity after addition of a substrate for the luciferase reporter. The resulting data indicate which treatments stimulate activity from the promoter fragment cloned into the reporter construct.

Seed cells. Grow cells on an opaque 96-well plate (Corning, cat. # 3917). Seeding densities will vary by cell line; for 293T cells, use 10,000 cells per well. It may be helpful to simultaneously grow cells on a clear plate (Corning, cat. # 3595) at an identical density to allow for visual inspection of population confluence and health through a normal light microscope.

Transfect cells. Prepare the transfection mixture by adding 0.2-0.4 µl per well of FuGene 6 transfection reagent (Promega, cat. # E2691) to 4 µl per well of serum-free medium, then adding 0.03-0.06 µg per well of construct and 0.01-0.03 µg per well of a pRL renilla control vector (used to control for cell number and transfection efficiency, Promega, cat. # E2261). The exact amounts of these two plasmids should be empirically determined for each assay in order to obtain optimal luciferase and renilla signals. (Note that the constitutive promoter of the renilla vector is quite strong and, in some cases, a larger construct/renilla ratio may be necessary than the typical values given here.) Mix according to the manufacturer's instructions, then add to cells.

Add chemicals or apply other treatment. Depending on the hypothesis being tested, add chemicals, transfect additional plasmids, or apply another treatment to the cells.

Measure luciferase activity. 24 to 48 hours after the initial transfection, assay luciferase activity using a Dual-Luciferase Reporter Assay kit (Promega, cat. # E1910). Begin by aspirating the medium from the cells, then add 25 µl per well of the included passive lysis buffer (dilute the 5x stock to a 1x working solution with distilled water). Place the cells on a shaker with gentle movement for at least 20 minutes to ensure lysis.

Following lysis, add 100 µl of the provided luciferase assay reagent to each well. Use a multichannel pipettor to do this quickly, as the luminescence signal degrades with time. Measure the luminescence of each well in a luminescence-equipped plate reader such as a Cary Varian Eclipse fluorescence spectrophotometer with a gate time of 200 ms and an emission slit of 2.5 nm around a target emission wavelength of 560 nm (the first two of these parameters may be adjusted to optimize signal capture). Next, add 100 µl per well of the provided "Stop & Glo" reagent to quench the luciferase reaction and begin the renilla luminescence. Measure the luminescence of each well again, changing the target emission wavelength from 560 nm to 500 nm.

For data analysis, divide the first (luciferase) luminescence reading by the second (renilla) luminescence reading. This provides a signal value for each well that is normalized by transfection efficiency. Average by condition to obtain a readout of the relative activity of the luciferase promoter construct under different treatments.

Example application: Importance of ERRα for SIRT3 promoter activity in 293T cells

We used the reversible *SIRT3-PSMD13* promoter construct to verify the effect of ERRα binding on *SIRT3* promoter activity in 293T cells. To do this, we generated both forward and reverse *SIRT3* promoter reporter constructs, making versions for each with either wildtype sequence or a mutated ERRα binding site, as described above. We also used Gateway cloning techniques to generate an HA-tagged ERRα overexpression plasmid (starting from the HsCD00079872 ORF in a pDONR221 entry clone from the PlasmID database of the Dana-Farber / Harvard Cancer Center DNA Resource Core).

We then seeded an opaque 96-well plate with 10,000 293T cells per well. Cells were grown in Dulbecco's Modified Eagle Medium (DMEM) (Life Technologies, cat. # 11995) with 10% fetal bovine serum (FBS) (HyClone, cat. # SH30910.03) and 1% penicillin-streptomycin supplement (Life Technologies, cat. #15140). The next day, we mixed and applied to each well 4 µl DMEM, 0.2 µl FuGene6 transfection reagent, 0.03 µg renilla plasmid, and 0.06 µg of a reporter plasmid construct. We additionally combined and added 4 µl DMEM, 0.2 µl FuGene6, and 0.02 µg ERRα-HA expression plasmid or vector control (as well as 0.02 µg PCDNA3.1 empty vector for comparison to wells overexpressing a PGC-1α construct - data not shown). Forty-eight hours later, we assayed luciferase activity as described above and saw that ERRα overexpression increased promoter activity from the wildtype sequence promoter construct in the *SIRT3* direction (Figure 2.2A), but not from the mutated promoter in the *SIRT3* direction (Figure 2.2A) or from either sequence variant in the *PSMD13* direction (Figure 2.2B). This verified that the previously reported activation of the *SIRT3* promoter by ERRα was exhibited by our system.

Example application: Effect of rapamycin on SIRT3 promoter activity in 293T cells

Because SIRT3 expression is known to be upregulated by calorie restriction, we also tested the responsiveness of our longer *SIRT3* promoter construct to rapamycin (Sigma, cat. # R0395), a small molecule that inhibits the nutrient-sensing TOR pathway and has been used in certain contexts as a calorie restriction mimetic (Harrison et al., 2009; Zoncu et al., 2011). To do this, we seeded 293T cells into 24 wells of a 96-well plate at 10,000 cells per well. The next day, we mixed and applied to each well 4 µl DMEM, 0.4 µl FuGene6 transfection reagent, 0.03 µg renilla plasmid, and 0.06 µg of a reporter plasmid construct or promoterless vector control. The following day, we treated with DMSO or one of two concentrations of rapamycin, to final

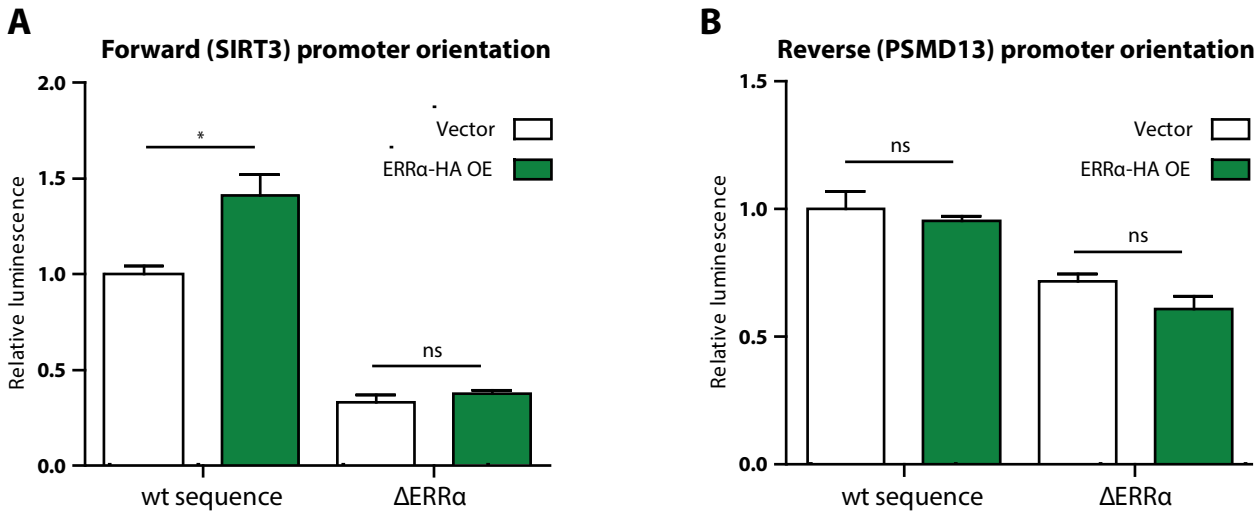

Figure 2.2. Luciferase reporter results after transfection of wildtype sequence or mutated estrogen-related receptor α (ERRα) reporter constructs plus vector (empty bars) or ERRα-HA overexpression constructs (filled bars) in human 293T cells. Promoters were oriented in the A) forward or B) reverse orientation relative to *SIRT3*. N = 4 wells per condition. * indicates $p < 0.05$. Two-tailed student's t test was used for p values.

concentrations of 0, 0.1, or 100 nm of rapamycin in 0.01% DMSO. Forty-eight hours later we assayed luciferase activity as described above and observed that increasing rapamycin dosage led to increased activity from the *SIRT3* promoter construct (Figure 2.3).

Verifying reporter results with complementary methods

Multiple molecular biology methods may be used to verify the results of the luciferase reporter system. Quantitative polymerase chain reaction (qPCR) is conceptually similar, as it assays promoter activity by measuring the amount of RNA transcript detected by a pair of primers specific to the gene of interest. A standard western blot can also be used to estimate sirtuin expression by measuring protein level.

Quantitative PCR

Quantitative PCR protocol. Begin by extracting RNA with an RNEasy Mini kit (Qiagen, cat. #74104). One well of a six-well plate (or 10 mg of tissue) is sufficient for each biological replicate. Reverse transcribe RNA into cDNA with an iScript cDNA synthesis kit (Bio-Rad, cat. # 170-8891), using 1 µg of RNA as starting material.

Quantitative PCR may be performed using 2x LightCycler 480 SYBR Green I Master mix (Roche, cat. #04707516001) on a LightCycler 480 thermal cycler (Roche). Halve the 20 µl reaction volume called for by the manufacturer's protocol and use 5 µl of master mix, 0.5 µl each of the forward and reverse primers (at 10 µM stock concentration), and 4 µl of a 1:50 working cDNA dilution for each qPCR reaction. Run two technical replicates for each biological replicate. In addition, prepare a set of six standards, beginning with a 1:4 dilution of pooled cDNA and serially diluting 1:4 five times to create a basis for software estimation of the relative

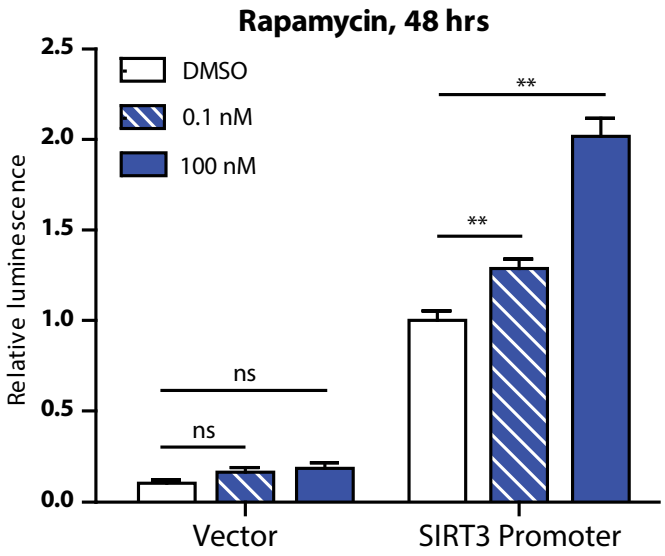

Figure 2.3. Luciferase reporter results after transfection of the longer-form *SIRT3* reporter construct or vector control plus DMSO (empty bars), 0.1 nM rapamycin (striped bars), or 100 nM rapapmycin (filled bars). N = 4 wells per condition. ** indicates $p < 0.01$. Two-tailed student's t test was used for p values.

concentrations of target RNA in each sample. Run each plate through 45 amplification cycles, following manufacturer's instructions, and end with a melting curve to verify homogeneity of the amplified DNA.

Before concentration estimates for the gene of interest in each sample can be compared to one another, they must be normalized by the levels of a reference gene within the same sample. We found that β2 microglobulin (B2M), ribosomal protein S16 (RPS16), and peptidylprolyl isomerase A (PPIA) were generally stable in expression across different treatments in human 293T cells and made good reference genes. In cases where detection of small perturbations in target gene level was important, we ran all three and used the geometric mean of their expression as reference.

Verification of ERRα results by qPCR. To assay SIRT3 expression in 293T cells following overexpression of the ERRα-HA construct described above, we seeded 100,000 cells per well in a six-well plate. The next day, we treated each well with a mix of 8 µl FuGene6 and 0.5 µg ERRα-HA or vector. Two days later, we extracted RNA, synthesized cDNA, and analyzed SIRT3 expression by qPCR. Consistent with our luciferase data, we saw that SIRT3 mRNA was upregulated with ERRα overexpression (Figure 2.4A, Figure 2.4B). For this data, n = 3 and B2M was used as the reference gene.

We also created an ERRα knockdown 293T cell line using the shRNA construct TRCN0000330191 from the RNAi consortium (via the Dana-Farber / Harvard Cancer Center RNAi Core facility). We conducted qPCR on these cells and saw the complementary result, that ERRα knockdown led to lower SIRT3 transcript levels (Figure 2.4C, Figure 2.4D). For this data,

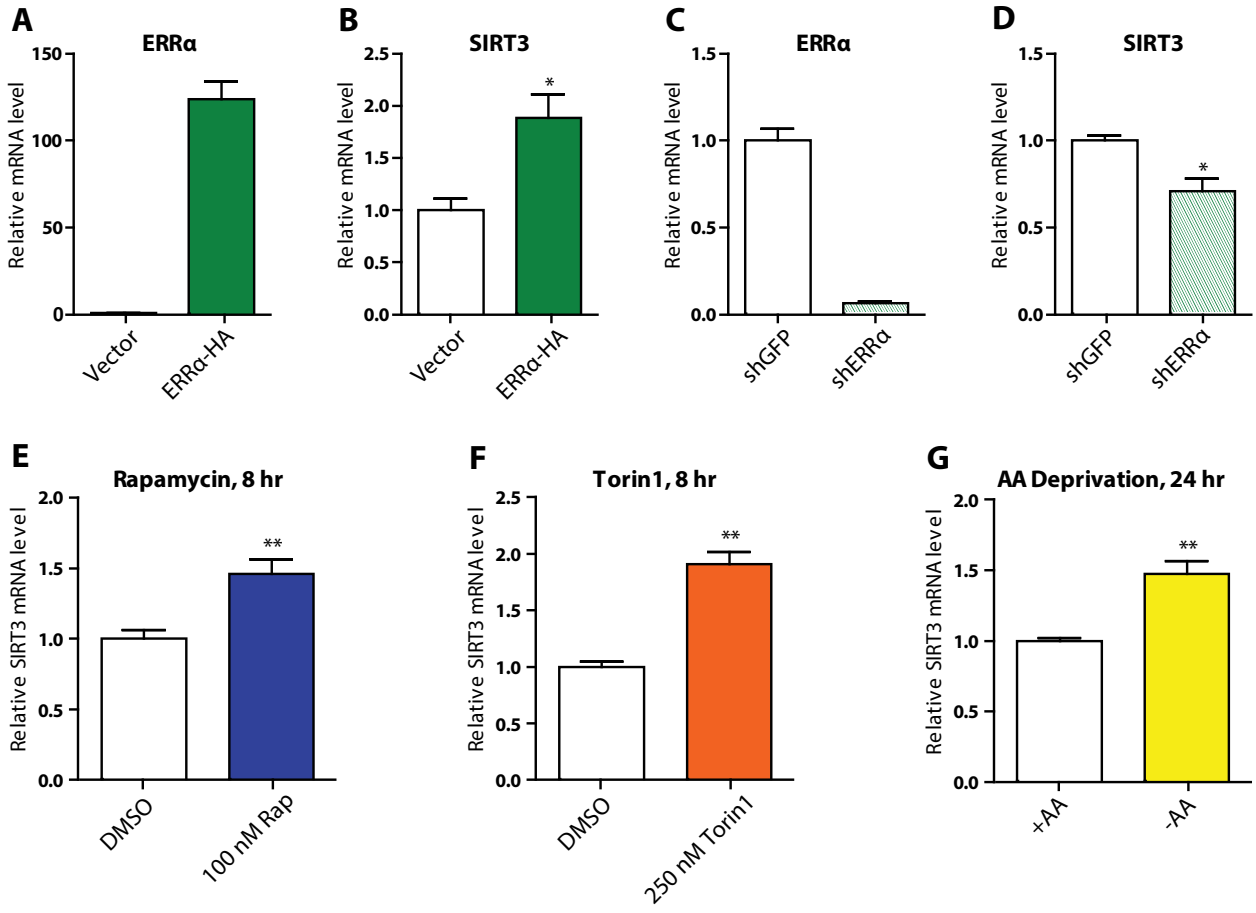

Figure 2.4. Quantitative PCR results. A) Verification of ERRα overexpression in 293T cells and B) effect on SIRT3 expression following transfection with vector control (empty bar) or ERRα-HA (filled bar). C) Verification of ERRα knockdown in 293T cells and D) effect on SIRT3 expression with control knockdown (empty bar) compared to ERRα knockdown (striped bar). E) SIRT3 expression following 8-hour treatment with DMSO control (empty bar) or 100 nM rapamycin (filled bar). F) SIRT3 expression following 8-hour treatment with DMSO control (empty bar) or 250 nM Torin1 (filled bar). G) SIRT3 expression following 24-hour treatment with control culture medium (empty bar) or culture medium lacking amino acids (filled bar). * indicates $p < 0.05$; ** indicates $p < 0.01$. Two-tailed student's t test was used for p values.

n = 3 and B2M was used as the reference gene. Primer sequences used are given in Table 2.2; the ERRα pair is from Schreiber et al. (2003).

Verification of rapamycin results by qPCR. To verify the rapamycin luciferase results, we inhibited the TOR pathway in three different ways. We inhibited by treatment with rapamycin for 8 hours at 100 nM (Figure 2.4E); by treatment with the small molecule Torin1, which inhibits the catalytic site of mTOR (Thoreen et al., 2009), for 8 hours at 250 nM (Figure 2.4F); and by 24-hour amino acid deprivation (Figure 2.4G). In all three cases, inhibition of the TOR pathway led to greater expression of SIRT3, validating our luciferase results. In this case, n = 4, and we used the geometric mean of B2M, RPS16, and PPIA expression as a reference. Primer sequences used are given in Table 2.2.

Western blot

Additional verification may be performed by western blot, which looks at protein rather than mRNA levels. We used this to further verify the upregulation of SIRT3 expression by rapamycin treatment because it represented a novel finding.

Western blot protocol. Briefly, obtain whole cell lysate by applying 1% NP40 buffer (1% NP40 detergent with 150 mM NaCl, 50 mM Tris [pH 8], 1 mM dithiothreitol, plus 1x Roche cOmplete Mini protease inhibitor tablets [cat. # 11836170001] and 1% each of Sigma phosphatase inhibitor cocktail #s 2 [cat. # P5726] and 3 [cat. # P0044]) to a pellet of collected cells. Use 150 µl of lysis buffer for mostly confluent cells in a 35 mm well, or 300 µl for cells in a 10 cm dish (providing a more concentrated lysate). Separate the proteins by running the lysate

Table 2.2. Sequences of qPCR primers used in this study. All sequences are for human genes.

Gene	Direction	Sequence
SIRT3	Forward	5'-AGCCCTCTTCATGTTCCGAAGTGT-3'
	Reverse	5'-TCATGTCAACACCTGCAGTCCCTT-3'
ERRα	Forward	5'-AAGACAGCAGCCCCAGTGAA-3'
	Reverse	5'-ACACCCAGCACCAGCACCT-3'
B2M	Forward	5'-AGATGAGTATGCCTGCCGTGTGAA-3'
	Reverse	5'-TGCTGCTTACATGTCTCGATCCCA-3'
PPIA	Forward	5'-AGCATACAGGTCCTGGCATCTTGT-3'
	Reverse	5'-CAAAGACCACATGCTTGCCATCCA-3'
RPS16	Forward	5'-AGATCAAAGACATCCTCATCCAG-3'
	Reverse	5'-TGAGTTTTGAGTCACGATGGG-3'

on a polyacrylamide gel (Bio-Rad, cat. # 345-0043), transfer to nitrocellulose membrane (Bio-Rad, cat. # 162-0112), and blot for the protein of interest using standard molecular biology techniques.

Verification of rapamycin results by western blot. For detection of human SIRT3, we used Cell Signaling C73E3 (cat. # 2627) as the primary antibody at a dilution of 1:1000 in 3% BSA with 0.02% sodium azide (note that this antibody detects human but not mouse SIRT3, while Cell Signaling D22A3 [cat. # 5490] detects both). We observed that our western blot reproduced at the protein level the induction of SIRT3 expression that we saw at the RNA level. In 293T cells grown in DMEM with 10% FBS and 1% penicillin-streptomycin, inhibition of the TOR pathway by 100 nM rapamycin for 48 hours (Figure 2.5A) or 250 nM Torin1 for 48 hours (Figure 2.5B) led to an increase in SIRT3 expression, as did inhibition of the mTOR target p70-S6 kinase (S6K) via the S6K inhibitor PF-4708671 (Pearce et al., 2010) at 10 μM for 24 hours (Figure 2.5C). An 8-hour time course of 100 nM rapamycin treatment displayed gradual SIRT3 induction (Figure 2.5D). In these experiments we used phosphorylation of S6K (Cell Signaling, cat. # 9234, 1:1000) as a marker of mTOR pathway activation (except in the case of direct S6K inhibition, where we used phosphorylation of ribosomal protein S6 [Cell Signaling, cat. # 4856, 1:1000]). HSP60 (Abcam, cat. # ab3080, 1:5000) was used as a control for total amount of mitochondria, and the loading controls were total S6K (Cell Signaling, cat. # 9202, 1:1000) or total S6 (Cell Signaling, cat. # 2317, 1:1000) and α-tubulin (Santa Cruz Biotechnology, cat. # sc-8035, 1:5000).

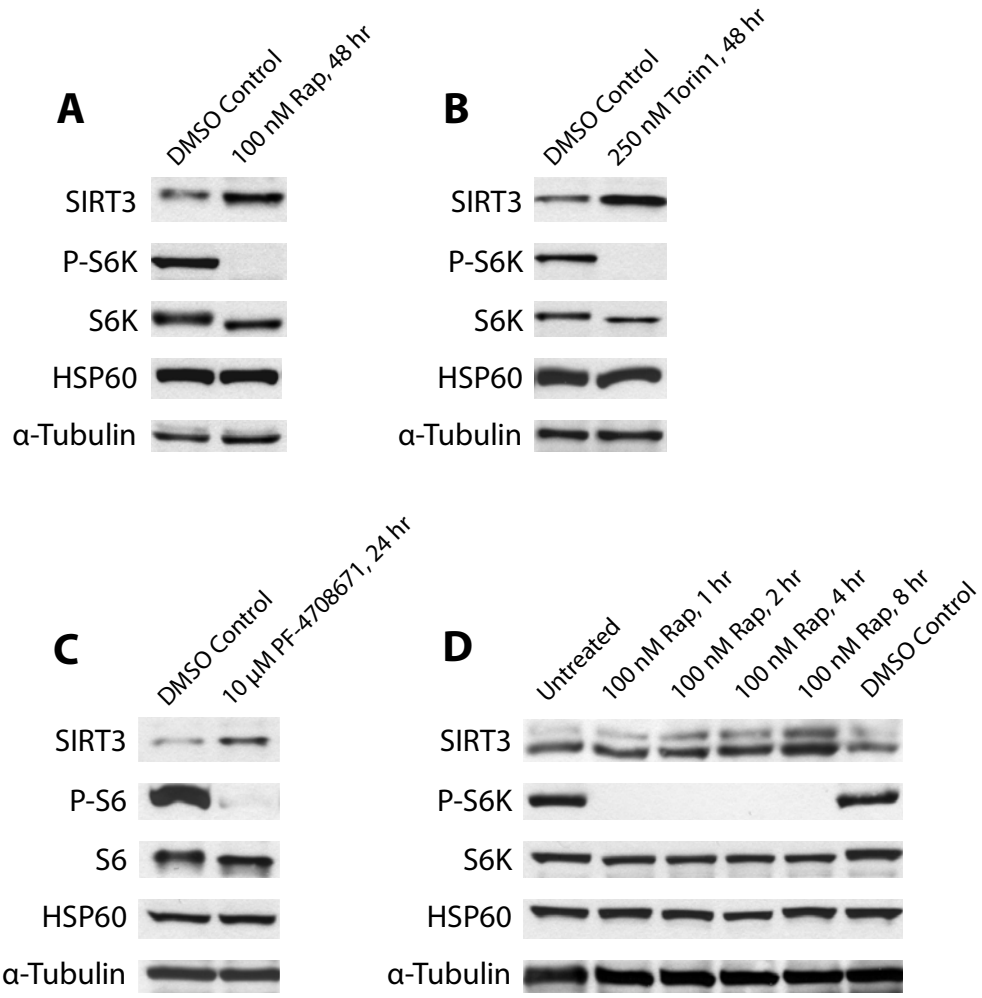

Figure 2.5. Western blot results. SIRT3 protein level after treatment with A) rapamycin, B) Torin1, or C) PF-4708671, an inhibitor of p70-S6 kinase (S6K); D) rapamycin-induced increase in SIRT3 protein level over 8 hours.

Summary

In this chapter we have detailed the development of a luciferase-based plasmid reporter system to measure activation of the human *SIRT3* promoter, we have validated its activity, and we have shown that SIRT3 expression is upregulated by inhibition of the nutrient-sensing TOR pathway in 293T cells. Not only can this system be used with cell lines in culture, as described above, but it could also see future utilization as a diagnostic tool for use with primary tumor cell lines to assay the level of *SIRT3* activation. Furthermore, future studies using such a system may identify small molecule compounds and proteins that activate or inhibit SIRT3 expression. Because SIRT3 exerts a range of metabolic effects on tumors, including fighting against the Warburg effect, the knowledge gained by implementations of this system could have important diagnostic, prognostic, and therapeutic consequences.

Acknowledgments

F. K. S. was supported by NIH Training Grant No. T32 DK007260. M. C. H. was supported by an American Cancer Society New Scholar Award and the Glenn Foundation for Medical Research.

References

Bell EL, Emerling BM, Ricoult SJ, Guarente L (2011) SirT3 suppresses hypoxia inducible factor 1alpha and tumor growth by inhibiting mitochondrial ROS production. *Oncogene* **30**, 2986-2996.

Bellizzi D, Dato S, Cavalcante P, Covello G, Di Cianni F, Passarino G, Rose G, De Benedictis G (2007) Characterization of a bidirectional promoter shared between two human genes related to aging: SIRT3 and PSMD13. *Genomics* **89**, 143-150.

Chakrabarti P, English T, Karki S, Qiang L, Tao R, Kim J, Luo Z, Farmer SR, Kandror KV (2011) SIRT1 controls lipolysis in adipocytes via FOXO1-mediated expression of ATGL. *J. Lipid Res.* **52**, 1693-1701.

Cohen HY, Miller C, Bitterman KJ, Wall NR, Hekking B, Kessler B, Howitz KT, Gorospe M, de Cabo R, Sinclair DA (2004) Calorie restriction promotes mammalian cell survival by inducing the SIRT1 deacetylase. *Science* **305**, 390-392.

Finley LW, Carracedo A, Lee J, Souza A, Egia A, Zhang J, Teruya-Feldstein J, Moreira PI, Cardoso SM, Clish CB, Pandolfi PP, Haigis MC (2011) SIRT3 opposes reprogramming of cancer cell metabolism through HIF1alpha destabilization. *Cancer Cell* **19**, 416-428.

Hallows WC, Yu W, Smith BC, Devries MK, Ellinger JJ, Someya S, Shortreed MR, Prolla T, Markley JL, Smith LM, Zhao S, Guan KL, Denu JM (2011) Sirt3 promotes the urea cycle and fatty acid oxidation during dietary restriction. *Mol. Cell* **41**, 139-149.

Harrison DE, Strong R, Sharp ZD, Nelson JF, Astle CM, Flurkey K, Nadon NL, Wilkinson JE, Frenkel K, Carter CS, Pahor M, Javors MA, Fernandez E, Miller RA (2009) Rapamycin fed late in life extends lifespan in genetically heterogeneous mice. *Nature* **460**, 392-395.

Hirschey MD, Shimazu T, Goetzman E, Jing E, Schwer B, Lombard DB, Grueter CA, Harris C, Biddinger S, Ilkayeva OR, Stevens RD, Li Y, Saha AK, Ruderman NB, Bain JR, Newgard CB, Farese RV Jr, Alt FW, Kahn CR, Verdin E (2010) SIRT3 regulates mitochondrial fatty-acid oxidation by reversible enzyme deacetylation. *Nature* **464**, 121-125.

Houtkooper RH, Pirinen E, Auwerx J (2012) Sirtuins as regulators of metabolism and healthspan. *Nat. Rev. Mol. Cell Biol*. **13**, 225-238.

Jeong SM, Xiao C, Finley LW, Lahusen T, Souza AL, Pierce K, Li YH, Wang X, Laurent G, German NJ, Xu X, Li C, Wang RH, Lee J, Csibi A, Cerione R, Blenis J, Clish CB, Kimmelman A, Deng CX, Haigis MC (2013) SIRT4 has tumor-suppressive activity and regulates the cellular metabolic response to DNA damage by inhibiting mitochondrial glutamine metabolism. *Cancer Cell* **23**, 450-463.

Kim HS, Patel K, Muldoon-Jacobs K, Bisht KS, Aykin-Burns N, Pennington JD, van der Meer R, Nguyen P, Savage J, Owens KM, Vassilopoulos A, Ozden O, Park SH, Singh KK, Abdulkadir SA, Spitz DR, Deng CX, Gius D (2010) SIRT3 is a mitochondria-localized tumor suppressor

required for maintenance of mitochondrial integrity and metabolism during stress. *Cancer Cell* **17**, 41-52.

Kong X, Wang R, Xue Y, Liu X, Zhang H, Chen Y, Fang F, Chang Y (2010) Sirtuin 3, a new target of PGC-1alpha, plays an important role in the suppression of ROS and mitochondrial biogenesis. *PLoS One* **5**, e11707.

Lin JM, Collins PJ, Trinklein ND, Fu Y, Xi H, Myers RM, Weng Z (2007) Transcription factor binding and modified histones in human bidirectional promoters. *Genome Res*. **17**, 818-827.

Lin SJ, Defossez PA, Guarente, L (2000) Requirement of NAD and SIR2 for life-span extension by calorie restriction in Saccharomyces cerevisiae. *Science* **289**, 2126-2128.

Pearce LR, Alton GR, Richter DT, Kath JC, Lingardo L, Chapman J, Hwang C, Alessi DR (2010) Characterization of PF-4708671, a novel and highly specific inhibitor of p70 ribosomal S6 kinase (S6K1). *Biochem. J*. **431**, 245-255.

Sebastián C, Zwaans BM, Silberman DM, Gymrek M, Goren A, Zhong L, Ram O, Truelove J, Guimaraes AR, Toiber D, Cosentino C, Greenson JK, MacDonald AI, McGlynn L, Maxwell F, Edwards J, Giacosa S, Guccione E, Weissleder R, Bernstein BE, Regev A, Shiels PG, Lombard DB, Mostoslavsky R (2012) The histone deacetylase SIRT6 is a tumor suppressor that controls cancer metabolism. *Cell* **151**, 1185-99.

Schreiber SN, Knutti D, Brogli K, Uhlmann T, Kralli A (2003) The transcriptional coactivator PGC-1 regulates the expression and activity of the orphan nuclear receptor estrogen-related receptor alpha (ERRalpha). *J. Biol. Chem.* **278**, 9013-9018.

Tao R, Coleman MC, Pennington JD, Ozden O, Park SH, Jiang H, Kim HS, Flynn CR, Hill S, Hayes McDonald W, Olivier AK, Spitz DR, Gius D (2010) Sirt3-mediated deacetylation of evolutionarily conserved lysine 122 regulates MnSOD activity in response to stress. *Mol. Cell* **40**, 893-904.

Thoreen CC, Kang SA, Chang JW, Liu Q, Zhang J, Gao Y, Reichling LJ, Sim T, Sabatini DM, Gray NS (2009) An ATP-competitive mammalian target of rapamycin inhibitor reveals rapamycin-resistant functions of mTORC1. *J. Biol. Chem*. **284**, 8023-8032.

Xi H, Yu Y, Fu Y, Foley J, Halees A, Weng Z (2007) Analysis of overrepresented motifs in human core promoters reveals dual regulatory roles of YY1. *Genome Res*. **17**, 798-806.

Zoncu R, Efeyan A, Sabatini DM (2011) mTOR: from growth signal integration to cancer, diabetes and ageing. *Nat. Rev. Mol. Cell Biol*. **12**, 21-35.

CHAPTER III

Nuclear respiratory factor 2 induces SIRT3 expression

F. Kyle Satterstrom[1,2], William R. Swindell[3,5], Gaëlle Laurent[2], Martha L. Bulyk[3,4], and Marcia C. Haigis[2]

[1] Harvard School of Engineering and Applied Sciences, Cambridge, Massachusetts 02138

[2] Department of Cell Biology, Harvard Medical School, Boston, Massachusetts 02115

[3] Division of Genetics, Department of Medicine, Brigham and Women's Hospital and Harvard Medical School, Boston, Massachusetts 02115

[4] Department of Pathology, Brigham and Women's Hospital and Harvard Medical School, Boston, Massachusetts 02115

[5] Current address: Department of Dermatology, University of Michigan, Ann Arbor, Michigan 02005

This work is a complete manuscript recently submitted for potential publication. Kyle Satterstrom performed the bioinformatic analysis and the experiments described in this chapter, with bioinformatic advice from William Swindell and Martha Bulyk, and experimental assistance from Gaëlle Laurent (chromatin immunoprecipitation).

Abstract

The mitochondrial deacetylase SIRT3 regulates several important metabolic processes. SIRT3 is transcriptionally upregulated in multiple tissues during nutrient stresses such as calorie restriction and fasting, but the molecular mechanism of this induction is unclear. We conducted a bioinformatic study to identify transcription factor(s) involved in SIRT3 induction. Our analysis identified an enrichment of binding sites for nuclear respiratory factor 2 (NRF-2), a transcription factor known to play a role in the expression of mitochondrial genes, in the DNA sequences of *SIRT3* and genes with closely correlated expression patterns. *In vitro*, knockdown or overexpression of NRF-2 modulated SIRT3 levels, and the NRF-2α subunit directly bound to the SIRT3 promoter. Our results suggest that NRF-2 is a transcriptional regulator of SIRT3 expression and may shed light on how SIRT3 is upregulated during nutrient stress.

Introduction

The NAD^+-dependent mitochondrial deacetylase sirtuin-3 (SIRT3) is central to the regulation of cellular metabolism, including the adaptation to nutrient stresses such as fasting and calorie restriction (CR) (Lombard et al., 2007; Hebert et al., 2013). SIRT3 protein levels are upregulated by fasting and calorie restriction in liver, where it stimulates fatty acid oxidation (Hirschey et al., 2010) and activates key nodes of ketone body production (Shimazu et al., 2010) and the urea cycle (Hallows et al., 2011). SIRT3 mRNA levels are also upregulated by calorie restriction in brown adipose tissue, where SIRT3 activates mitochondrial thermogenesis (Shi et al., 2005). In addition, SIRT3 mediates some of the beneficial effects of CR, such as the activation of mitochondrial superoxide dismutase to reduce oxidative stress (Qiu et al., 2010; Tao et al., 2010) and the prevention of age-related hearing loss in mice (Someya et al., 2010).

Conversely, livers of mice fed a chronic high-fat diet exhibit reduced SIRT3 mRNA and protein levels (Hirschey et al., 2011), indicating that SIRT3 expression is dynamically regulated by nutrient intake.

Surprisingly, little is known about the molecular control of SIRT3 expression. In murine adipocytes and hepatocytes, the transcription factor estrogen-related receptor α (ERRα) has been shown to induce SIRT3 expression in conjunction with peroxisome proliferator-activated receptor γ coactivator 1-α (PGC-1α) (Kong et al., 2010; Giralt et al., 2011). In this study, we employed a bioinformatic approach to identify additional transcription factors which regulate SIRT3 expression. We searched publicly available microarray data to identify datasets with an induction of SIRT3 by either CR or fasting and then computationally identified transcription factor binding motifs enriched in the regulatory regions of *SIRT3* and co-induced genes. Our bioinformatic analysis and experimental validation in cell culture identified nuclear respiratory factor 2 (NRF-2) as a novel transcriptional regulator of SIRT3 expression.

Results

Bioinformatic analysis

To identify transcription factors involved in SIRT3 induction, we undertook a systematic bioinformatic approach (Figure 3.1A). We first identified datasets in which SIRT3 mRNA expression was increased with CR in neocortex (GSE11291; Barger et al., 2008), cochlea (GSE4786, Someya et al., 2007), and liver (GSE26267, Streeper et al., 2012), and with fasting in kidney (GSE24504, Hakvoort et al., 2011). We conducted gene set enrichment analysis (Table 3.1) to determine that this induction was part of a larger metabolic adaptation. Next, based on the rationale that co-expressed genes may share common transcriptional regulators, we identified

Figure 3.1 (Next page). Bioinformatic identificiation of NRF-2 binding site enrichment in DNA sequences of *SIRT3* and co-expressed genes. A) Overview of bioinfomatic steps analyzing transcription factor binding motif enrichment in the DNA sequences of *SIRT3* and co-expressed genes. B) Top 25 most-SIRT3-correlated genes (by Pearson's r) in the mouse neocortex dataset. C) Enrichment of selected gene ontology terms in top 50 most-SIRT3-correlated genes in neocortex (full results in Supplementary File 3.2). D-F) Heat maps of transcription factor motif enrichment in the (D) 25 most SIRT3-correlated genes, (E) 50 most SIRT3-correlated genes, and (F) 100 most-SIRT3-correlated genes (by expression levels across samples) for the neocortex dataset. All genes = analyzed most-SIRT3-correlated genes from all genes in dataset. Mitochondrial = analyzed most-SIRT3-correlated mitochondrial genes in dataset. Top ten motifs are shown, ordered by motif's maximum AUC score, a measure of enrichment. Red = greater enrichment; white = less enrichment. * indicates $q < 0.05$; ** indicates $q < 0.01$. G) Overlap of significantly enriched transcription factor motifs identified in (D-F), showing results from analyzing the 25 (red circle), 50 (blue circle), and 100 (yellow circle) most-SIRT3-correlated genes for the neocortex dataset.

Figure 3.1 (Continued).

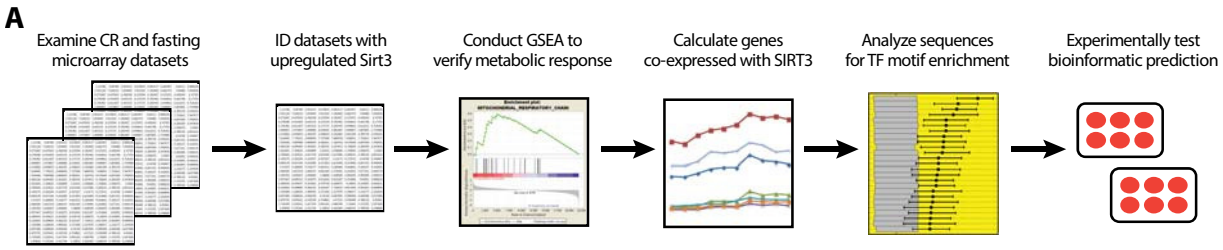

B

Gene	Description	Correlation
SIRT3	NAD-dependent deacetylase involved in regulation of cellular energy metabolism	1.000
NDUFB3	Accessory subunit to complex I of electron transport chain	0.974
TIPIN	Involved in DNA damage response, cell cycle progression	0.971
TMEM141	Multi-pass membrane protein	0.964
EDC4	Plays role in mRNA decapping during mRNA degradation	0.962
SYF2	Potentially involved in splicing of pre-mRNA transcripts	0.960
FAM173A	Single-pass membrane protein	0.957
H2AFZ	Histone H2A variant	0.956
DAPK2	Kinase which plays a role in cell survival, apoptosis, and autophagy	0.955
PRDX5	Reduces hydroperoxides, involved in redox signaling	0.951
TYW5	tRNA hydroxylase, component of wybutosine biosynthesis pathway	0.951
METTL5	Probable methyltransferase	0.949
NAE1	Component of E1 NEDD8-activating enzyme; able to bind β-amyloid precursor	0.949
PNKP	Involved in NHEJ and BER pathways of DNA repair	0.948
NAA20	Catalytic subunit of complex which acetylates N-terminal methionine	0.947
APITD1	DNA-binding component of Fanconi Anemia core complex involved in DNA repair	0.947
FGFR1OP	Required for anchoring microtubules to the centrosome	0.946
SLC35B3	Transports 3' P-adenosine 5' P-sulfate from cytosol to Golgi lumen	0.944
GRHPR	Has glyoxylate/hydroxypyruvate reductase and D-glycerate dehydrogenase activity	0.944
MAGOH	Core component of multiprotein exon junction complex on mRNAs	0.942
PUS10	Catalyzes isomerization of uridine to pseudouridine in structural RNA	0.942
MPPE1	Required for transport of GPI-anchored proteins from ER to Golgi	0.941
HSD11B1	Interconverts cortisone and cortisol	0.940
CHRAC1	Binds DNA for packing into chromatin	0.940
CCZ1	Lysosomal membrane protein	0.940

C

Gene Ontology Term	Corrected P Value
Metabolic Process	2.60E-06
Intracellular	6.19E-05
Catalytic Activity	7.85E-05
Membrane-Bounded Organelle	7.85E-05
Oxidoreductase Activity	4.57E-03
Primary Metabolic Process	1.23E-02
Catabolic Process	1.41E-02
Proteasome Core Complex	1.43E-02
Threonine-Type Endopeptidase Activity	1.43E-02
RNA Processing	1.43E-02
RNA Metabolic Process	1.43E-02
Macromolecule Metabolic Process	1.43E-02
NADH Dehydrogenase Activity	1.43E-02
Spliceosomal Complex	1.81E-02
NADP or NADPH Binding	1.98E-02
NAD or NADH Binding	2.79E-02
N-Acetyltransferase Activity	2.79E-02
Acyltransferase Activity	2.79E-02
Endopeptidase Activity	2.79E-02
Nitrogen Compound Metabolic Process	2.79E-02
Cell Redox Homeostasis	3.19E-02
Nucleic Acid Metabolic Process	3.19E-02
Respiratory Chain	3.20E-02
Cellular Response to Stress	3.57E-02
Cofactor Binding	3.95E-02

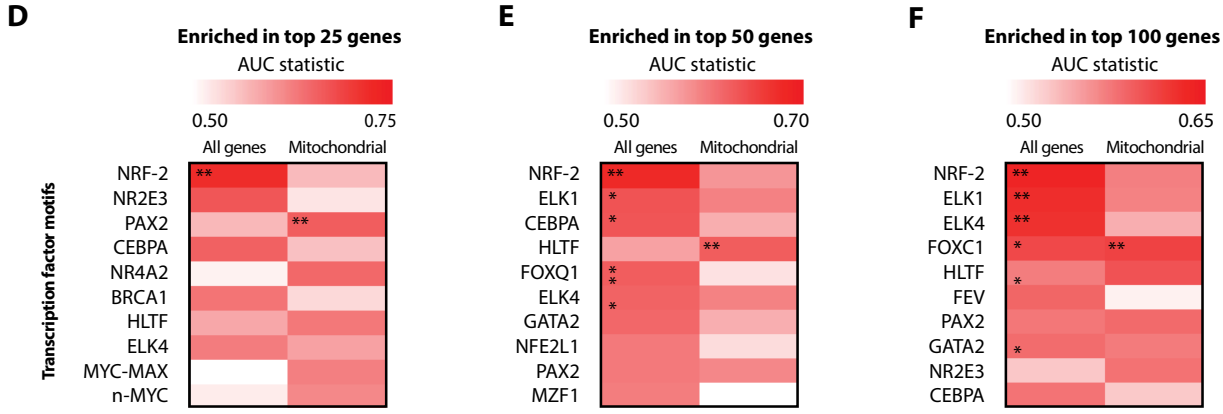

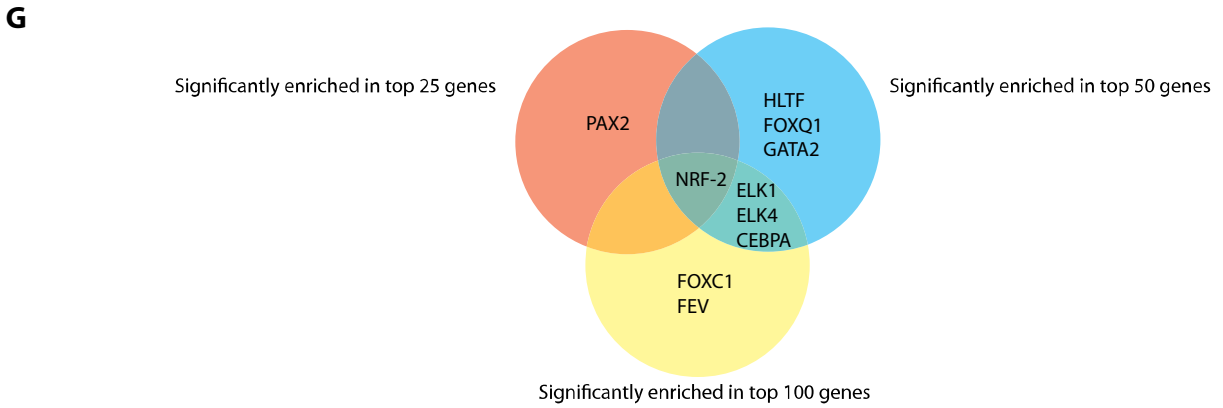

Table 3.1. Gene set enrichment analysis summary for datasets with significant induction of Sirt3 in mouse tissue by calorie restriction or fasting. The false discovery rate (FDR) rankings for the kidney dataset are an average across four time points.

Dataset	# gene sets with FDR < 0.05 and nominal pval < 0.01	Top ten enriched gene sets with CR (by FDR)
Neocortex	9	Replication Fork Structural Constituent of Ribosome Ribonuclease Activity Neuropeptide Hormone Activity Organellar Ribosome Mitochondrial Respiratory Chain Proton Transporting Two Sector ATPase Complex Endoribonuclease Activity Cellular Respiration Endonuclease Activity
Cochlea	72	Ligase Activity Protein Folding Microbody Part mRNA Binding GTPase Activity Peroxisomal Part Structural Constituent of Ribosome Phosphatase Inhibitor Activity Organellar Ribosome Mitochondrial Ribosome
Liver	21	Mitochondrial Membrane Part Mitochondrial Membrane Organelle Inner Membrane Mitochondrial Inner Membrane Mitochondrial Envelope Mitochondrial Part Mitochondrion Structural Constituent of Ribosome Cellular Respiration Envelope
Kidney	12 hrs: 10 24 hrs: 9 48 hrs: 7 72 hrs: 3	Fatty Acid Metabolic Process Fatty Acid Oxidation Monocarboxylic Acid Metabolic Process Cellular Lipid Catabolic Process Solute Sodium Symporter Activity Peroxisomal Part Lipid Catabolic Process Microbody Part Microbody Peroxisome

the genes most closely co-induced with SIRT3 in each dataset (Figure 3.1B, Supplementary File 3.1). Groups of 25, 50, and 100 genes were analyzed, allowing for greater statistical power than an analysis of *SIRT3* alone. Gene ontology analysis showed that the genes most closely co-induced with SIRT3 were enriched in metabolism-related annotations, as well as processes such as the cellular response to stress (Figure 3.1C, Supplementary File 3.2), suggesting that many co-regulated genes are functionally related to SIRT3. For each dataset, a DNA sequence analysis algorithm (Warner et al., 2008) was then used to calculate the enrichment of a set of transcription factor motifs in 20 kbp of sequence surrounding i) the most-SIRT3-correlated genes overall or ii) the most-SIRT3-correlated mitochondrial genes (as determined by inclusion in the MitoCarta, Pagliarini et al., 2008; Supplementary File 3.3). The mitochondrial group was included because SIRT3 is a mitochondrial protein, and factors which regulate its expression may act specifically on nuclear-encoded mitochondrial genes during processes induced by nutrient stress such as mitochondrial biogenesis (e.g. Scarpulla, 2002).

The highest-scoring transcription factor motif identified by this study was nuclear respiratory factor 2 (NRF-2, also known as GA binding protein, or GABP) (Rosmarin et al., 2004) from the neocortex dataset, regardless of number of genes analyzed (Figure 3.1D, Figure 3.1E, Figure 3.1F; for the other datasets, Figure 3.2; full results for all datasets are in Supplementary File 3.4). NRF-2 was also the only motif significantly enriched across the analyses of 25, 50, and 100 genes (Figure 3.1G). NRF-2 is an E26 transformation specific (ETS)-family transcription factor that is important for the expression of many mitochondrial genes (Scarpulla, 2002). NRF-2 is bound and co-activated by PGC-1α, and it is central to mitochondrial biogenesis and metabolism (Mootha et al., 2004; Baldelli et al., 2013). All ten nuclear-encoded cytochrome c oxidase subunits have functional NRF-2 binding sites

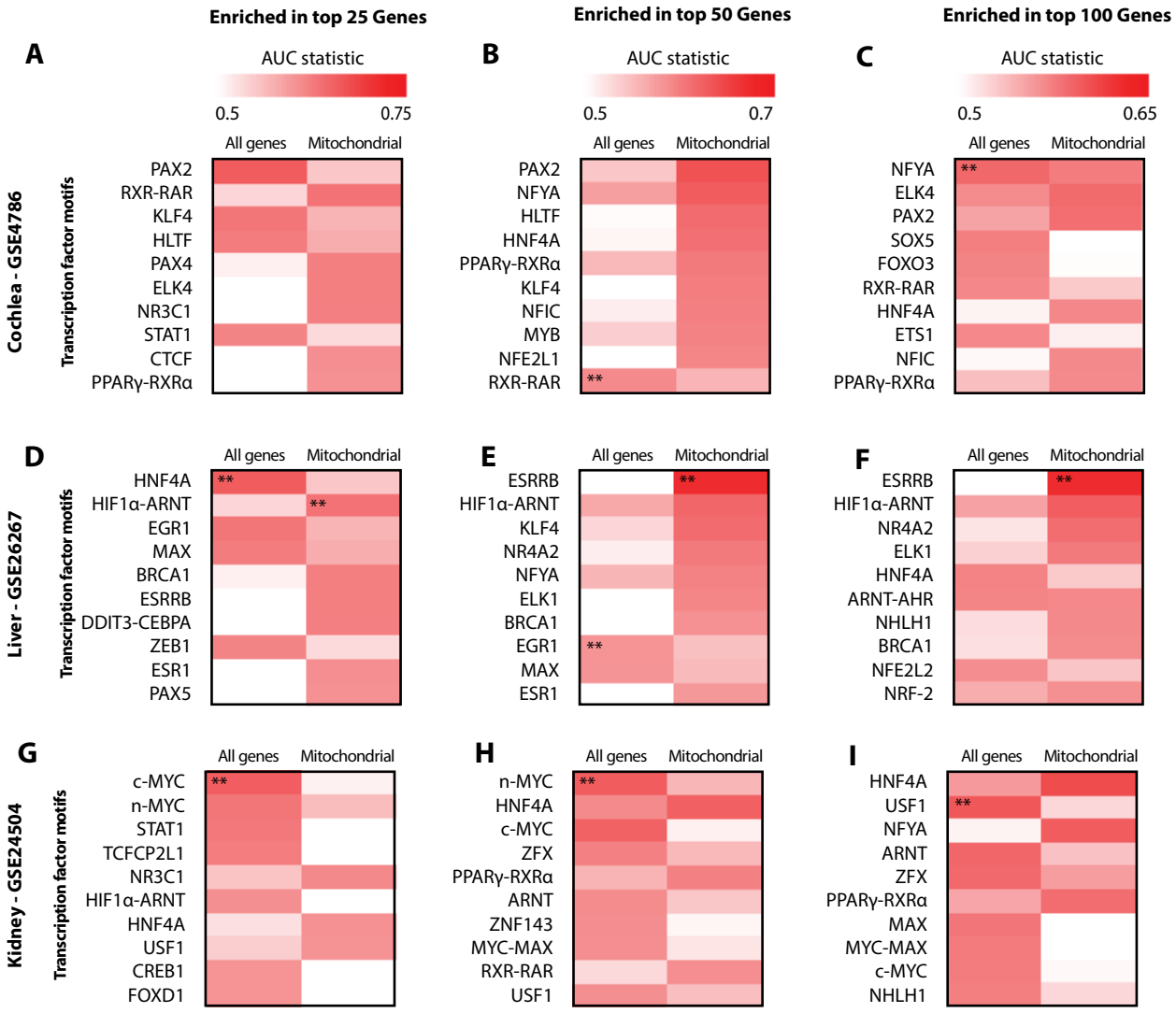

Figure 3.2. Heat maps of transcription factor motif enrichment in DNA sequences of *SIRT3* and co-expressed genes for cochlea (A-C), liver (D-F), and kidney (G-I) datasets based on sequence analysis of the top 25, 50, and 100 SIRT3-correlated genes in each dataset. Top ten motifs are shown, ordered by motif's maximum AUC score. Full results are given in Supplementary File 3.4. AUC = area under curve, a measure of enrichment. All genes = analyzed most-SIRT3-correlated genes from all genes in dataset; Mitochondrial = analyzed most-SIRT3-correlated mitochondrial genes in dataset. * indicates $q < 0.05$; ** indicates $q < 0.01$.

(Ongwijitwat and Wong-Riley, 2005), and recognition sites for NRF-2 are also present in the promoters of ATP synthase subunit β and succinate dehydrogenase subunits B, C, and D (Scarpulla, 2002). SIRT3 directly interacts with several components of the electron transport chain, including ATP synthase subunit β and succinate dehydrogenase subunit A (Finley et al., 2011; Vassilopoulos et al., 2014), and one of its few known regulators is PGC-1α. This functional overlap supports our bioinformatic finding of NRF-2 as a candidate regulator of *SIRT3*.

Analysis of SIRT3 promoter

To investigate whether NRF-2 regulated SIRT3 expression, we first probed whether NRF-2 binding sites were present in the *SIRT3* promoter. *SIRT3* shares a short bidirectional promoter with the 26S proteasome non-ATPase regulatory subunit 13 (*PSMD13*) (Bellizzi et al., 2007). The two genes are coded on opposite strands, with their 5' ends toward each other and less than 1 kbp apart. Because of the bidirectional promoter, any binding sites in the *SIRT3* promoter are also in the *PSMD13* promoter. Dissection of the promoter using a separate sequence analysis tool (MAPPER, http://genome.ufl.edu/mapper/; Marinescu et al., 2005) identified several transcription factor binding motifs (Figure 3.3A). Notably, NRF-2 was the only overlap between our significant DNA sequence analysis results for the neocortex dataset and the MAPPER results (Figure 3.3B). Moreover, NRF-2 sites often occur in tandem (Virbasius and Scarpulla, 1991), and the best-conserved region of the entire *SIRT3* promoter is a pair of NRF-2 consensus sequences (Figure 3.3C). NRF-2 is also known to direct transcription from many bidirectional promoters (Collins et al., 2007). Taken together with the motif enrichment results above, our findings strongly suggested that NRF-2 may play a role in

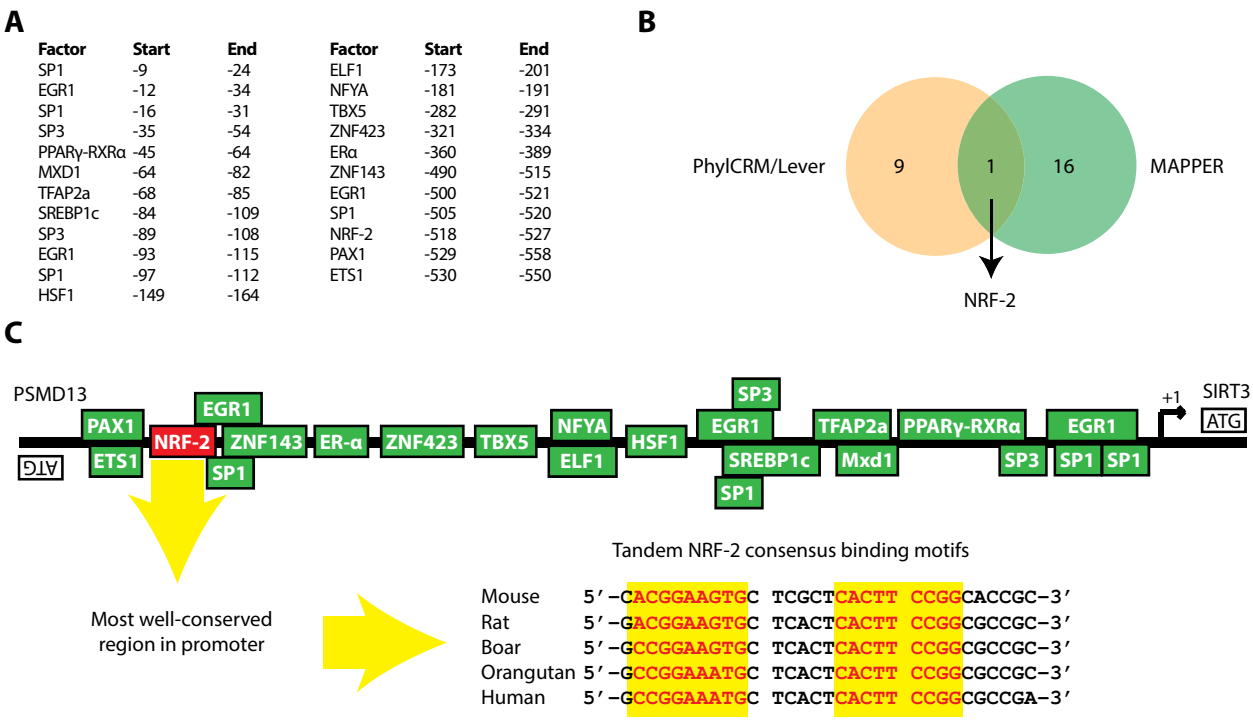

Figure 3.3. Analysis of *SIRT3* promoter. A) List of transcription factor binding sites identified by MAPPER in the mouse *SIRT3* promoter. B) Overlap of enriched transcription factor motifs identified by analysis of SIRT3 correlated genes in the neocortex dataset (pink circle) with transcription factors identified in the *SIRT3* promoter (green circle). C) Schematic of *PSMD13-SIRT3* promoter, highlighting tandem NRF-2 binding sites in yellow and showing evolutionary sequence conservation.

regulating SIRT3 expression, and perhaps PSMD13 expression as well, via the *PSMD13-SIRT3* promoter.

Experimental investigation of NRF-2 and SIRT3

We tested experimentally whether NRF-2 regulated SIRT3 and PSMD13 gene expression using human 293T cells. NRF-2 functions as a heterodimer, with the α subunit binding DNA and the β subunit facilitating binding between heterodimers (Batchelor et al, 1998). When NRF-2α and NRF-2β1 were transiently overexpressed together (Figure 3.4A, Figure 3.4B), SIRT3 mRNA levels were significantly induced ($p = 0.046$ for HA-tagged NRF-2, $p = 0.003$ for untagged NRF-2, Figure 3.4C) to a greater degree than known NRF-2 target mitochondrial DNA polymerase subunit γ-2 (POLG2) ($p = 0.26$ for HA-tagged NRF-2, $p = 0.44$ for untagged NRF-2, Figure 3.4D). PSMD13 levels were not significantly affected ($p = 0.21$ for HA-tagged NRF-2, $p = 0.77$ for untagged NRF-2, Figure 3.4E), and were likewise only weakly correlated with SIRT3 expression in the four datasets examined (Supplementary File 3.1). Conversely, when the DNA-binding NRF-2α subunit was knocked down (Figure 3.4F), SIRT3 mRNA levels significantly dropped ($p = 0.005$, Figure 3.4G). These data demonstrate that SIRT3 expression responded dynamically to NRF-2 levels.

Having identified the presence of canonical NRF-2 binding sites in the *SIRT3* promoter and characterized the response of SIRT3 expression to NRF-2 overexpression, we next tested whether the response to NRF-2 occurred via the *SIRT3* promoter. A luciferase reporter plasmid driven by the shared promoter in either the SIRT3 or PSMD13 direction (Satterstrom and Haigis, 2014) was transfected into 293T cells. NRF-2 was then overexpressed and luminescence measured. Overexpression of NRF-2 increased activation of the reporter when driven by the

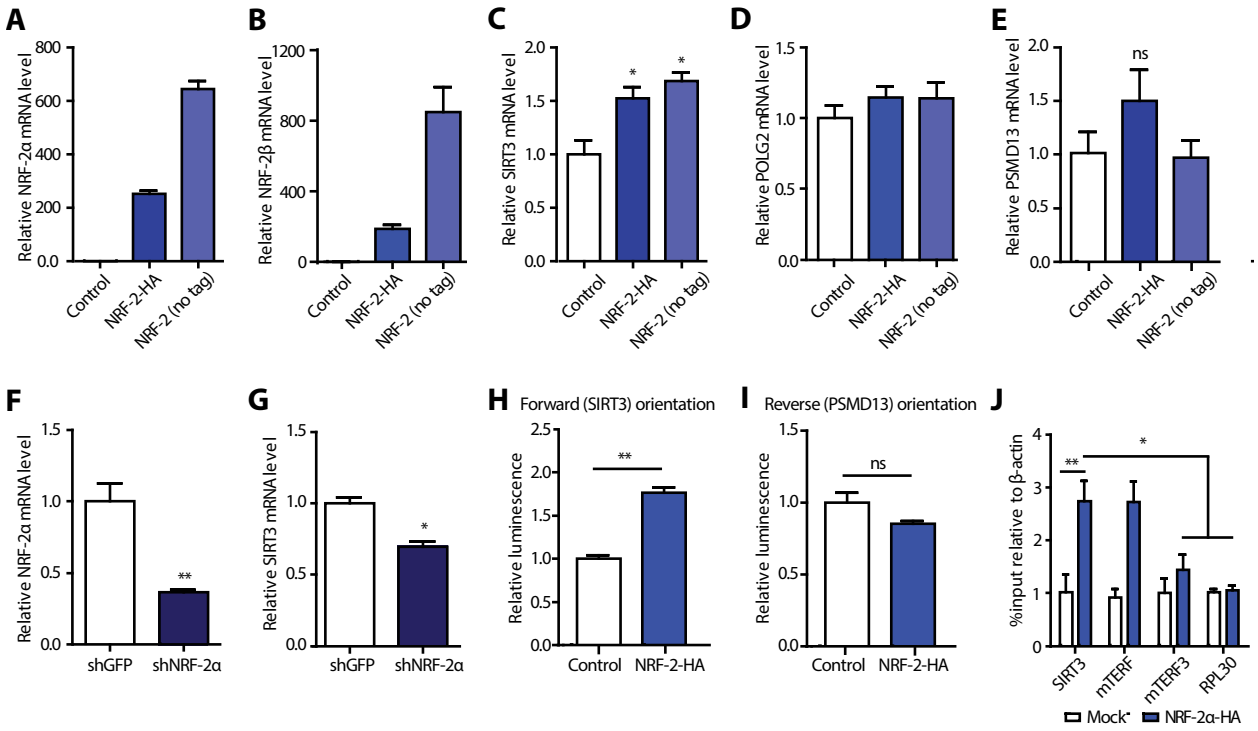

Figure 3.4. Experimental investigation of NRF-2 control of the *SIRT3* promoter. A) Validation of NRF-2α overexpression and B) NRF-2β1 overexpression in 293T cells by quantitative PCR. The two subunits together compose NRF-2. C) Effect of NRF-2 overexpression on mRNA levels of SIRT3, D) mitochondrial DNA polymerase subunit γ-2, and E) PSMD13. F) Validation of NRF-2α knockdown in 293T cells and G) effect on SIRT3 mRNA levels. H) Relative luminescence from forward (SIRT3) and I) reversed (PSMD13) bidirectional promoter luciferase reporter following overexpression of vector control or NRF-2-HA in 293T cells. J) Chromatin immunoprecipitation of HA tag in 293T cells following overexpression of NRF-2-HA, showing percent input (relative to β-actin) of SIRT3 and positive (mTERF) and negative (mTERF3, RPL30) NRF-2 controls. For A-G, n = 3 samples per condition, and B2M was used as the reference gene; for H-I, n = 4 samples per condition; for J, n = 3 separate precipitations; for all, bars are standard error. * indicates $p < 0.05$; ** indicates $p < 0.01$. Two-tailed student's t test was used for p values.

SIRT3 promoter ($p < 0.01$, Figure 3.4H) but did not have a significant effect when the promoter was inserted in the PSMD13 direction (activity decreased, $p = 0.09$, Figure 3.4I). Together with the quantitative PCR data, this data suggests that NRF-2 may control SIRT3 expression by direct interaction with the *SIRT3* promoter.

To test physical binding of the *SIRT3* promoter by NRF-2, a chromatin immunoprecipitation was performed in 293T cells transiently overexpressing HA-tagged NRF-2α, the DNA-binding subunit of the NRF-2 heterodimer. Following chromatin isolation, HA tag was immunoprecipitated and qPCR was used to quantify levels of target DNA. Immunoprecipitation and quantification were carried out three times. Using β-actin to normalize background across experiments, *SIRT3* was significantly enriched in the NRF-2α-treated condition compared to the untreated condition ($p = 0.005$). This enrichment was to approximately the same degree as genes known to be transcriptionally regulated by NRF-2, such as mitochondrial transcription termination factor (*mTERF*) ($p = 0.99$) (Bruni et al., 2010), and to a significantly greater degree than non-NRF-2-regulated genes such as *mTERF3* ($p = 0.01$) and ribosomal protein L30 (*RPL30*) ($p = 0.002$) (Figure 3.4J). These results suggest that NRF-2α physically binds the SIRT3 promoter in order to affect SIRT3 gene expression.

Discussion

In this study, we have discovered that nuclear respiratory factor 2 (NRF-2) is a novel regulator of SIRT3 expression. We used a bioinformatic analysis to show that NRF-2 binding sites are highly enriched in the regulatory regions of *SIRT3* and genes that are similarly induced by calorie restriction. We have also demonstrated that SIRT3 mRNA levels respond to overexpression or knockdown of NRF-2 in 293T cells, and that the same effect occurs when

using a luciferase reporter with the *SIRT3* promoter. Finally, we have shown by chromatin immunoprecipitation that the α subunit of NRF-2 binds the *SIRT3* promoter directly, suggesting a model wherein NRF-2 binds the *SIRT3* promoter, leading to expression of SIRT3 mRNA. Our data also suggest that *SIRT3* and *PSMD13* are regulated independently, as NRF-2 induces expression of SIRT3 but not PSMD13 under the conditions studied.

NRF-2 binds and is co-activated by PGC-1α, leading to an increase in its induction of target genes (Mootha et al., 2004, Baldelli et al., 2013). Because PGC-1α is induced in certain tissues by fasting or calorie restriction (Lehman et al., 2000), this pathway may underlie the upregulation of SIRT3 and other mitochondrial genes in CR. Noteably, ERRα, which is already known to play a role in activating SIRT3 transcription, is also co-activated by PGC-1α (Shreiber et al., 2003). Both NRF-2 and ERRα drive the expression of oxidative genes as well as each other (Mootha et al., 2004), but they may be active at different times or in different tissues; in support of this idea, NRF-2 was a significant result for our analysis of the neocortex dataset, while one significant result for our analysis of the liver dataset was ERRβ (which has a nearly identical binding motif to ERRα; ERRα was not in the set of Jaspar motifs). Further study is therefore needed to determine the importance of these transcription factors for the induction of SIRT3 in different physiological contexts.

Our analysis additionally identified multiple transcription factors of interest which may be involved in the regulation of SIRT3 expression. CCAAT/enhancer-binding protein α (CEBPα), whose motif was enriched in the neocortex dataset, and c-MYC, whose motif was enriched in the kidney dataset, regulate metabolic processes and would be reasonable candidate regulators of SIRT3. CEBPα regulates transcription of the human fat mass and obesity-associated gene (FTO) (Ren et al., 2014), and the proto-oncogene c-MYC is well known for its

role in cancer metabolism (reviewed in Miller et al., 2012). Additionally, our inspection of the *SIRT3* promoter identified binding sites for transcription factors known to interact with NRF-2, including SP1 and SP3 (Galvagni et al., 2001), or share common targets with it, including ZNF143 (Gérard et al., 2007) and Egr1 (Fromm and Rhode, 2004). Finally, ETS-1, ELF-1, ELK1, and ELK4 are all members of the same ETS family of transcription factors as NRF-2. It is possible that one or more was identified because of its similar binding motif without actually playing a role in SIRT3 expression; it is also possible that they are important in different contexts, or, when they are co-expressed, multiple factors may bind the same promoter element to activate gene expression with different strengths (Takahashi et al., 2008).

Our findings are an important step toward elucidating the molecular regulation upstream of SIRT3 expression. SIRT3 levels are increased in multiple tissues during nutrient stresses such as calorie restriction. CR is associated with increased lifespan (Anderson and Weindruch, 2010), as is a *SIRT3* allele with increased transcriptional activity (Bellizzi et al., 2005). We have shown that NRF-2 plays a role in the induction of SIRT3, and this may help to uncover the molecular pathways activated by calorie restriction and to inform therapies that delay the onset of age-related disease.

Methods

Analysis of SIRT3 levels in microarray datasets

Microarray series data and corresponding platform annotations from CR/fasting experiments were downloaded from the Gene Expression Omnibus at http://www.ncbi.nlm.nih.gov/geo/. Significance of the effect on SIRT3 was determined using a

two-tailed student's t-test with a significance threshold of $p < 0.05$. In cases where the platform had more than one probe for SIRT3, each probe was examined individually.

Gene set enrichment analysis

Gene set enrichment analysis of each dataset showing a significant induction of SIRT3 by CR/fasting was performed using the GSEA version 2.0.10 java program from http://www.broadinstitute.org/gsea/downloads.jsp. Data files were prepared with the Broad GEOImporter preprocess utility and were analyzed for enrichment of gene ontology-related gene sets as contained in the c5.all.v3.1.symbols.gmt gene sets database. Datasets were collapsed from probes to gene symbols using default settings and 1000 permutations were conducted. Gene set permutations were used because none of the datasets had a sufficient number of samples per condition to allow use of phenotype permutations. Datasets which showed no significant induction of any gene sets were not included in subsequent analysis.

Calculation of co-regulated gene sets

The robust multiarray average (RMA) algorithm as implemented in the Bioconductor package "affy" (Gautier et al., 2004) for R was used to background adjust and normalize the raw data files for each dataset that showed upregulation of SIRT3 and gene ontology-related gene sets upon CR (except for GSE24504, for which the GEO series matrix was used). Correlations (Pearson's r) were then computed between the SIRT3 probe and each probe in the array. To control for probe specificity, probes whose label contained an _s_ or _x_ were removed from datasets generated from the Affymetrix Mouse Genome 430 2.0 Array unless doing so would

leave the gene without any valid probes. For genes with multiple probes, correlations were averaged to compute a single correlation value for the gene.

Gene ontology analysis

Analysis of overrepresented gene ontology terms was carried out within the Cytoscape software program using the BiNGO plugin (Maere et al., 2005), with the whole *mus musculus* annotation as the reference set. The hypergeometric statistical test and Benjamini & Hochberg FDR correction options were used.

DNA sequence analysis

Analysis was conducted using the PhylCRM-Lever algorithm (Warner et al., 2008). The sequence analysis looked at 20 kbp for each gene, from -10 kbp to +10 kbp surrounding the transcription start site. Motif enrichment was calculated for all 130 mammalian motifs hosted by version 4 of the JASPAR database (Portales-Casamar et al., 2010; http://jaspar.genereg.net/). The analysis included weighting based on conservation of transcription factor motifs across genomes of multiple species: mouse (mm9), rat (rn4), human (hg18), chimpanzee (panTro2), rhesus macaque (rheMac2), cow (bosTau3), dog (canFam2), and chicken (galGal3). SIRT3 itself was included in lists of SIRT3-correlated genes.

Additional DNA sequence analysis was performed using MAPPER (Marinescu et al., 2005). MAPPER database runs with default filtering options examined 2 kbp of *mus musculus* DNA sequence upstream of the transcription start, using TRANSFAC, MAPPER, and JASPAR models.

Cell culture

Human embryonic kidney 293T cells were grown in Dulbecco's Modified Eagle Medium (Life Technologies, cat. # 11995) with 10% fetal bovine serum (HyClone) and 1% penicillin-streptomycin supplement (Life Technologies) and maintained in an incubator at standard tissue culture conditions (37°C, 5% CO_2). A control knockdown line was created using a GFP shRNA construct, and a 293T NRF-2α knockdown cell line was created using shRNA construct TRCN0000235698 from the RNAi consortium (both via the Dana-Farber / Harvard Cancer Center RNAi Core facility).

Expression and reporter plasmids

HA-tagged overexpression plasmids for NRF-2α and NRF-2β1 were generated using Gateway cloning techniques, starting from the HsCD00080063 and HsCD00370955 entry clones, respectively, from the PlasmID database of the Dana-Farber / Harvard Cancer Center DNA Resource Core. Untagged overexpression plasmids were generated via Gateway cloning techniques from HsCD00296808 and HsCD00338810. The reversible *PSMD13-SIRT3* promoter reporter construct was cloned as described (chapter II; Satterstrom and Haigis, 2014). Plasmid DNA was transfected into 293T cells using FuGene6 (Roche) according to the manufacturer's instructions, and cells were allowed to grow for 48 hours prior to analysis.

Luciferase

Cells were grown in an opaque 96-well plate. Following co-transfection of the SIRT3 reporter plasmid and the pRL renilla control vector (Promega), the Dual-Luciferase Reporter

Assay System (Promega) was used according to manufacturer's instructions. Sample luminescence was assayed with a Cary Varian Eclipse fluorescence spectrophotometer.

Chromatin immunoprecipitation

Chromatin immunoprecipitation (ChIP) was performed with the SimpleChIP Enzymatic Chromatin IP Kit (Cell Signaling) with antibodies against HA tag (Cell Signaling), histone H3 (Cell Signalig), or normal rabbit IgG (Cell Signaling). Relative quantities of precipitated DNA fragments were obtained using quantitative PCR.

Quantitative PCR

For overexpression experiments in cells, RNA was extracted using RNEasy Mini Kits (Qiagen) and cDNA was synthesized using iScript cDNA Synthesis Kits (Bio-Rad). For both overexpression experiments and ChIP analysis, quantitative PCR was performed with 2x PerfeCTa SYBR Green FastMix (Quanta). Control primers for ChIP analysis were from Bruni et al. (2010); other primer sequences are given in Table 3.2 (except RPL30, Cell Signaling). For non-ChIP analysis, β2 microglobulin (B2M) was used as a reference gene.

Acknowledgments

F. K. S. was supported by NIH Training Grant No. T32 DK007260. M. L. B. was supported in part by NIH Grant No. R01 DK088718. M. C. H. was supported by an American Cancer Society New Scholar Award and the Glenn Foundation for Medical Research.

Table 3.2. Sequences of primers used in this study. All sequences are for human genes. The control mTERF, mTERF3, and β-actin ChIP sequences are from Bruni et al. (2010).

Gene	Purpose	Direction	Sequence
SIRT3	qPCR	Forward	5'-AGCCCTCTTCATGTTCCGAAGTGT-3'
		Reverse	5'-TCATGTCAACACCTGCAGTCCCTT-3'
NRF-2α	qPCR	Forward	5'-GGCGCGTAGGTTTGTTCTAC-3'
		Reverse	5'-ACTCCAGCCATGACTAAAAGAGA-3'
NRF-2β1	qPCR	Forward	5'-ACCAACCAGTGGGATGGGTCAG-3'
		Reverse	5'-GCACATTCCACCCGGCTCTCAAT-3'
POLG2	qPCR	Forward	5'-AAGGTTGCTTTGGATGTAGGAAGA-3'
		Reverse	5'-GGCCACACAGAAATCCCATT-3'
B2M	qPCR	Forward	5'-AGATGAGTATGCCTGCCGTGTGAA-3'
		Reverse	5'-TGCTGCTTACATGTCTCGATCCCA-3'
SIRT3	ChIP	Forward	5'-CATGACAGCAGGAAGACCCC-3'
		Reverse	5'-CAAACGCCGGAGAGTTTTGT-3'
mTERF	ChIP	Forward	5'-GACCAACGACATCACCTCTGC-3'
		Reverse	5'-CACCCATCCACTGTAGTTCGC-3'
mTERF3	ChIP	Forward	5'-CTGTCTCCCCGCGTAACC-3'
		Reverse	5'-CTCCTCAGCCCGCCCTAC-3'
β-actin	ChIP	Forward	5'-CCCAGCCATGTACGTTGCTA-3'
		Reverse	5'-CGTCACCGGAGTCCATCAC-3'

References

Anderson RM, Weindruch R (2010) Metabolic reprogramming, caloric restriction and aging. *Trends Endocrinol. Metab.* **21**, 134-141.

Baldelli S, Aquilano K, Ciriolo MR (2013) Punctum on two different transcription factors regulated by PGC-1α: nuclear factor erythroid-derived 2-like 2 and nuclear respiratory factor 2. *Biochim. Biophys. Acta* **1830**, 4137-4146.

Barger JL, Kayo T, Vann JM, Arias EB, Wang J, Hacker TA, Wang Y, Raederstorff D, Morrow JD, Leeuwenburgh C, Allison DB, Saupe KW, Cartee GD, Weindruch R, Prolla TA (2008) A low dose of dietary resveratrol partially mimics caloric restriction and retards aging parameters in mice. *PLoS One* **3**, e2264.

Batchelor AH, Piper DE, de la Brousse FC, McKnight SL, Wolberger C (1998) The structure of GABPalpha/beta: an ETS domain- ankyrin repeat heterodimer bound to DNA. *Science* **279**, 1037-1041.

Bellizzi D, Rose G, Cavalcante P, Covello G, Dato S, De Rango F, Greco V, Maggiolini M, Feraco E, Mari V, Franceschi C, Passarino G, De Benedictis G (2005) A novel VNTR enhancer within the SIRT3 gene, a human homologue of SIR2, is associated with survival at oldest ages. *Genomics* **85**, 258-263.

Bellizzi D, Dato S, Cavalcante P, Covello G, Di Cianni F, Passarino G, Rose G, De Benedictis G (2007) Characterization of a bidirectional promoter shared between two human genes related to aging: SIRT3 and PSMD13. *Genomics* **89**, 143-150.

Bruni F, Polosa PL, Gadaleta MN, Cantatore P, Roberti M (2010) Nuclear respiratory factor 2 induces the expression of many but not all human proteins acting in mitochondrial DNA transcription and replication. *J. Biol. Chem.* **285**, 3939-3948.

Collins PJ, Kobayashi Y, Nguyen L, Trinklein ND, Myers RM (2007) The ets-related transcription factor GABP directs bidirectional transcription. *PLoS Genet.* **3**, e208.

Finley LW, Haas W, Desquiret-Dumas V, Wallace DC, Procaccio V, Gygi SP, Haigis MC (2011) Succinate dehydrogenase is a direct target of sirtuin 3 deacetylase activity. *PLoS One* **6**, e23295.

Fromm L, Rhode M (2004) Neuregulin-1 induces expression of Egr-1 and activates acetylcholine receptor transcription through an Egr-1-binding site. *J. Mol. Biol.* **339**, 483-494.

Galvagni F, Capo S, Oliviero S (2001) Sp1 and Sp3 physically interact and co-operate with GABP for the activation of the utrophin promoter. *J. Mol. Biol.* **306**, 985-996.

Gautier L, Cope L, Bolstad BM, Irizarry RA (2004) affy--analysis of Affymetrix GeneChip data at the probe level. *Bioinformatics* **20**, 307-315.

Gérard MA, Krol A, Carbon P (2007) Transcription factor hStaf/ZNF143 is required for expression of the human TFAM gene. *Gene* **401**, 145-153.

Giralt A, Hondares E, Villena JA, Ribas F, Díaz-Delfín J, Giralt M, Iglesias R, Villarroya F (2011) Peroxisome proliferator-activated receptor-gamma coactivator-1alpha controls transcription of the Sirt3 gene, an essential component of the thermogenic brown adipocyte phenotype. *J. Biol. Chem.* **286**, 16958-16966.

Hakvoort TB, Moerland PD, Frijters R, Sokolović A, Labruyère WT, Vermeulen JL, Ver Loren van Themaat E, Breit TM, Wittink FR, van Kampen AH, Verhoeven AJ, Lamers WH, Sokolović M (2011) Interorgan coordination of the murine adaptive response to fasting. *J. Biol. Chem.* **286**, 16332-16343.

Hallows WC, Yu W, Smith BC, Devries MK, Ellinger JJ, Someya S, Shortreed MR, Prolla T, Markley JL, Smith LM, Zhao S, Guan KL, Denu JM (2011) Sirt3 promotes the urea cycle and fatty acid oxidation during dietary restriction. *Mol. Cell* **41**, 139-149.

Hebert AS, Dittenhafer-Reed KE, Yu W, Bailey DJ, Selen ES, Boersma MD, Carson JJ, Tonelli M, Balloon AJ, Higbee AJ, Westphall MS, Pagliarini DJ, Prolla TA, Assadi-Porter F, Roy S, Denu JM, Coon JJ (2013) Calorie restriction and SIRT3 trigger global reprogramming of the mitochondrial protein acetylome. *Mol. Cell* **49**, 186-199.

Hirschey MD, Shimazu T, Goetzman E, Jing E, Schwer B, Lombard DB, Grueter CA, Harris C, Biddinger S, Ilkayeva OR, Stevens RD, Li Y, Saha AK, Ruderman NB, Bain JR, Newgard CB, Farese RV Jr, Alt FW, Kahn CR, Verdin E (2010) SIRT3 regulates mitochondrial fatty-acid oxidation by reversible enzyme deacetylation. *Nature* **464**, 121-125.

Hirschey MD, Shimazu T, Jing E, Grueter CA, Collins AM, Aouizerat B, Stančáková A, Goetzman E, Lam MM, Schwer B, Stevens RD, Muehlbauer MJ, Kakar S, Bass NM, Kuusisto J, Laakso M, Alt FW, Newgard CB, Farese RV Jr, Kahn CR, Verdin E (2011) SIRT3 deficiency and mitochondrial protein hyperacetylation accelerate the development of the metabolic syndrome. *Mol. Cell* **44**, 177-190.

Kong X, Wang R, Xue Y, Liu X, Zhang H, Chen Y, Fang F, Chang Y (2010) Sirtuin 3, a new target of PGC-1alpha, plays an important role in the suppression of ROS and mitochondrial biogenesis. *PLoS One* **5**, e11707.

Lehman JJ, Barger PM, Kovacs A, Saffitz JE, Medeiros DM, Kelly DP (2000) Peroxisome proliferator-activated receptor gamma coactivator-1 promotes cardiac mitochondrial biogenesis. *J. Clin. Invest.* **106**, 847-856.

Lombard DB, Alt FW, Cheng HL, Bunkenborg J, Streeper RS, Mostoslavsky R, Kim J, Yancopoulos G, Valenzuela D, Murphy A, Yang Y, Chen Y, Hirschey MD, Bronson RT, Haigis M, Guarente LP, Farese RV Jr, Weissman S, Verdin E, Schwer B (2007) Mammalian Sir2 homolog SIRT3 regulates global mitochondrial lysine acetylation. *Mol. Cell. Biol.* **24**, 8807-8814.

Maere S, Heymans K, Kuiper M (2005) BiNGO: a Cytoscape plugin to assess overrepresentation of gene ontology categories in biological networks. *Bioinformatics* **21**, 3448-9.

Marinescu VD, Kohane IS, Riva A (2005) MAPPER: a search engine for the computational identification of putative transcription factor binding sites in multiple genomes. *BMC Bioinformatics* **6**, 79.

Miller DM, Thomas SD, Islam A, Muench D, Sedoris K (2012) c-Myc and cancer metabolism. *Clin. Cancer Res*. **18**, 5546-5553.

Mootha VK, Handschin C, Arlow D, Xie X, St Pierre J, Sihag S, Yang W, Altshuler D, Puigserver P, Patterson N, Willy PJ, Schulman IG, Heyman RA, Lander ES, Spiegelman BM (2004) Errα and Gabpa/b specify PGC-1α-dependent oxidative phosphorylation gene expression that is altered in diabetic muscle. *Proc. Natl. Acad. Sci. U. S. A.* **101**, 6570-6575.

Ongwijitwat S, Wong-Riley MT (2005) Is nuclear respiratory factor 2 a master transcriptional coordinator for all ten nuclear-encoded cytochrome c oxidase subunits in neurons? *Gene* **360**, 65-77.

Pagliarini DJ, Calvo SE, Chang B, Sheth SA, Vafai SB, Ong SE, Walford GA, Sugiana C, Boneh A, Chen WK, Hill DE, Vidal M, Evans JG, Thorburn DR, Carr SA, Mootha VK (2008) A mitochondrial protein compendium elucidates complex I disease biology. *Cell* **134**, 112-123.

Portales-Casamar E, Thongjuea S, Kwon AT, Arenillas D, Zhao X, Valen E, Yusuf D, Lenhard B, Wasserman WW, Sandelin A (2010) JASPAR 2010: the greatly expanded open-access database of transcription factor binding profiles. *Nucleic Acids Res.* **38**, D105-D110.

Qiu X, Brown K, Hirschey MD, Verdin E, Chen D (2010) Calorie restriction reduces oxidative stress by SIRT3-mediated SOD2 activation. *Cell Metab.* **12**, 662-7.

Ren W, Guo J, Jiang F, Lu J, Ding Y, Li A, Liang X, Jia W (2014) CCAAT/enhancer-binding protein α is a crucial regulator of human fat mass and obesity associated gene transcription and expression. *Biomed. Res. Int*. **2014**, 406909.

Rosmarin AG, Resendes KK, Yang Z, McMillan JN, Fleming SL (2004) GA-binding protein transcription factor: a review of GABP as an integrator of intracellular signaling and protein-protein interactions. *Blood Cells Mol. Dis.* **32**, 143-154.

Satterstrom FK, Haigis MC (2014) Luciferase-based reporter to monitor the transcriptional activity of the SIRT3 promoter. *Methods Enzymol.* **543**, 141-163.

Scarpulla RC (2002) Nuclear activators and coactivators in mammalian mitochondrial biogenesis. *Biochim. Biophys. Acta* **1576**, 1-14.

Shi T, Wang F, Stieren E, Tong Q (2005) SIRT3, a mitochondrial sirtuin deacetylase, regulates mitochondrial function and thermogenesis in brown adipocytes. *J. Biol. Chem.* **280**, 13560-13567.

Shimazu T, Hirschey MD, Hua L, Dittenhafer-Reed KE, Schwer B, Lombard DB, Li Y, Bunkenborg J, Alt FW, Denu JM, Jacobson MP, Verdin E (2010) SIRT3 deacetylates mitochondrial 3-hydroxy-3-methylglutaryl CoA synthase 2 and regulates ketone body production. *Cell Metab.* **12**, 654-661.

Schreiber SN, Knutti D, Brogli K, Uhlmann T, Kralli A (2003) The transcriptional coactivator PGC-1 regulates the expression and activity of the orphan nuclear receptor estrogen-related receptor alpha (ERRalpha). *J. Biol. Chem.* **278**, 9013-9018.

Someya S, Yamasoba T, Weindruch R, Prolla TA, Tanokura M (2007) Caloric restriction suppresses apoptotic cell death in the mammalian cochlea and leads to prevention of presbycusis. *Neurobiol. Aging* **28**, 1613-1622.

Someya S, Yu W, Hallows WC, Xu J, Vann JM, Leeuwenburgh C, Tanokura M, Denu JM, Prolla TA (2010) Sirt3 mediates reduction of oxidative damage and prevention of age-related hearing loss under caloric restriction. *Cell* **143**, 802-812.

Streeper RS, Grueter CA, Salomonis N, Cases S, Levin MC, Koliwad SK, Zhou P, Hirschey MD, Verdin E, Farese RV Jr (2012) Deficiency of the lipid synthesis enzyme, DGAT1, extends longevity in mice. *Aging (Albany NY)* **4**, 13-27.

Takahashi K, Hayashi N, Shimokawa T, Umehara N, Kaminogawa S, Ra C (2008) Cooperative regulation of Fc receptor gamma-chain gene expression by multiple transcription factors, including Sp1, GABP, and Elf-1. *J. Biol. Chem.* **283**, 15134-15141.

Tao R, Coleman MC, Pennington JD, Ozden O, Park SH, Jiang H, Kim HS, Flynn CR, Hill S, Hayes McDonald W, Olivier AK, Spitz DR, Gius D (2010) Sirt3-mediated deacetylation of evolutionarily conserved lysine 122 regulates MnSOD activity in response to stress. *Mol. Cell* **40**, 893-904.

Vassilopoulos A, Pennington JD, Andresson T, Rees DM, Bosley AD, Fearnley IM, Ham A, Flynn CR, Hill S, Rose KL, Kim HS, Deng CX, Walker JE, Gius D (2014) SIRT3 Deacetylates ATP Synthase F1 Complex Proteins in Response to Nutrient- and Exercise-Induced Stress. *Antioxid. Redox Signal.* **21**, 551-564.

Virbasius JV, Scarpulla RC (1991) Transcriptional activation through ETS domain binding sites in the cytochrome c oxidase subunit IV gene. *Mol. Cell. Biol.* **11**, 5631-5638.

Warner JB, Philippakis AA, Jaeger SA, He FS, Lin J, Bulyk ML (2008) Systematic identification of mammalian regulatory motifs' target genes and functions. *Nat. Methods* **5**, 347-353.

CHAPTER IV

Calorie restriction reverses age-related changes in gene expression and isoform usage in mouse liver

F. Kyle Satterstrom[1,2,3], Lydia W. S. Finley[2,3], Joshua M. Gorham[4], Danos C. Christodoulou[4], Jonathan G. Seidman[4], and Marcia C. Haigis[2,3]

[1] Harvard School of Engineering and Applied Sciences, Cambridge, Massachusetts 02138

[2] Department of Cell Biology, Harvard Medical School, Boston, Massachusetts 02115

[3] The Paul F. Glenn Labs for the Biological Mechanisms of Aging, Harvard Medical School, Boston, Massachusetts 02115

[4] Department of Genetics, Harvard Medical School, Boston, Massachusetts 02115

This work utilized tissue samples from mice which had been calorie restricted by Lydia Finley. Kyle Satterstrom designed the study, extracted new RNA from tissue samples, and performed the majority of the data analysis described in this chapter, with assistance from Danos Christodoulou (normalized gene expression values and isoform scores). Joshua Gorham performed the high-throughput sequencing.

Abstract

Calorie restriction (CR), which increases lifespan in several model organisms, is known to reverse age-related changes in gene expression. However, it is not known whether CR is also able to reverse age-related changes in the relative proportions of different isoforms expressed from the same locus. We used high-throughput RNA sequencing (RNA-seq) to examine gene expression in liver and heart tissue of aged short-term calorie-restricted mice, aged control mice, and young control mice. We found that calorie restriction reversed many age-related changes in gene expression, with changes more pronounced in liver than in heart. Using a scoring system to quantify differences in read profile between samples, our data suggested that calorie restriction reversed many age-related changes in isoform usage as well. These data suggest a new mechanism which calorie restriction may use in achieving its biological effects.

Introduction

Calorie restriction (CR) increases lifespan in several model organisms, including yeast, worms, flies, and mice (Weindruch et al., 1986), although the exact mechanisms are not clear. On a molecular level, CR also reverses age-related changes in gene expression (Lee et al., 1999). To date, most studies of gene expression in CR have used microarrays, which generally do not give a finer level of granularity than expression for the gene as a whole. Recently, high-throughput RNA sequencing (RNA-seq) techniques have been developed which provide information about the RNA expression of each base along the DNA coding for a gene. When transcripts are sequenced, the number which map to any given base is termed that base's read depth, and the progression of read depths along a gene's DNA strand is termed the gene's read profile. Read profiles allow assessment of not only overall expression levels but also of factors

such as start site usage and exon usage, enabling an assessment of differential isoform expression.

Despite the significant attention that calorie restriction has received, RNA-seq methods have not yet been used to determine whether CR can reverse age-related changes in isoform usage. One recent RNA-seq study of calorie-restricted mice demonstrated that CR can affect which mRNA isoform of a gene is preferentially expressed in skeletal muscle (Dhahbi et al., 2012), but this study did not compare young versus old samples. To determine whether CR could reverse age-related changes in overall gene expression as well as isoform usage, we performed high-throughput RNA sequencing on liver and heart tissue from young (5 month) control mice, aged (21 month) control mice, and aged (21 month) mice that had been 40% calorie restricted for 11 weeks. We assayed overall gene expression changes, and we also applied a scoring system (Christodoulou et al., 2014) to quantify the differences in read profile between samples, enabling the identification of specific genes which may have experienced a change in the relative expression of their different isoforms.

Results

Gene expression

The RNA-seq data show that aging (i.e. comparing the young control and the aged control samples) and calorie restriction (comparing the aged control and aged CR samples) each led thousands of genes to change expression levels significantly between samples (full results in Supplementary File 4.1). Volcano plots (Figure 4.1) show that more genes in the liver were up with aging (8329) than were down with aging (2438) (Table 4.1). In fact, the number up with aging was more than 50% of all genes (15694) which had at least 10 reads in either sample (the

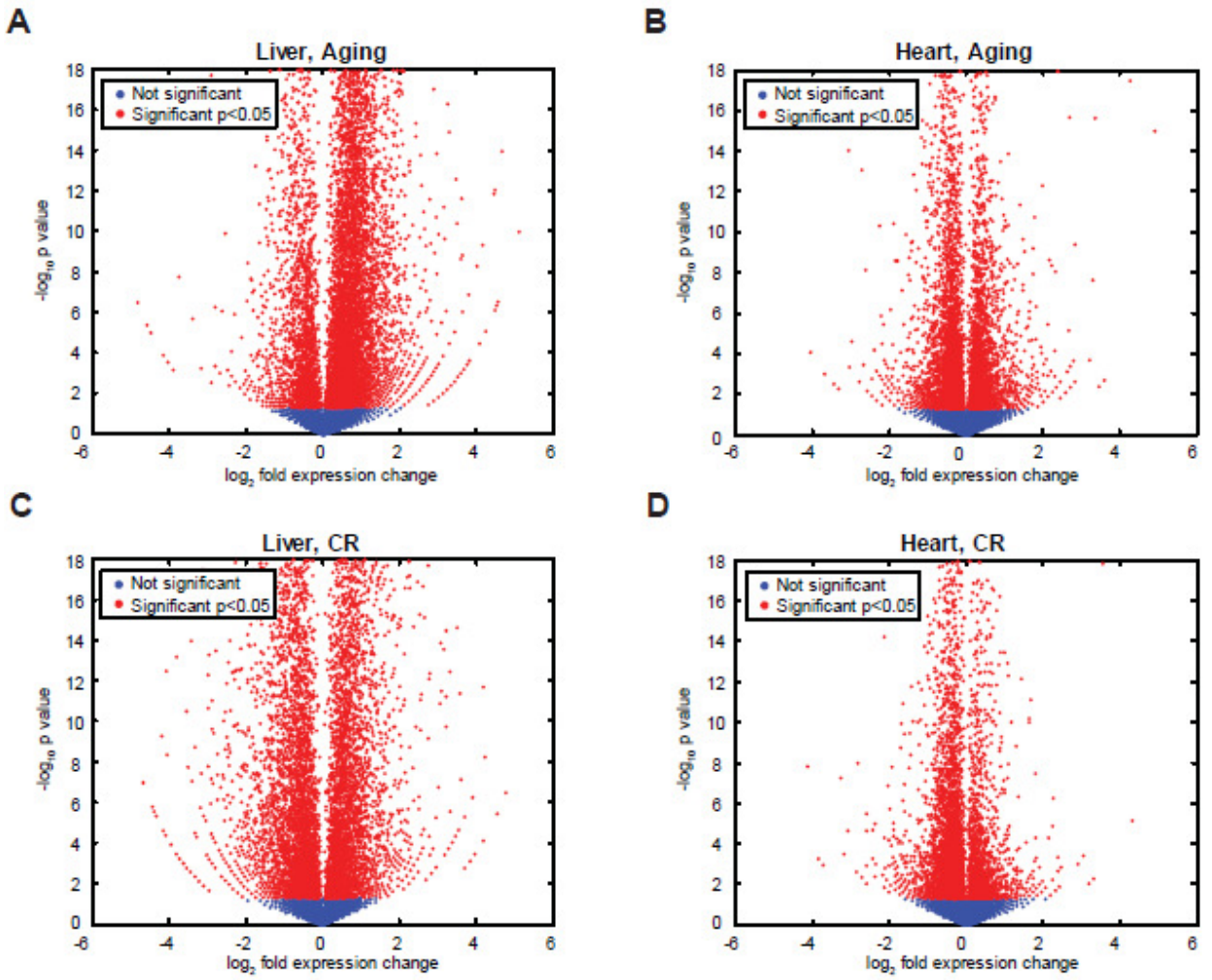

Figure 4.1. Volcano plots of gene expression results. Plots are shown for A) liver, young control vs. aged control samples; B) heart, young control vs. aged control samples; C) liver, aged control vs. aged CR samples; and D) heart, aged control vs. aged CR samples. Only genes which had at least 10 reads in one or both of the samples being compared were included.

Table 4.1. Overview of gene expression results. Within each organ, results are shown for three different read thresholds. Each comparison involves two samples (i.e. aging compares young control with aged control; CR compares aged control with aged). A gene was included in the analysis if either of the two samples being compared had a number of reads equal to or higher than the specified minimum reads per gene threshold. Median FC = median fold change among all genes in the analysis for the given treatment.

	Liver			**Heart**		
Min reads/gene:	10	100	1000	10	100	1000
Aging						
Genes	**15694**	**11176**	**3541**	**15902**	**10563**	**2555**
Median FC	1.365	1.378	1.396	0.962	0.961	0.951
Up with aging	**8329**	**7073**	**2450**	**2383**	**1964**	**719**
Percentage	53%	63%	69%	15%	19%	28%
Down with aging	**2438**	**1980**	**829**	**3669**	**3178**	**1226**
Percentage	16%	18%	23%	23%	30%	48%
CR						
Genes	**15871**	**11435**	**3875**	**15926**	**10492**	**2520**
Median FC	0.997	1.024	1.111	0.931	0.933	0.966
Up with CR	**5717**	**4883**	**2033**	**1505**	**1253**	**597**
Percentage	36%	43%	52%	9%	12%	24%
Down with CR	**5358**	**4370**	**1592**	**4317**	**3620**	**1085**
Percentage	34%	38%	41%	27%	35%	43%
Overlap						
Up w/ aging & down w/ CR	**4556**	**3985**	**1481**	**1059**	**964**	**394**
Percentage of up with aging	55%	56%	60%	44%	49%	55%
Percentage of down with CR	85%	91%	93%	25%	27%	36%
Down w/ aging & up w/ CR	**2051**	**1762**	**734**	**633**	**563**	**294**
Percentage of down with aging	84%	89%	89%	17%	18%	24%
Percentage of up with CR	36%	36%	36%	42%	45%	49%

minimum to enable proper statistical analysis of gene expression changes and corresponding significance levels), while only 16% of genes had decreased expression with age. Calorie restriction had a more even effect, with 36% of liver genes up with CR and 34% down with CR. These effects became more pronounced for genes with a higher expression level – for all genes which met a 1000 read requirement, for example, 69% were increased with aging and 52% were increased with CR.

Gene expression changes in the heart were less pronounced than in the liver. While 69% of genes were either increased or decreased by aging in the liver, only 38% of genes were changed in the heart. With calorie restriction, 70% of genes were changed in the liver, while only 36% were changed in the heart. Aging and CR both increased the expression levels of more genes than they decreased in the liver, but they had the opposite effect in the heart. As in the liver, the percentage of total genes whose expression changed significantly increased when looking at only genes with higher overall expression levels (Table 4.1). This is in part due to our method of calculating p values, which gains increased statistical certainty with increased read depth, but it also demonstrates that the changes in gene expression were not being driven by weakly expressed genes. The percentage of total genes whose expression changed significantly was also much higher in our study than in the wildtype mice of several microarray studies of aging liver (e.g. GSE3129, Boylston et al., 2006; GSE34378, Jonker et al., 2013) or aging heart (e.g. GSE8146 Reiter et al., 2007; GSE11291, Barger et al., 2008); this is likely due to the greater sensitivity of our experimental method as well as the greater statistical power of calculating a gene's p value with Bayesian inference based on read depth rather than with a t-test based on one expression value per sample.

Reversal of age-related expression changes by CR

Interestingly, many of the gene expression changes that happened with aging were reversed by CR. This was most striking in the liver, where 84% of the genes that were down with age were also up with CR. Similarly, 85% of the genes that were down with CR were also up with age. This is depicted visually in Figure 4.2. For each segment of Figure 4.2A, the top 10 most-changed genes are shown (Figure 4.2B), and gene ontology analysis was also conducted to determine enriched GO terms among the genes in each segment (the top 10 are shown) (Figure 4.2C) (likewise for Figures 4.2D-F). In the liver, the genes whose age-related expression changes were reversed by CR were enriched in GO terms related to metabolism, including "metabolic process" and "electron transport chain." This shows the high sensitivity of metabolic genes, especially in the liver, to aging and calorie restriction, and it is consistent with a hypothesis of calorie restriction showing anti-aging effects.

Just as the heart had less pronounced gene expression changes than the liver overall, it also exhibited a smaller proportion of age-related changes that were reversed by CR (Figure 4.3). Nonetheless, several hundred genes did show reversed changes, and over 40% of the genes increased by CR had also been down with age. This included genes such as mitochondrial 3-hydroxy-3-methylglutaryl-CoA synthase 2 (HMGCS2), whose protein product is the rate-limiting step in the production of ketone bodies and which is normally activated as a metabolic adaptation to reduced nutrient intake (Shimazu et al., 2010). The cardioprotective gene uncoupling protein 1 (UCP1) (Hoerter et al., 2004) was also increased by CR, though not affected by age. GO term analysis of genes in the heart which were affected by aging and/or CR identified similar sets of metabolism-related terms for all groups.

Figure 4.2 (Next page). Overview of reversal of age-related changes in gene expression in mouse liver by CR. A) Venn diagrams showing genes whose expression significantly ($p < 0.05$) increased with age (yellow), decreased with calorie restriction (blue), or both. Only genes which had at least 10 reads in one or both of the samples being compared were included. B) The top ten genes increased with age but not affected by CR (ranked by highest FC_{age}), the top ten genes increased with age and decreased by CR (ranked by FC_{age}/FC_{CR}), and the top ten genes decreased with CR but not affected by age (ranked by lowest FC_{CR}). C) Top ten gene ontology terms enriched in genes from each diagram region of (A) (by p value; redundant terms were omitted). D) Venn diagrams showing genes whose expression significantly ($p < 0.05$) decreased with age (green), increased with calorie restriction (tan), or both. Only genes which had at least 10 reads in one or both of the samples being compared were included. E) The top ten genes decreased with age but not affected by CR (ranked by lowest FC_{age}), the top ten genes decreased with age and increased by CR (ranked by FC_{CR}/FC_{age}), and the top ten genes increased with CR but not affected by age (ranked by highest FC_{CR}). F) Top ten gene ontology terms enriched in genes from each diagram region of (D) (by p value; redundant terms were omitted). FC = fold change. For the FC rankings, genes with fewer than 100 reads in any sample, RIKEN cDNAs, and hypothetical protein loci were included in the analysis but omitted from the list shown.

Figure 4.2 (Continued).

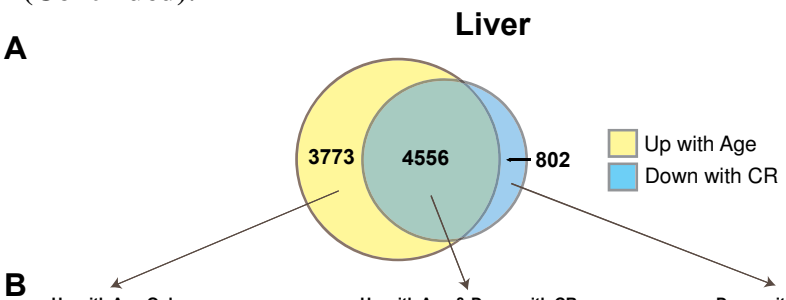

B

Up with Age Only

Genes	FC (Age)
CYP2B9	54.6
MMD2	18.1
CYP2B13	10.4
HAPLN4	9.51
SREBF1	7.85
SLP1	7.39
PER2	6.78
TOMM40	6.13
MARCO	5.42
PER3	5.12
.	
.	
.	

Up with Age & Down with CR

Genes	FC (Age)	FC (CR)
CIDEA	61.1	0.012
CYP46A1	40.6	0.056
NPAS2	2.15	0.011
GPRC5B	22.2	0.156
TEM5	8.12	0.080
ADAM11	9.94	0.099
LAD1	1.32	0.017
CYP4A12A	1.42	0.019
CYP4A12B	1.38	0.019
SEMA5B	5.58	0.084
.		
.		
.		

Down with CR Only

Genes	FC (CR)
PITX3	0.000
ELOVL3	0.026
SLCO1A1	0.030
ARNTL	0.046
CDKN1A	0.046
CFD	0.053
MUP20	0.055
LY6D	0.082
MUP7	0.086
MUP11	0.095
.	
.	
.	

C

Enriched GO Terms	Enriched GO Terms	Enriched GO Terms
Metabolic process	Metabolic process	Response to stimulus
Cellular metabolic process	Cellular metabolic process	Immune system process
Macromolecule metabolic process	Macromolecule metabolic process	Metabolic process
Nitrogen compound metabolic process	Regulation of metabolic process	Positive regulation of biological process
Biosynthetic process	Regulation of cellular metabolic process	Regulation of metabolic process
Small molecule metabolic process	Biological regulation	Developmental process
Nucleic acid metabolic process	Regulation of primary metabolic process	System development
Gene expression	Regulation of biological process	Cellular metabolic process
Biological regulation	Regulation of cellular process	Regulation of primary metabolic process
Protein metabolic process	Regulation of gene expression	Immune response
.	.	.
.	.	.
.	.	.

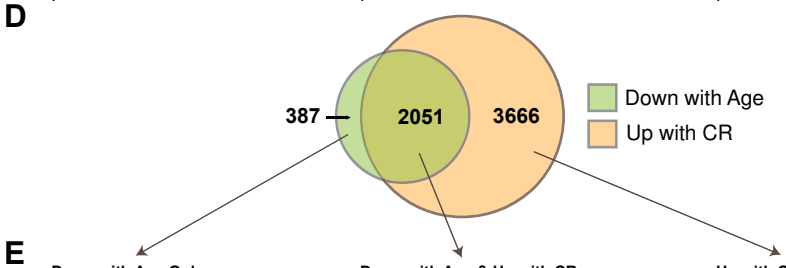

E

Down with Age Only

Genes	FC (Age)
TFF3	0.038
SERPINA4	0.100
SCARA5	0.108
CIB3	0.193
SLCO1A1	0.196
HSD3B5	0.208
MUP20	0.317
CFD	0.324
MUP21	0.331
EIF4EBP3	0.333
.	
.	
.	

Down with Age & Up with CR

Genes	FC (Age)	FC (CR)
MT2	0.065	4.11
MT1	0.134	8.04
S100A6	0.226	11.6
RPL22L1	0.282	10.5
ATP5E	0.210	7.02
FAM25C	0.184	6.00
SUMO1	0.262	6.89
LEAP2	0.250	6.49
NDUFA13	0.246	6.11
RPS27A	0.241	5.92
.		
.		
.		

Up with CR Only

Genes	FC (CR)
SULT2A3	(inf)
FMO3	2550
SULT2A2	873
SULT2A1	320
SULT1E1	172
CUX2	47.5
LRTM1	28.7
A1BG	23.3
SULT2A7	18.5
NNMT	13.5
.	
.	
.	

F

Enriched GO Terms	Enriched GO Terms	Enriched GO Terms
Nuclear division	Metabolic process	Metabolic process
Mitosis	Cellular metabolic process	Cellular metabolic process
M phase of mitotic cell cycle	Tanslation	Macromolecule metabolic process
Organelle fission	Generation of precursor metabolites	Nitrogen compound metabolic process
Cell division	Oxidation reduction	Small molecule metabolic process
Cellular process	Electron transport chain	Biosynthetic process
Cell cycle	Macromolecule metabolic process	Nucleic acid metabolic process
Mitotic cell cycle	Biosynthetic process	Gene expression
Immune response	Small molecule metabolic process	Protein metabolic process
Complement activation	Cellular protein metabolic process	Catabolic process
.	.	.
.	.	.
.	.	.

Figure 4.3 (Next page). Overview of reversal of age-related changes in gene expression in mouse heart by CR. A) Venn diagrams showing genes whose expression significantly ($p < 0.05$) increased with age (yellow), decreased with calorie restriction (blue), or both. Only genes which had at least 10 reads in one or both of the samples being compared were included. B) The top ten genes increased with age but not affected by CR (ranked by highest FC_{age}), the top ten genes increased with age and decreased by CR (ranked by FC_{age}/FC_{CR}), and the top ten genes decreased with CR but not affected by age (ranked by lowest FC_{CR}). C) Top ten gene ontology terms enriched in genes from each diagram region of (A) (by p value; redundant terms were omitted). D) Venn diagrams showing genes whose expression significantly ($p < 0.05$) decreased with age (green), increased with calorie restriction (tan), or both. Only genes which had at least 10 reads in one or both of the samples being compared were included. E) The top ten genes decreased with age but not affected by CR (ranked by lowest FC_{age}), the top ten genes decreased with age and increased by CR (ranked by FC_{CR}/FC_{age}), and the top ten genes increased with CR but not affected by age (ranked by highest FC_{CR}). F) Top ten gene ontology terms enriched in genes from each diagram region of (D) (by p value; redundant terms were omitted). FC = fold change. For the FC rankings, genes with fewer than 100 reads in any sample, RIKEN cDNAs, and hypothetical protein loci were included in the analysis but omitted from the list shown.

Figure 4.3 (Continued).

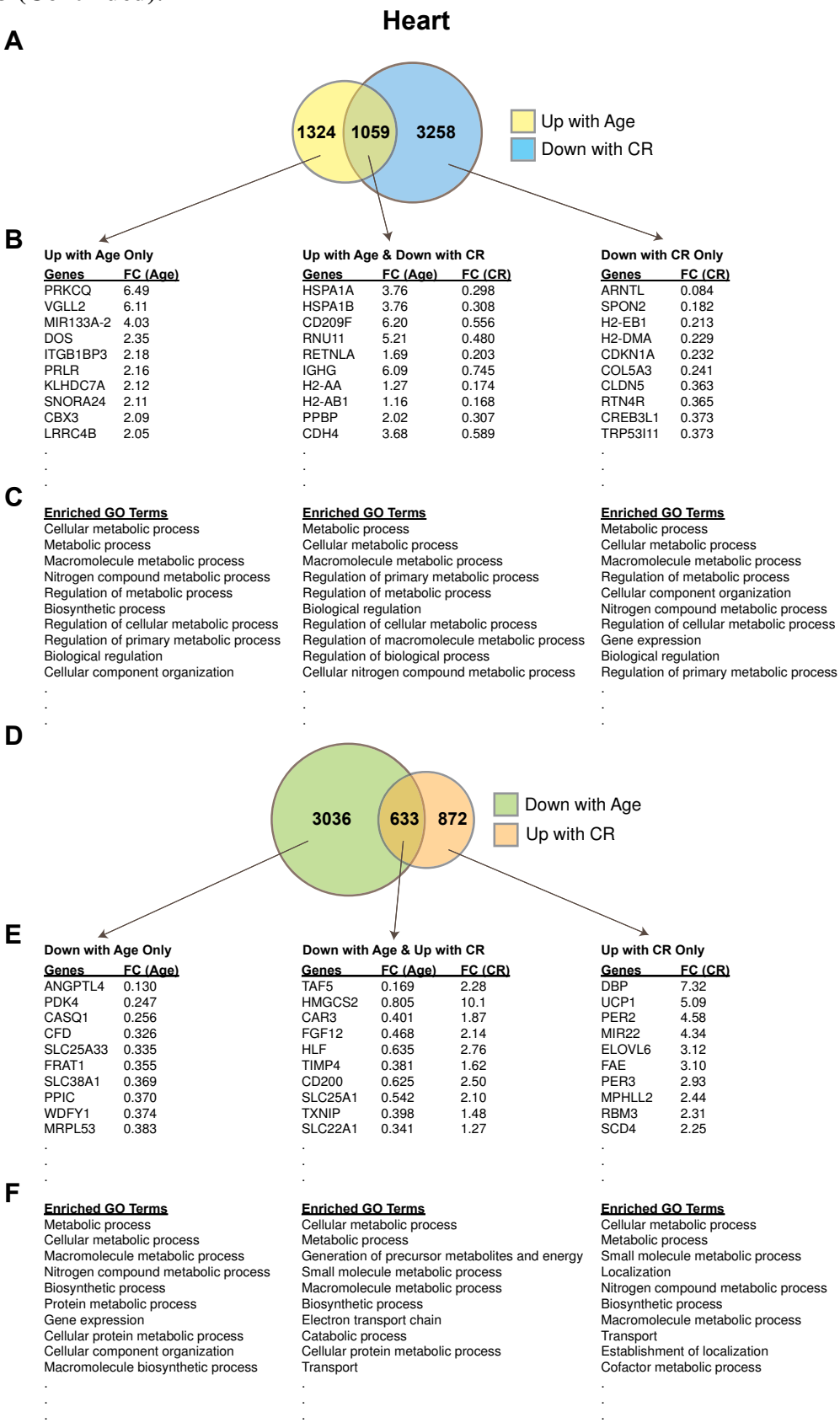

Plots of the raw numbers of reads for each gene between samples also show that gene expression changed to a greater degree in the liver than in the heart (Figure 4.4). In the liver, the R^2 for the trend line between the aged control and the young control sample was 0.863 (Figure 4.4A), while in the heart it was 0.953 for the plot of aged control sample vs. young control sample (Figure 4.4B). This reflects more variation in a gene's reads between the young and aged control samples in the liver than in the heart. The same holds true for the effect of calorie restriction, where the R^2 values for plots of aged CR sample vs. aged control sample were 0.486 in the liver (Figure 4.4C) and 0.989 in the heart (Figure 4.4D). Overall, gene expression in the liver was more perturbed by aging and CR than gene expression in the heart.

Gene expression validation

To confirm the RNA-seq results, we used a separate approach to measure expression changes with age and calorie restriction. Beginning with the same RNA (unpooled), we conducted quantitative PCR of several genes from the liver samples that exhibited pronounced changes with both aging and CR in the RNA-seq data to verify that the results were similar (Figure 4.5). For example, SIRT3, which was decreased with age and induced with CR in the liver RNA-seq data, exhibited the same pattern when assayed by qPCR (Figure 4.5E; for qPCR data, $p = 0.10$ for effect of aging and $p = 0.029$ for effect of CR; both are highly significant in RNA-seq data). Together, these and the other genes shown in Figure 4.5 validate the gene expression values obtained by RNA-seq.

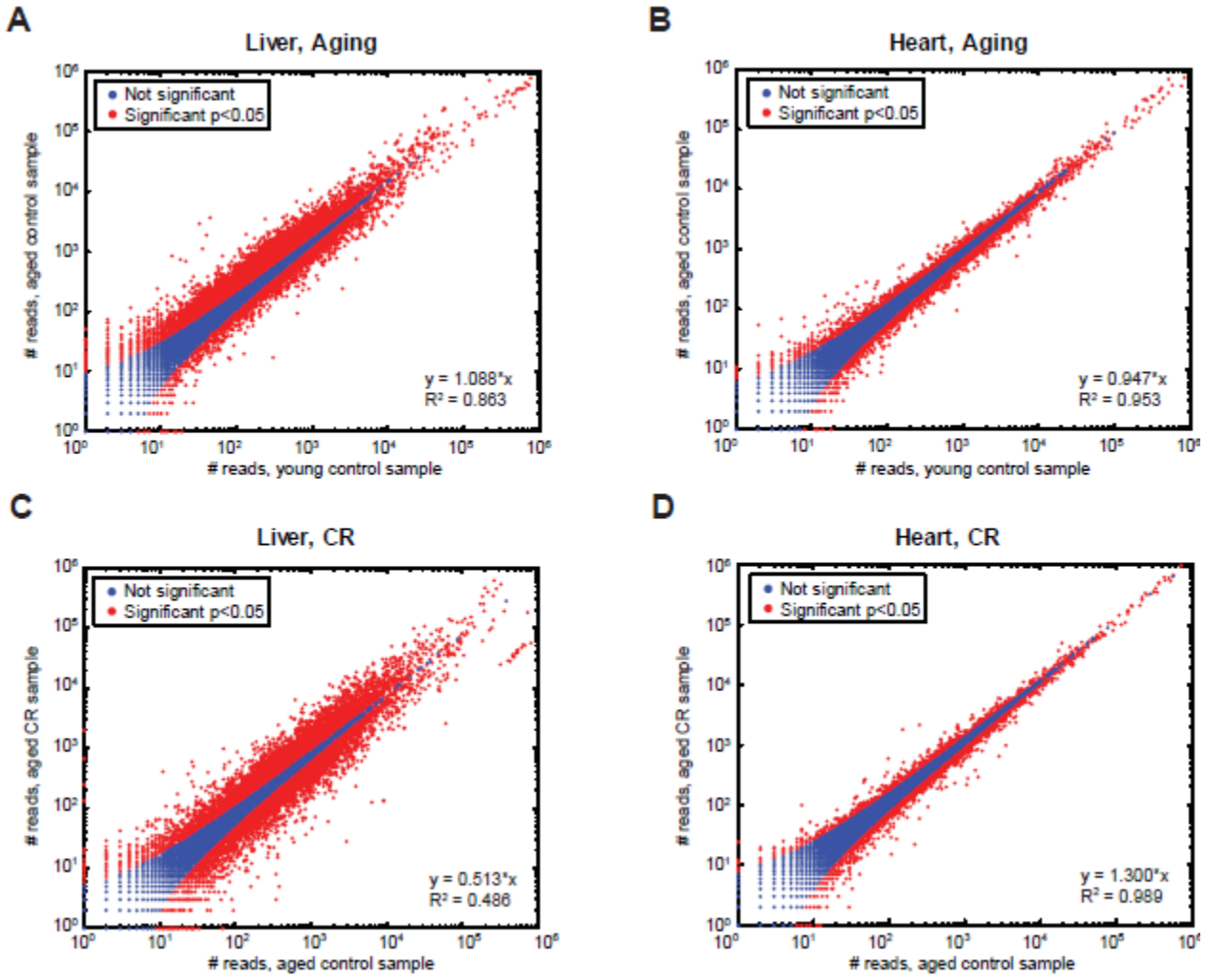

Figure 4.4. Comparison of the number of raw RNA-seq reads between samples for each gene. Plots are shown for A) the young control vs. aged control samples in the liver; B) the young control vs. aged control samples in the heart; C) the aged control vs. aged CR samples in the liver; and D) the aged control vs. aged CR samples in the heart. Only genes which had at least 10 reads in one or both of the samples being compared were included. Least-squares regression lines and R^2 values were calculated for the data, with the y-intercept of each line set to zero.

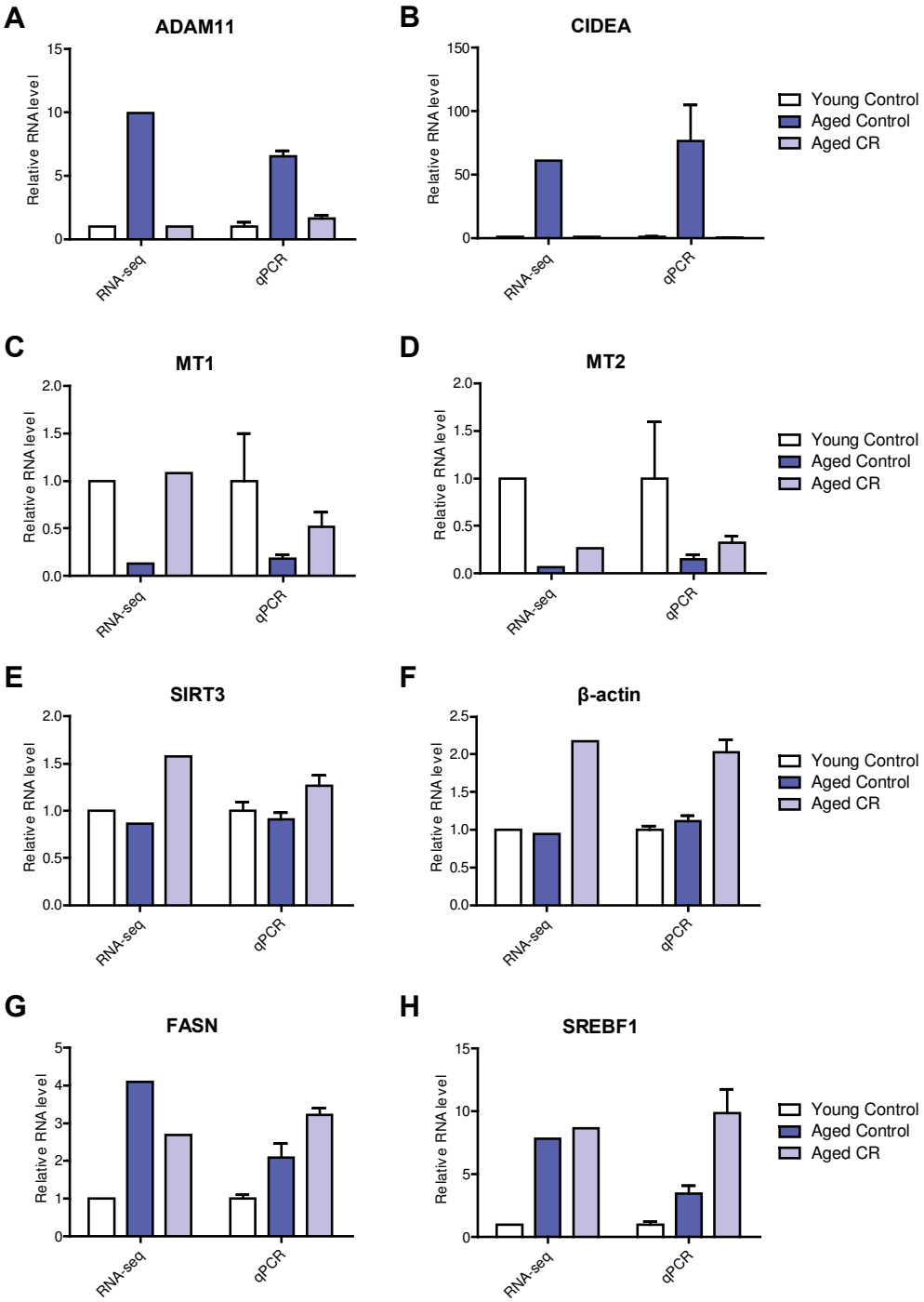

Figure 4.5. Validation of RNA-seq gene expression results by qPCR in the liver. Comparisons of RNA-seq gene expression results with those obtained by quantitative PCR, starting with the same RNA, for A) disintegrin and metalloproteinase domain-containing protein 11 (ADAM11), B) cell death activator CIDE-A (CIDEA), C) metallothionein 1 (MT1), D) metallothionein 2 (MT2), E) sirtuin 3 (SIRT3), F) β-actin, G) fatty acid synthase (FASN), and H) sterol regulatory element-binding transcription factor 1 (SREBF1). Genes were selected that exhibited a pronounced age- or CR-related change in expression. Heat shock protein 90kDa α, class B member 1 (HSP90AB1) was used as the reference gene. n = 4 samples per condition.

Isoform scores

Because RNA-seq provides nucleotide-level detail of transcript expression, we were also able to calculate "isoform scores" to quantify the difference in RNA-seq read profiles (the number of reads, or read depth, along a gene's DNA sequence) for each gene between two samples. These are scores of arbitrary units following the methodology of Christodoulou et al. (2014), where a larger score indicates a larger difference in read profile between samples at annotated transcription start sites for a gene (start sites used listed in Supplementary File 4.1). This score captures alternate start site usage, as well as any other effect which changes the relative proportion of a gene's reads which lie in that section of the gene. For the purposes of this study, we have termed this value an "isoform score." This was a novel application, and we investigated whether isoform scores were more plastic under aging and CR in one tissue than in another, as well as whether isoform scores were higher in genes with significantly changed expression levels than in genes whose overall expression level was unchanged.

Just as gene expression in the liver was more plastic under aging and CR in the liver than in the heart, isoform scores were higher in the liver as well (full results in Supplementary File 4.1). Under both aging and CR, the average score for all genes was higher in the liver, and more genes had a non-zero score in the liver (Table 4.2, Figure 4.6). Isoform scores were in general higher in genes with a significant change in overall expression level, suggesting that perhaps the underlying biological process could be an up- or downregulation of one isoform while expression of other isoforms remained constant. There were exceptions to this, however – in the comparison between the control and CR liver samples, scores were essentially indistinguishable between the changed vs. unchanged genes with at least 100 reads, and at the 1000 read threshold the average isoform score of the unchanged genes was higher. There was also no significant

Table 4.2. Summary statistics for isoform scores. Within each organ, results are shown for three different read thresholds. "Changed" genes refers to genes whose expression is significantly up or down ($p < 0.05$) with the given treatment or between the two tissues. "Unchanged" genes have no significant difference. P values for scores of changed vs. unchanged genes were calculated with a two-tailed student's t-test. A gene was included in the analysis if either of the two samples being compared had a number of reads equal to or higher than the specified minimum reads per gene threshold.

	Liver			**Heart**		
Min reads/gene:	10	100	1000	10	100	1000
Aging						
Genes	15694	11176	3541	15902	10563	2555
Genes with non-zero score	6668	6158	2230	2758	2413	583
Percentage	42%	55%	63%	17%	23%	23%
Avg score, all genes	**18.49**	**25.06**	**35.03**	**2.46**	**3.31**	**4.26**
Avg score, changed genes	23.04	27.02	36.38	3.25	3.69	4.49
Avg score, unchanged genes	8.55	16.70	18.19	1.98	2.86	3.52
Pval, changed vs. unchanged	2E-101	1.6E-21	6.3E-07	2.2E-14	3.7E-04	0.24
CR						
Genes	15871	11435	3875	15926	10492	2520
Genes with non-zero score	6189	5728	2150	1906	1639	389
Percentage	39%	50%	55%	12%	16%	15%
Avg score, all genes	**15.80**	**21.14**	**28.12**	**1.25**	**1.64**	**2.25**
Avg score, changed genes	18.21	21.38	27.65	1.63	1.86	2.59
Avg score, unchanged genes	10.24	20.13	34.89	1.03	1.45	1.57
Pval, changed vs. unchanged	1.4E-36	0.21	0.032	1.8E-08	5.6E-03	0.044

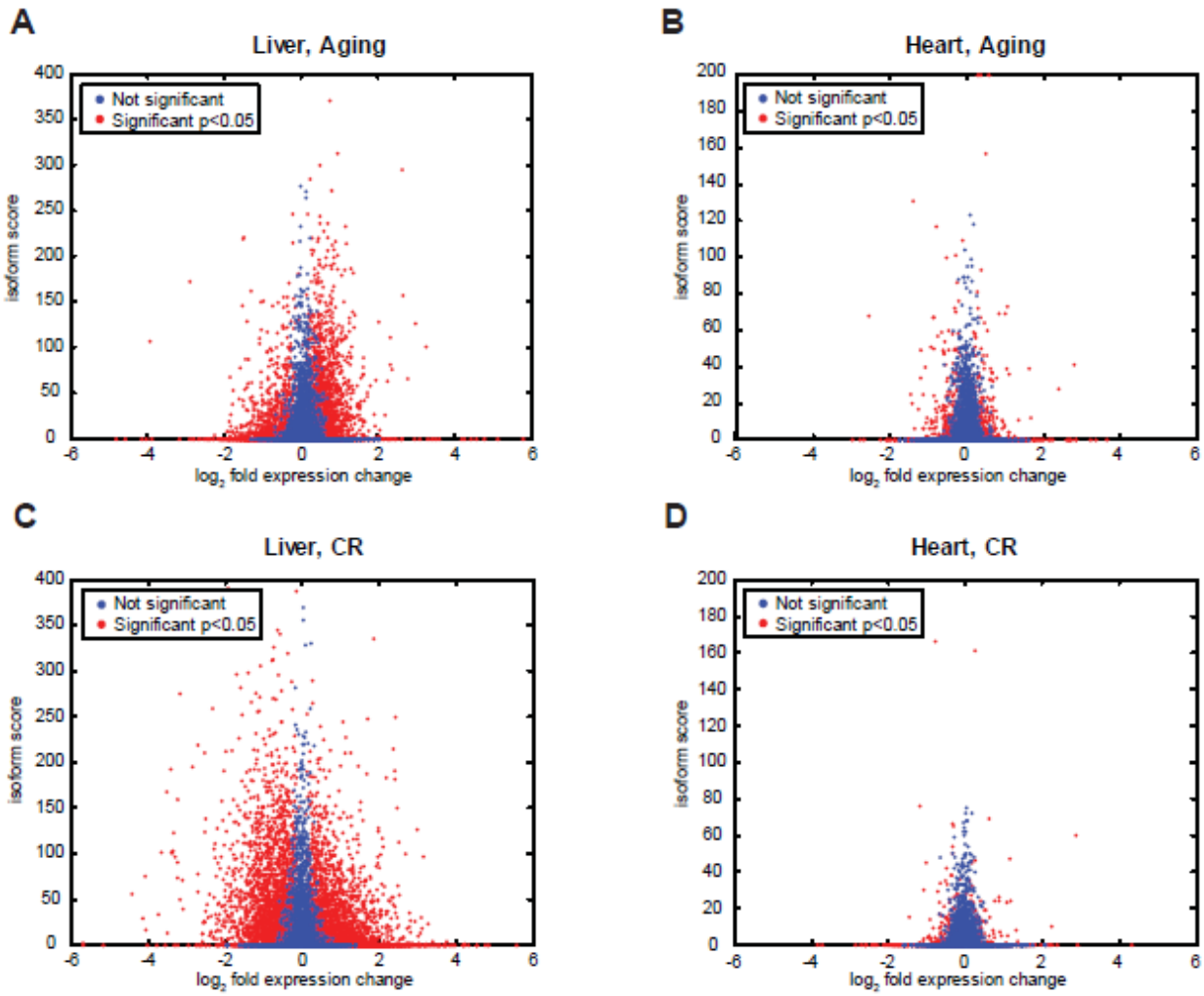

Figure 4.6. Comparison of isoform score with fold gene expression change for RNA-seq results. Plots are shown for A) liver, young control vs. aged control samples; B) heart, young control vs. aged control samples; C) liver, aged control vs. aged CR samples; and D) heart, aged control vs. aged CR samples. Only genes which had at least 10 reads in one or both of the samples being compared were included. The red (significant $p < 0.05$) or blue (not significant) refers to significance of gene expression change with aging or calorie restriction.

difference between changed and unchanged genes' isoform scores with aging in heart at the 1000 read threshold. Thus isoform scores were not uniformly higher in genes with significantly changed overall expression level, allowing for the possibility that some genes had expression of one isoform increase while expression of another isoform decreased.

Reversal of age-related changes in read profile by CR

We next analyzed whether any of the changes in read profile with age were reversed by CR. To examine this, we created a "meta" score defined as: (isoform score for aging) + (isoform score for CR) – 2*(isoform score between young and CR samples). The genes which scored most highly on this metric would have nearly identical isoform usage between the young control and aged CR samples, and both would be very different from the aged control sample. We calculated this score for each gene, and the top 25 genes by "meta" score are given in Table 4.3 for the liver and Table 4.4 for the heart. The top result in the liver (and also the top overall result), *SEC31A*, is thought to have three isoforms and is a component of the coat protein complex II which promotes the budding of vesicles from the endoplasmic reticulum. The top result in the heart, *NT5E*, is a membrane protein which hydrolyzes the phosphate from extracellular nucleotides, turning them into membrane-permeable nucleosides. Read profiles for *SEC31A* are given in Figure 4.7, which shows that the young control sample and the aged CR sample use primarily the 5'-most transcription start site, while the aged control sample seems to have relatively higher usage of an alternative downstream transcription start site. These data suggest that CR is capable of reversing age-related changes in the relative proportion of isoforms expressed from a given locus.

Table 4.3. Liver genes with changes in isoform usage in aging that are reversed by CR. Top 25 genes are shown, ranked by "meta" score. C/Y = isoform score for aging. CR/C = isoform score for calorie restriction. CR/Y = isoform score for CR sample compared to young sample. Higher isoform scores indicate larger change in isoform usage. "Meta" score calculated by (C/Y)+(CR/C)-2*(CR/Y). Putative uncharacterized proteins and unnamed Riken cDNAs are not shown.

Gene	Description	C/Y	CR/C	CR/Y	Meta
SEC31A	Protein transport protein Sec31A	586	422	3	1002
WDTC1	WD and tetratricopeptide repeats 1	400	391	0	791
FASTK	Fas activated serine/threonine kinase	378	341	0	719
ACAA2	3-ketoacyl-CoA thiolase	300	370	6	658
WAC	WW domain-containing adapter protein	325	312	0	637
PCF11	Pre-mRNA cleavage complex II protein Pcf11	264	356	0	620
ABL1	Tyrosine-protein kinase ABL1	336	313	15	619
B4GALNT1	β-1,4 N-acetylgalactosaminyltransferase 1	404	279	42	599
TUG1	Taurine upregulated gene 1	313	282	6	583
MOV10	Putative helicase MOV-10	262	320	2	578
MBD6	Methyl-CpG binding domain protein 6	416	259	49	577
NCOR1	Nuclear receptor co-repressor 1	290	306	16	564
ZDHHC16	Zinc finger DHHC domain-containing protein 16	271	290	0	561
FGFR4	Fibroblast growth factor receptor 4 precursor	318	229	2	543
MLL2	Histone-lysine N-methyltransferase MLL2	253	282	0	535
CIC	Protein capicua homolog	348	227	28	519
INF2	Inverted formin-2	233	329	24	514
ANKS1	Ankyrin repeat and SAM domain-containing protein	286	231	7	503
GPR137	Integral membrane protein GPR137	278	236	6	502
NDST1	Bifunctional heparan sulfate	238	270	5	498
LRRC16A	Leucine-rich repeat-containing protein 16A	235	266	5	491
HNF4A	Hepatocyte nuclear factor 4-alpha	271	212	0	483
NPR2	Atrial natriuretic peptide receptor 2 precursor	262	257	19	481
GORASP2	Golgi reassembly-stacking protein 2	371	145	18	480

Table 4.4. Heart genes with changes in isoform usage in aging that are reversed by CR. Top 25 genes are shown, ranked by "meta" score. C/Y = isoform score for aging. CR/C = isoform score for calorie restriction. CR/Y = isoform score for CR sample compared to young sample. Higher isoform scores indicate larger change in isoform usage. "Meta" score calculated by (C/Y)+(CR/C)-2*(CR/Y). Putative uncharacterized proteins and unnamed Riken cDNAs are not shown.

Gene	Description	C/Y	CR/C	CR/Y	Meta
NT5E	5'-nucleotidase	117	67	0	184
SENP1	Sentrin-specific protease 1	123	48	10	151
ACTG1	Actin, cytoplasmic 2	66	52	0	118
TENC1	tensin-like C1 domain-containing phosphatase	150	1	17	117
SCS	GTP-specific succinyl-CoA synthetase β subunit	50	55	0	105
GPR157	G-protein coupled receptor 157	89	14	0	103
AGRN	Agrin	43	60	0	103
NFYA	Nuclear transcription factor Y subunit α	93	5	0	98
ARL6IP6	ADP-ribosylation factor-like protein	55	41	0	96
PCX	Pyruvate carboxylase, mitochondrial	44	50	0	94
CCAR1	Cell division cycle and apoptosis regulator	99	16	12	91
TCF4	Transcription factor 4	86	17	7	89
PCM1	Pericentriolar material 1 protein	38	50	0	88
WDFY1	WD repeat and FYVE domain containing 1	131	0	22	87
SULF2	Extracellular sulfatase Sulf-2 precursor	71	16	0	87
ACP2	Lysosomal acid phosphatase precursor	81	5	0	86
UNC93B1	Protein unc-93 homolog B1	84	0	0	84
ACAD10	Acyl-CoA dehydrogenase family member 10	46	38	0	84
LSP1	Lymphocyte-specific protein 1	9	79	2	84
FADS2	Fatty acid desaturase 2	60	22	0	82
CCL21B	C-C motif chemokine 21a	40	51	6	79
USP4	Ubiquitin carboxyl-terminal hydrolase 4	59	29	5	78
TMEM57	Macoilin	66	12	0	78
CYP4B1	Cytochrome P450 4B1	69	12	2	77

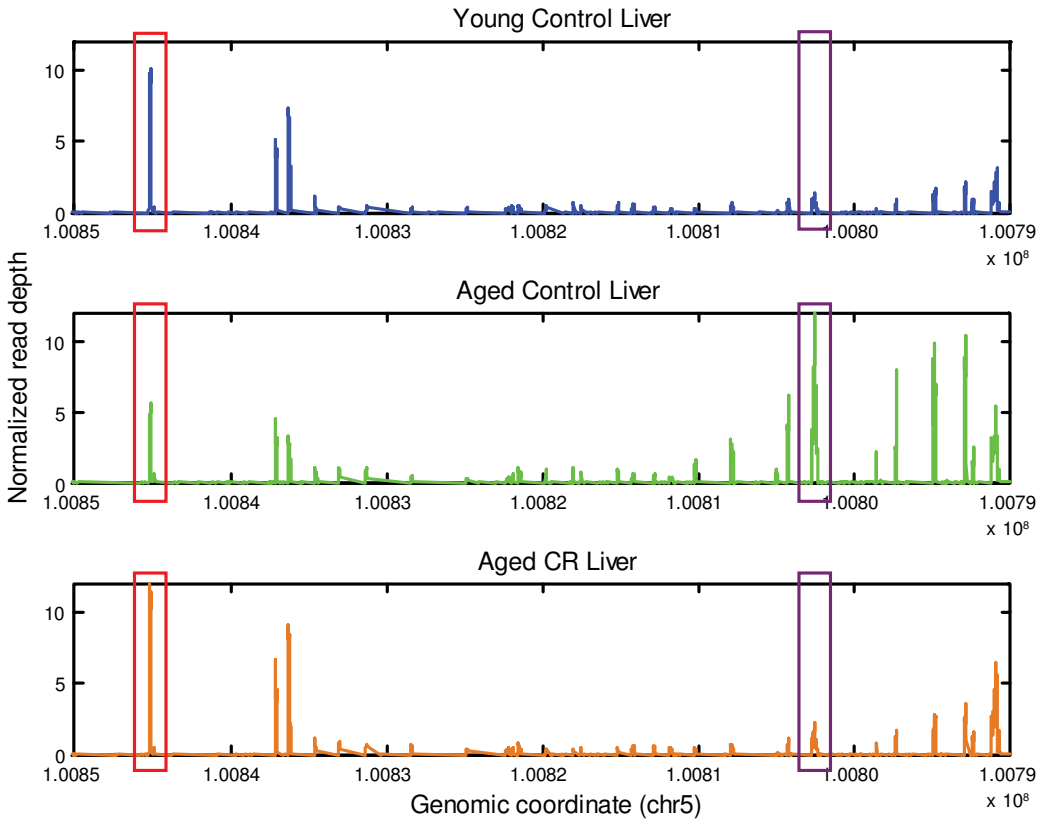

Figure 4.7. Liver read profiles for *SEC31A*, the gene with the highest overall "meta" score, along the mouse (-) strand of chromosome 5. The 5'-most transcription start site is shown in a red box. An alternate downstream transcription start site is shown in a purple box. At any given location along the gene, a higher read profile indicates a larger number of transcripts which map to that segment of the gene.

To gain a clearer understanding of the pathways which the top "meta" scoring genes participated in, we conducted gene ontology analysis to identify enriched GO terms in the top 100 liver and heart genes. Top results for the liver (Table 4.5) included the terms "metabolic process" and "fatty acid beta oxidation," while top results for the heart (Table 4.6) also included terms such as "response to stimulus," "developmental process," "cell differentiation," and "insulin receptor signaling pathway." Thus the genes whose age-related changes in isoform usage are reversed by calorie restriction seem to lie in primarily metabolic pathways in the liver and, although the genes are lower-scoring overall, in a broader array of pathways in the heart.

Examination of SIRT3

Finally, we used the high granularity of the RNA-seq data to take a close look at the expression of SIRT3. The mouse *SIRT3* gene has seven exons and gives rise to three different transcript variants (Figure 4.8A; described in Yang et al., 2010). The first exon has two alternative versions – exons 1a and 1b – which are incorporated into the transcript in a mutually exclusive manner. At the 5' end of exon 2, there is also an 8 bp insertion which is sometimes omitted from transcripts containing exon 1b, providing a third possible transcript variant. In our *SIRT3* RNA-seq data, although we did not observe a shift in isoform usage with aging or CR, we did see a significant difference between liver and heart transcripts in the rate of incorporation of the 8 bp insertion. Based on comparing the integrated read profile of the insertion with that of the rest of exon 2, we calculated that the insert was incorporated in heart transcripts approximately 48% as often as in transcripts from the liver (quantified in Figure 4.8B, visualized in Figure 4.8C). This difference was highly significant ($p = 3.9 \times 10^{-4}$).

Table 4.5. Top 20 gene ontology terms enriched in 100 liver genes with highest "meta" score. Redundant terms omitted. Corr p value = corrected p value.

GO Term	GO ID	Corr p value
Metabolic process	8152	8.35E-06
Cellular metabolic process	44237	2.22E-05
Macromolecule metabolic process	43170	9.96E-05
Regulation of gene-specific transcription from RNA pol II promoter	10551	3.11E-04
Regulation of gene-specific transcription	32583	7.76E-04
Fatty acid beta-oxidation	6635	3.76E-03
Nucleoside, nucleotide and nucleic acid metabolic process	6139	3.76E-03
Regulation of macromolecule biosynthetic process	10556	4.17E-03
Regulation of transcription	45449	4.17E-03
Biosynthetic process	9058	4.31E-03
Lipid modification	30258	4.31E-03
Nitrogen compound metabolic process	6807	4.90E-03
Post-translational protein modification	43687	5.41E-03
Regulation of cellular biosynthetic process	31326	5.41E-03
Positive regulation of transcription	45941	5.41E-03
Regulation of biosynthetic process	9889	5.41E-03
Macromolecule biosynthetic process	9059	5.41E-03
Fatty acid catabolic process	9062	5.41E-03
Nucleic acid metabolic process	90304	5.41E-03
Transcription	6350	5.41E-03

Table 4.6. Top 20 gene ontology terms enriched in 100 heart genes with highest "meta" score. Redundant terms omitted. Corr p value = corrected p value.

GO Term	GO ID	Corr p value
Metabolic process	8152	6.05E-08
Cellular metabolic process	44237	3.59E-07
Cellular component organization	16043	1.19E-05
Response to stimulus	50896	1.19E-05
Macromolecule metabolic process	43170	2.23E-04
Nucleoside, nucleotide and nucleic acid metabolic process	6139	1.19E-03
Nucleic acid metabolic process	90304	1.19E-03
Response to chemical stimulus	42221	1.67E-03
Developmental process	32502	1.96E-03
Cell differentiation	30154	2.48E-03
Nervous system development	7399	2.48E-03
Cellular nitrogen compound metabolic process	34641	2.48E-03
Cell development	48468	2.48E-03
Organelle organization	6996	2.81E-03
Anatomical structure development	48856	2.91E-03
Regulation of macromolecule biosynthetic process	10556	2.91E-03
Response to external stimulus	9605	3.41E-03
Insulin receptor signaling pathway	8286	3.80E-03
Cellular biosynthetic process	44249	4.16E-03
Locomotion	40011	4.26E-03

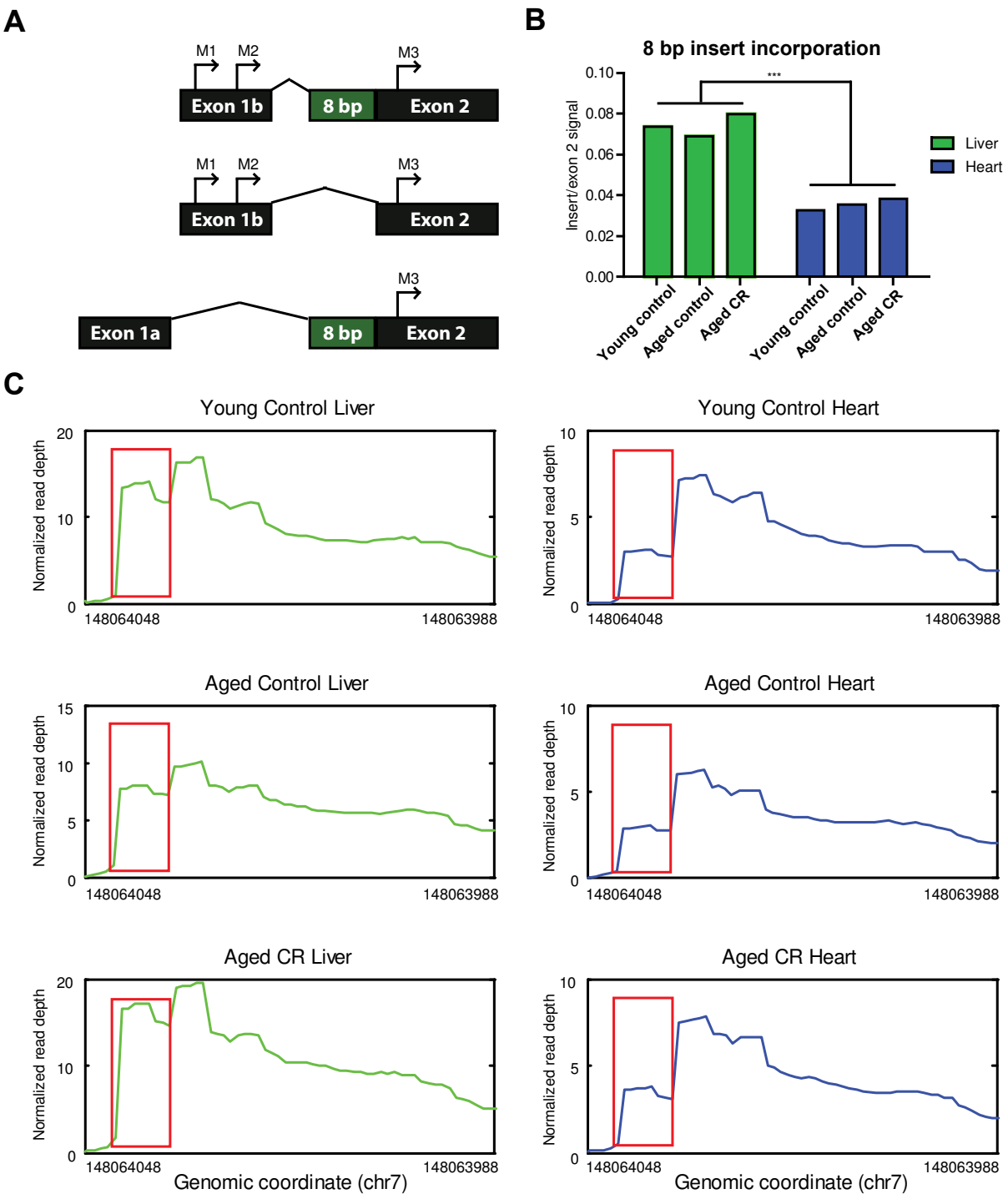

Figure 4.8. Comparison of 8 bp insert incorporation in mouse SIRT3 transcripts from liver and heart. A) Schematic of the three possible mouse SIRT3 transcript isoforms, adapted from Yang et al. (2010). Possible translation start codons are labeled M1, M2, and M3. Only the first two of seven exons are shown. B) Integrated read profiles for the 8 bp insert relative to the rest of exon 2 for the *SIRT3* gene. C) Read profiles along the beginning of *SIRT3* exon 2 on the mouse (-) strand of chromosome 7. Red box shows 8 bp insert. *** indicates $p < 0.001$. Two-tailed student's t test was used for P values.

The 8 bp insertion is thought to function as a method for controlling which of three possible translation start sites are used to produce full-length SIRT3 protein (Yang et al., 2010). Two of the start sites (M1 and M2) are in exon 1b, upstream of the 8 bp insertion, while the other (M3) is in exon 2, downstream of the insertion. Because M1 and M2 are not present in exon 1a, the only SIRT3 protein produced by these transcripts begins with M3. When exon 1b is incorporated, any of the three start sites may be used. However, when the insertion is present, use of either M1 or M2 will result in premature termination at a stop codon early in exon 2. Thus, the only full-length SIRT3 protein capable of being produced from a transcript with the insertion is the form beginning with M3. Our data therefore suggests that the heart may have a higher proportion of SIRT3 protein beginning with M1 or M2 than the liver. All three of these protein isoforms are reported to be enzymatically active, but the M3 form may be targeted to mitochondria with a lower efficiency (Yang et al., 2010). If this is the case, then SIRT3 protein in the heart may localize to the mitochondria with greater efficiency than SIRT3 protein in the liver. Further study will be necessary to verify this and to explore functional consequences of the regulation of SIRT3 isoform expression.

Discussion

We conducted RNA-seq on liver and heart tissue from young control, aged control, and aged short-term calorie-restricted mice. On the level of gene expression, we found that aging and calorie restriction both changed the expression levels of thousands of genes in the liver and heart, with gene expression changed to a greater degree in the liver. Many of the age-related changes were reversed by CR. This effect was also greater in the liver, where over 80% of genes decreased by age were reversed by CR, and over 80% of genes down with CR had been

increased by age. Gene ontology analysis showed these genes to be involved in metabolic processes, and RNA-seq expression levels were validated by qPCR.

Aging and CR also changed read profiles for certain genes, as quantified by isoform scores. As with gene expression, changes were more dramatic in the liver than heart. We defined a "meta" score to identify genes whose changes in isoform score with aging were reversed by CR, and we identified many genes for which this occurred. CR reversed age-related changes in isoform score in both genes which had a significant change in overall expression and also in genes which did not. In the liver, gene ontology analysis found that these genes were primarily metabolic, but in the heart they were involved in a wider array of pathways.

Taken together, our data show the promise of RNA-seq methods for investigating previously unexplored gene expression phenomena. The mechanisms by which calorie restriction extends lifespan remain unclear, and the reversal of age-related changes in the relative proportion of isoforms expressed from a given locus is a novel potential mechanism by which CR may regulate genes in the cell.

Methods

Mice

Mice were obtained and calorie-restricted as described (Cerletti et al., 2012). Briefly, aged C57BL/6 mice (National Institutes of Aging) and young C57BL/6 mice (Jackson Laboratories) were fed an AIN-93M diet (BioServ, NJ). After calculation of baseline food intake, aged mice were randomly divided into control and CR groups while young mice were entirely kept as controls. Calorie restriction was then carried out according to established protocols (Pugh et al., 1999) as described (Cerletti et al., 2012). Aged mice were 18 months old

at the beginning of the feeding schedule, and young mice were 2 months old. For the first week, control mice were fed 90% and CR mice were fed 80% of their *ad libitum* food intake (3 g/day). CR mice were then switched to 60% of their *ad libitum* intake (2.3 g/day), and the feeding schedule continued for 11 weeks. Liver tissue and heart tissue were then obtained.

RNA-seq

RNA was extracted from homogenized harvested tissue using TRIzol (Life Technologies), and the aqueous phase was purified using RNEasy kits (Qiagen). For both liver and heart, equal amounts of RNA from four mice per condition were pooled to produce RNA samples representing young control, aged control, and aged calorie-restricted mice. For each of these six samples, an RNA-seq library was constructed using 5' poly-A selection and PCR techniques (Christodoulou et al., 2014) and high-throughput RNA sequencing was carried out using an Illumina HiSeq flowcell sequencer. Following sequencing, raw sequence read data was aligned to the mouse mm9 genome using TopHat (Trapnell et al., 2009). Statistics for the alignment are given in Table 4.7. Gene expression profiles were calculated by normalizing read depth on each gene, and a Bayesian p value was calculated to determine the significance of gene expression changes (Audic & Claverie 1997; Christodoulou et al., 2011). Isoform scores were generated to quantify the difference in genes' read profiles between two samples following Christodoulou et al. (2014).

Quantitative PCR

Synthesis of cDNA was carried out with iScript cDNA Synthesis Kits (Bio-Rad), starting from the same RNA used to construct the RNA-seq library. Quantitative PCR was performed

Table 4.7. Statistics for the alignment of the raw RNA-seq reads to the mouse genome using TopHat.

Sample	Number raw reads (total)	Aligned (total)	Percentage aligned	Aligned as paired-ends	Aligned single
Young Control Liver	45603788	43390553	95.1%	35595308	7795245
Aged Control Liver	69275854	65508388	94.5%	55455516	10052872
Aged CR Liver	71615068	57315897	80.0%	51269762	6046135
Young Control Heart	61137582	51988470	85.0%	47960490	4027980
Aged Control Heart	58762002	47431651	80.7%	43499522	3932129
Aged CR Heart	69899858	57452236	82.1%	52435822	5016414

with 2x PerfeCTa SYBR Green FastMix (Quanta). Primers for SIRT3 are from Kong et al. (2010); primer sequences are given in Table 4.8. Heat shock protein 90kDa α, class B member 1 (HSP90AB1) had stable expression across RNA-seq samples and was used as a reference gene.

Gene ontology analysis

Analysis of overrepresented gene ontology terms was conducted within the Cytoscape software program (Cline et al., 2007) using the BiNGO plugin (Maere et al., 2005), with the whole *mus musculus* annotation as the reference set. The hypergeometric statistical test and Benjamini & Hochberg FDR correction options were used.

Acknowledgements

This work was supported in part by NIH Training Grant No. T32 DK007260. Thanks are due to Steve DePalma and Michael Parfenov of Harvard Medical School for their assistance processing the raw data files.

Table 4.8. Sequences of qPCR primers used in this study. All sequences are for mouse genes. The SIRT3 sequences are from Kong et al. (2010).

Gene	Direction	Sequence
ADAM11	Forward	5'-AAAGCCACAGTTGGACACCA-3'
	Reverse	5'-ATACTGCGAGGACAGGAGGT-3'
CIDEA	Forward	5'-CATACATCCAGCTCGCCCTT-3'
	Reverse	5'-CGTAACCAGGCCAGTTGTGA-3'
MT1	Forward	5'-AGATCTCGGAATGGACCCCA-3'
	Reverse	5'-AGGAGCAGCAGCTCTTCTTG-3'
MT2	Forward	5'-TCGTCGATCTTCAACCGCC-3'
	Reverse	5'-CACTTGTCGGAAGCCTCTTTG-3'
SIRT3	Forward	5'-GCTGCTTCTGCGGCTCTATAC-3'
	Reverse	5'-GAAGGACCTTCGACAGACCGT-3'
β-actin	Forward	5'-AGCCATGTACGTAGCCATCC-3'
	Reverse	5'-CTCTCAGCTGTGGTGGTGAA-3'
FASN	Forward	5'-AAGCGGTCTGGAAAGCTGAA-3'
	Reverse	5'-CCTCTGAACCACTCACACCC-3'
SREBF1	Forward	5'-GACCCTACGAAGTGCACACA-3'
	Reverse	5'-TGTCGGGCTCAGAGTCACTA-3'
HSP90AB1	Forward	5'-TTTCAGGCAGAAATTGCCCAGCTC-3'
	Reverse	5'-TCTTGTCCAGGGCATCTGAAGCAT-3'

References

Audic S, Claverie JM (1997) The significance of digital gene expression profiles. *Genome Res*. **7**, 986-995.

Barger JL, Kayo T, Vann JM, Arias EB, Wang J, Hacker TA, Wang Y, Raederstorff D, Morrow JD, Leeuwenburgh C, Allison DB, Saupe KW, Cartee GD, Weindruch R, Prolla TA (2008) A low dose of dietary resveratrol partially mimics caloric restriction and retards aging parameters in mice. *PLoS One* **3**, e2264.

Boylston WH, DeFord JH, Papaconstantinou J (2006) Identification of longevity-associated genes in long-lived Snell and Ames dwarf mice. *Age (Dordr.)* **28**, 125-144.

Cerletti M, Jang YC, Finley LW, Haigis MC, Wagers AJ (2012) Short-term calorie restriction enhances skeletal muscle stem cell function. *Cell Stem Cell* **10**, 515-519.

Christodoulou DC, Gorham JM, Kawana M, DePalma SR, Herman DS, Wakimoto H (2011) Quantification of gene transcripts with deep sequencing analysis of gene expression (DSAGE) using 1 to 2 μg total RNA. *Curr. Protoc. Mol. Biol*. **25**, B.9.

Christodoulou DC, Wakimoto H, Onoue K, Eminaga S, Gorham JM, DePalma SR, Herman DS, Teekakirikul P, Conner DA, McKean DM, Domenighetti AA, Aboukhalil A, Chang S, Srivastava G, McDonough B, De Jager PL, Chen J, Bulyk ML, Muehlschlegel JD, Seidman CE, Seidman JG (2014) 5'RNA-Seq identifies Fhl1 as a genetic modifier in cardiomyopathy. *J. Clin. Invest*. **124**, 1364-1370.

Cline MS, Smoot M, Cerami E, Kuchinsky A, Landys N, Workman C, Christmas R, Avila-Campilo I, Creech M, Gross B, Hanspers K, Isserlin R, Kelley R, Killcoyne S, Lotia S, Maere S, Morris J, Ono K, Pavlovic V, Pico AR, Vailaya A, Wang PL, Adler A, Conklin BR, Hood L, Kuiper M, Sander C, Schmulevich I, Schwikowski B, Warner GJ, Ideker T, Bader GD (2007) Integration of biological networks and gene expression data using Cytoscape. *Nat. Protoc*. **2**, 2366-2382.

Dhahbi JM, Atamna H, Boffelli D, Martin DI, Spindler SR (2012) mRNA-Seq reveals complex patterns of gene regulation and expression in the mouse skeletal muscle transcriptome associated with calorie restriction. *Physiol. Genomics* **44**, 331-344.

Hoerter J, Gonzalez-Barroso MD, Couplan E, Mateo P, Gelly C, Cassard-Doulcier AM, Diolez P, Bouillaud F (2004) Mitochondrial uncoupling protein 1 expressed in the heart of transgenic mice protects against ischemic-reperfusion damage. *Circulation* **110**, 528-533.

Jonker MJ, Melis JP, Kuiper RV, van der Hoeven TV, Wackers PF, Robinson J, van der Horst GT, Dollé ME, Vijg J, Breit TM, Hoeijmakers JH, van Steeg H (2013) Life spanning murine gene expression profiles in relation to chronological and pathological aging in multiple organs. *Aging Cell* **12**, 901-909.

Kong X, Wang R, Xue Y, Liu X, Zhang H, Chen Y, Fang F, Chang Y (2010) Sirtuin 3, a new target of PGC-1alpha, plays an important role in the suppression of ROS and mitochondrial biogenesis. *PLoS One* **5**, e11707.

Lee CK, Klopp RG, Weindruch R, Prolla TA (1999) Gene expression profile of aging and its retardation by caloric restriction. *Science* **285**, 1390-1393.

Maere S, Heymans K, Kuiper M (2005) BiNGO: a Cytoscape plugin to assess overrepresentation of gene ontology categories in biological networks. *Bioinformatics* **21**, 3448-3449.

Pugh TD, Klopp RG, Weindruch R (1999) Controlling caloric consumption: protocols for rodents and rhesus monkeys. *Neurobiol. Aging* **20**, 157-165.

Reiter E, Jiang Q, Christen S (2007) Anti-inflammatory properties of alpha- and gamma-tocopherol. *Mol. Aspects Med*. **28**, 668-691.

Shimazu T, Hirschey MD, Hua L, Dittenhafer-Reed KE, Schwer B, Lombard DB, Li Y, Bunkenborg J, Alt FW, Denu JM, Jacobson MP, Verdin E (2010) SIRT3 deacetylates mitochondrial 3-hydroxy-3-methylglutaryl CoA synthase 2 and regulates ketone body production. *Cell Metab*. **12**, 654-661.

Trapnell C, Pachter L, Salzberg SL (2009) TopHat: discovering splice junctions with RNA-Seq. *Bioinformatics* **25**, 1105-1111.

Weindruch R, Walford RL, Fligiel S, Guthrie D (1986) The retardation of aging in mice by dietary restriction: longevity, cancer, immunity and lifetime energy intake. *J. Nutr*. **116**, 641-654.

Yang Y, Hubbard BP, Sinclair DA, Tong Q (2010) Characterization of murine SIRT3 transcript variants and corresponding protein products. *J. Cell. Biochem*. **111**, 1051-1058.

Zhou Z, Yon Toh S, Chen Z, Guo K, Ng CP, Ponniah S, Lin SC, Hong W, Li P (2003) Cidea-deficient mice have lean phenotype and are resistant to obesity. *Nat. Genet*. **35**, 49-56.

CHAPTER V

Conclusion

Calorie restriction (CR) extends lifespan and delays the onset of age-related diseases in several model organisms, and understanding how it works has the potential to bring significant advances in therapeutics for humans. CR induces a wide-ranging organismal metabolic adaptation, and SIRT3 is one of its primary effectors. SIRT3 expression is upregulated by CR in multiple tissues, and its activities include increasing the throughput of the mitochondrial electron transport chain, promoting the catabolism of fatty acids, upregulating the urea cycle, upregulating ketone body production, and helping to fight inflammation. As more and more of its downstream functions are uncovered, it is becoming increasingly clear that SIRT3 is a key cog in the machinery of CR. Two studies have shown that peroxisome proliferator-activated receptor γ coactivator 1-α (PGC-1α) coactivates estrogen-related receptor α (ERRα) in the induction of SIRT3 levels (Kong et al, 2010; Giralt et al, 2011). Yet the pathways upstream of SIRT3 have received no further attention. This dissertation sought to address that gap and to provide tools for studying *SIRT3* transcriptional activity, to identify additional transcription factors which may be involved in regulating SIRT3 expression, and to shed light on the effects of CR on SIRT3 and the entire genome using high-throughput RNA sequencing (RNA-seq).

Tools for studying SIRT3 activity

We developed a luciferase-based reporter construct to study transcriptional activity of the human *SIRT3* promoter. Chapter II detailed the design and development of this tool, describing the steps involved in its construction and validation. We showed that results from our reporter could be verified by both quantitative real-time PCR and Western blot, and we used it to

demonstrate that SIRT3 expression in human 293T cells is upregulated by inhibition of the nutrient-sensing Target of Rapamycin pathway. We subsequently used it in Chapter III as part of our investigation of transcription factors which regulate *SIRT3*. In the future, this tool could be used in research applications such as screening for small molecules or proteins that activate SIRT3 expression. Further, SIRT3 has reduced expression or is lost entirely in many breast cancer cell lines (Finley et al., 2011), and a decrease in its expression is a biomarker associated with poor outcome in patients (Desouki et al., 2014). This tool could therefore also be used in clinical practice as a diagnostic and prognostic tool for determining a cancer's genetic subtype and for helping to predict the course of disease.

Study of regulators of SIRT3 expression

Motivated by the relative lack of information about regulators of SIRT3 expression, we conducted a bioinformatic analysis to identify potential transcription factors involved in SIRT3 induction. Chapter III described this study, which identified nuclear respiratory factor 2 (NRF-2) as a top candidate and then verified that it binds the *SIRT3* promoter and controls SIRT3 expression. This makes NRF-2, after ERRα, the second transcription factor identified which directly binds the *SIRT3* promoter to control SIRT3 expression. Notably, NRF-2 and ERRα are both co-activated by PGC-1α (Mootha et al., 2004). Future study will be necessary to determine whether there are tissues or metabolic conditions where one of these transcription factors is more important for SIRT3 expression than the other. NRF-2 and ERRα can also co-induce each other (Mootha et al., 2004), and it will be interesting to see whether there are contexts where the two contribute cooperatively to SIRT3 expression. For example, Giralt et al. (2011) show that SIRT3 is upregulated by PGC-1α in brown adipocytes, and that ERRα is required for full induction. Yet

they do not explain the mechanisms of the partial SIRT3 induction seen when ERRα is knocked down. Our work strongly suggests that NRF-2 may be responsible for the upregulation of SIRT3 by PGC-1α observed in the absence of ERRα. By providing an additional link between PGC-1α – which is upregulated during CR – and SIRT3, our work also suggests that this pathway may be responsible for the upregulation of SIRT3 seen in multiple tissues during CR.

Effect of calorie restriction on isoform usage

We also applied new high-throughput RNA sequencing (RNA-seq) technologies to the study of CR. By supplying information about expression at the level of the individual DNA base, rather than the probe level supplied by microarrays, RNA-seq provides a more detailed look at gene expression than found in most of the CR datasets generated to date. Chapter IV used this information and showed for the first time that calorie restriction was capable of reversing not just age-related changes in gene expression, but age-related changes in the read profile generated for a gene as well. This suggested that different isoforms of the same gene were being expressed with age, and that the change was reversed with CR, even when overall expression of the gene remained stable. One of the mechanisms by which CR exerts its regulation of an organism's biology may therefore be a change of the relative isoform expression from an individual gene locus. Future study will be needed to identify specific isoforms with distinct biological effects whose relative expression changes with age and is reversed with CR. SIRT3 expression in our data was slightly decreased with age and significantly induced with CR in the liver, and although we did not observe an age- or CR-dependent shift in SIRT3 transcript isoform usage, we did observe a tissue-specific difference, as a particular 8bp insertion at the 5'

end of exon 2 was incorporated twice as often in liver transcripts as in heart transcripts. This may lead to a tissue-specific difference in SIRT3 protein isoform usage.

Limitations and future directions

The majority of experiments described in this dissertation have been conducted in cell culture models, and, although they are suggestive, one must exercise caution in generalizing the results of experiments conducted in cell culture to the biology of whole organisms. Cell culture is an extremely useful model system, but it does not capture every nuance of organism-level biology. Cells in culture are not exposed to paracrine signals or circulating factors from other cell types or tissues, as they would be *in vivo*, and the two-dimensional surface of a culture dish is a simplification of the three-dimensional microenvironment with a range of substrate stiffnesses encountered by the cell *in vivo*. Additional study is therefore necessary to draw organism-level conclusions based on the cell culture studies presented herein.

For example, further study could investigate whether the upregulation of SIRT3 following rapamycin treatment occurs *in vivo* – such as in particular tissues of mice administered rapamycin – and not just in cell culture. If so, techniques similar to the bioinformatic methods used to identify NRF-2 as a SIRT3 regulator could be employed to identify transcription factors involved in this regulation. In the vein of Fok et al. (2014), global gene expression studies could contribute to elucidating the degree of overlap between pathways activated by rapamycin and by calorie restriction. Functionally, it is known that SIRT3 plays a role in mediating some of the beneficial aspects of calorie restriction, and treatment of wildtype and SIRT3-knockout mice with rapamycin or vehicle control would determine whether the induction of SIRT3 plays a role in mediating the lifespan-extending effects of rapamycin.

Experiments to further determine the role played by NRF-2 in the regulation of SIRT3 could be conducted on both a cellular level and an organismal level. On a cellular level, a reduction of luminescence following mutation or deletion of the NRF-2 binding site in the SIRT3 promoter reporter would support direct regulation of the promoter by NRF-2. The NRF-2 overexpression studies presented in chapter III would present a fuller picture of NRF-2 activity with the inclusion of additional NRF-2 target genes as positive controls, and adding additional conditions to the chromatin immunopreciptation – such as the removal of serum – to partially mimic calorie restriction could potentially induce greater binding of the SIRT3 promoter by NRF-2, supporting a role for NRF-2 in the increase of SIRT3 expression in CR. On an organismal level, studies could include calorie restricting wildtype and tissue-specific NRF-2-knockout mice (whole-body deletion of NRF-2 is embryonic lethal) and then assaying SIRT3 induction in the target tissue of both groups. If NRF-2 is important for induction of SIRT3 by CR in that tissue, then its ablation should blunt the response by SIRT3. Existing datasets of calorie-restricted wildtype mice could also be analyzed to determine whether SIRT3 induction in CR is consistently co-incident with an induction of other NRF-2 targets.

Although the RNA-seq data described in chapter IV was generated from calorie-restricted mice rather than cells in culture, additional experiments could also be carried out for this study. In particular, validation needs to be carried out for the identified isoform switching events. This could include 5' rapid amplification of cDNA ends, or 5' RACE, which generates sequence data from mRNA transcripts and can serve as a method to independently verify the RNA-seq data. Once verified, particular isoforms could be knocked down in mice via lentiviral shRNA constructs to determine whether the switching plays a role in organisms' metabolic adaptation to calorie restriction.

Outlook

SIRT3 is a particularly interesting and important gene to study because its activity has been linked not only to mediating the benefits of CR in lower organisms, but also to longevity in humans: the possession of certain *SIRT3* alleles has been associated with survival to old ages, and the alleles associated with longevity may have higher levels of expression (Bellizzi et al., 2005; Albani et al., 2014). Thus, if we can understand how SIRT3 expression is regulated, we may be able to perturb these pathways to increase its expression, and if we can increase its expression, we may ultimately be able to stave off age-related disease and increase lifespan. A significant body of work remains to develop this strategy and determine whether and how it would function, but this dissertation has attempted to be a step in that direction.

References

Albani D, Ateri E, Mazzuco S, Ghilardi A, Rodilossi S, Biella G, Ongaro F, Antuono P, Boldrini P, Di Giorgi E, Frigato A, Durante E, Caberlotto L, Zanardo A, Siculi M, Gallucci M, Forloni G (2014) Modulation of human longevity by SIRT3 single nucleotide polymorphisms in the prospective study "Treviso Longeva (TRELONG)". *Age (Dordr)* **36**, 469-478.

Bellizzi D, Rose G, Cavalcante P, Covello G, Dato S, De Rango F, Greco V, Maggiolini M, Feraco E, Mari V, Franceschi C, Passarino G, De Benedictis G (2005) A novel VNTR enhancer within the SIRT3 gene, a human homologue of SIR2, is associated with survival at oldest ages. *Genomics* **85**, 258-263.

Desouki MM, Doubinskaia I, Gius D, Abdulkadir SA (2014) Decreased mitochondrial SIRT3 expression is a potential molecular biomarker associated with poor outcome in breast cancer. *Hum. Pathol*. **45**, 1071-1077.

Fok WC, Bokov A, Gelfond J, Yu Z, Zhang Y, Doderer M, Chen Y, Javors M, Wood WH 3rd, Zhang Y, Becker KG, Richardson A, Pérez VI (2014) Combined treatment of rapamycin and dietary restriction has a larger effect on the transcriptome and metabolome of liver. *Aging Cell* **13**, 311-319.

Giralt A, Hondares E, Villena JA, Ribas F, Díaz-Delfín J, Giralt M, Iglesias R, Villarroya F (2011) Peroxisome proliferator-activated receptor-gamma coactivator-1alpha controls transcription of the Sirt3 gene, an essential component of the thermogenic brown adipocyte phenotype. *J. Biol. Chem*. **286**, 16958-16966.

Kong X, Wang R, Xue Y, Liu X, Zhang H, Chen Y, Fang F, Chang Y (2010) Sirtuin 3, a new target of PGC-1alpha, plays an important role in the suppression of ROS and mitochondrial biogenesis. *PLoS One* **5**, e11707.

Mootha VK, Handschin C, Arlow D, Xie X, St Pierre J, Sihag S, Yang W, Altshuler D, Puigserver P, Patterson N, Willy PJ, Schulman IG, Heyman RA, Lander ES, Spiegelman BM (2004) Erralpha and Gabpa/b specify PGC-1alpha-dependent oxidative phosphorylation gene expression that is altered in diabetic muscle. *Proc. Natl. Acad. Sci. U. S. A*. **101**, 6570-6575.

APPENDIX A

Targeted screen of six calorie restriction mimetics identifies rapamycin as inducer of SIRT3 expression

F. Kyle Satterstrom[1,2] and Marcia C. Haigis[2]

[1] Harvard School of Engineering and Applied Sciences, Cambridge, Massachusetts 02138

[2] Department of Cell Biology, Harvard Medical School, Boston, Massachusetts 02115

Abstract

SIRT3 is upregulated in multiple tissues by nutrient stresses such as calorie restriction and fasting, though the molecular mechanism of this induction is unclear. We tested the effect on SIRT3 expression in human 293T cells of six different small molecule drugs: pioglitazone, 5-aminoimidazole-4-carboxamide ribonucleotide (AICAR), kaempferol, metformin, resveratrol, and rapamycin. These drugs were selected because each has been used as a calorie restriction mimetic, a stimulator of mitochondrial biogenesis, or (in the case of kaempferol) a stimulator of SIRT3 expression. Each drug was tested at two different concentrations for 24 and 48 hours, followed by measurement of SIRT3 expression level by quantitative PCR. In this experimental system, we observed robust and dose-dependent increases in SIRT3 expression with rapamycin, an inhibitor of the nutrient-sensing TOR pathway. We also observed sporadic induction of SIRT3 by AICAR and pioglitazone, no significant effect with kaempferol and metformin, and repression of SIRT3 transcript levels by resveratrol. Additional studies of SIRT3 expression verified SIRT3 induction by rapamycin treatment as well as other methods of inhibiting the TOR pathway.

Introduction

Calorie restriction (CR) extends lifespan and healthspan across a variety of species (reviewed in Anderson and Weindruch, 2010). CR induces an organismal metabolic adaptation involving a stimulation of mitochondrial function, and SIRT3 is important for this adaptation. In the liver, SIRT3 is upregulated by calorie restriction and activates the urea cycle (Hallows et al., 2011), ketone body production (Shimazu et al., 2010), and fatty acid oxidation (Hirschey et al., 2010). SIRT3 is also upregulated by CR in brown adipose tissue, where it activates

mitochondrial thermogenesis (Shi et al., 2005). SIRT3 additionally mediates some of the beneficial anti-oxidant effects of CR, such as the reduction of oxidative stress (Qiu et al., 2010; Tao et al., 2010) and the prevention of age-related hearing loss in mice (Someya et al., 2010).

However, as noted in earlier chapters, the mechanism of SIRT3 induction during CR is unclear. We tested the effect on SIRT3 expression of six small molecule drugs that have been used to mimic calorie restriction or to stimulate mitochondrial biogenesis, reasoning that either condition would lead to an upregulation of mitochondrial genes. In addition to identifying inducers of SIRT3 expression, we also hoped to gain insight into the mechanisms of SIRT3 induction by primarily using molecules with known targets or affected pathways.

Results

Targeted screen for small molecule inducers of SIRT3 expression

We chose pioglitazone, 5-aminoimidazole-4-carboxamide ribonucleotide (AICAR), kaempferol, metformin, resveratrol, and rapamycin as candidate calorie restriction-mimetic compounds. Each drug was tested in human embryonic kidney 293T cells at two different concentrations for 24 and 48 hours (Table A.1), followed by measurement of the mRNA expression levels of SIRT3 as well as peroxisome proliferator-activated receptor γ coactivator 1-α (PGC-1α). We used PGC-1α as a marker of CR-like effects because it is known to be activated during CR (Anderson et al, 2008) and to drive mitochondrial biogenesis (Scarpulla, 2011).

Pioglitazone is one of the class of drugs known as thiazolidinediones (TZDs) used to treat type II diabetes (reviewed in Phielix et al., 2011). TZDs are agonists of peroxisome proliferator-activated receptor γ (PPARγ). *In vivo*, one of the many consequences of activated PPARγ is release of the hormone adiponectin from adipose tissue, leading to increased glucose uptake by

Table A.1. Drugs and concentrations used in targeted screen for inducers of SIRT3 expression.

Drug	Affected Pathway	Durations Tested	Concentrations Tested
Pioglitazone	PPARγ agonist	1 day, 2 days	1 μM, 10 μM
AICAR	AMPK activator	1 day, 2 days	100 μM, 1 mM
Kaempferol	Oxidative stress	1 day, 2 days	10 μM, 100 μM
Metformin	Anti-diabetic drug	1 day, 2 days	10 μM, 1 mM
Resveratrol	SIRT1 activator	1 day, 2 days	10 μM, 50 μM
Rapamycin	mTOR inhibitor	1 day, 2 days	100 nM, 1 μM

muscle and liver and improved glucose homeostasis. *In vitro*, pioglitazone has been shown to stimulate mitochondrial biogenesis at concentrations of 1 μM and 10 μM (Ghosh et al., 2007; Fujisawa et al., 2009). We tested these concentrations and observed modest effects. One day of pioglitazone treatment had no significant effect, but after two days SIRT3 expression was increased at both concentrations tested, and the increase with 1 μM treatment was significant (Figure A.1A, $p = 0.026$). This significant result corresponded with a non-signficant increase in PGC-1α expression.

AICAR is an analog of adenosine monophosphate (AMP) and a stimulator of AMP-dependent protein kinase (AMPK) activity (Merrill et al., 1997). AMPK is an energy sensor which promotes mitochondrial biogenesis and ATP production through PGC-1α and nuclear respiratory factors 1 and 2 when the cellular ADP/ATP ratio climbs too high, as occurs during stimuli such as exercise (Bergeron et al., 2001; Reznick and Shulman, 2006; reviewed in Hardie et al., 2012). AICAR mimics a low cellular energy state and has been shown in cell culture to increases in cellular oxygen consumption and increase protein levels of electron transport chain subunits (Beeson et al., 2010; Jose et al., 2011). We tested concentrations of 100 μM and 1 mM, in line with these studies. We observed increased SIRT3 expression with both concentrations tested, leading to significant increases at two days (Figure A.1B, $p = 0.022$ for 100 μM, $p = 0.0012$ for 1 mM). PGC-1α transcript levels were increased with 1 mM treatment, but the effect was not significant ($p = 0.060$).

Kaempferol is a flavonoid found naturally in many foods. Intake of kaempferol is associated with lower lung cancer incidence in smokers (Cui et al., 2008), a phenomenon which is perhaps due to the induction of mitochondrial superoxide dismutase (SOD2) and apoptosis in lung cancer cells (Leung et al., 2007). SIRT3 is an activator of SOD2 (Qiu et al., 2010; Tao et

Figure A.1 (Next page). Targeted screen of calorie restriction mimetics for induction of SIRT3 transcript levels. Relative SIRT3 and PGC-1α transcript levels following addition of A) pioglitazone or DMSO control, B) AICAR or PBS control, C) kaempferol or DMSO control, D) metformin or PBS control, E) resveratrol or DMSO control, or F) rapamycin or DMSO control to the growth medium of human 293T cells at the indicated concentrations for one or two days. Blue bars = higher concentration tested; green bars = lower concentration tested; white bars = control condition. RPS16 was used as the reference gene for pioglitazone, kaempferol, and rapamycin treatments. B2M was used as the reference gene for resveratrol and metformin treatments. PPIA was used as the reference gene for AICAR treatment. Maximum final DMSO concentration in media was 0.2%. Data are a combination of two experiments with a total n = 6 per condition, except for pioglitazone (n = 5 for SIRT3 at 10 μM for 2 days), metformin (only one experiment, n = 3), and resveratrol (50 μM only included in one experiment, n = 3). * indicates $p < 0.05$, ** indicates $p < 0.01$, *** indicates $p < 0.001$ by two-tailed student's t-test.

Figure A.1 (Continued).

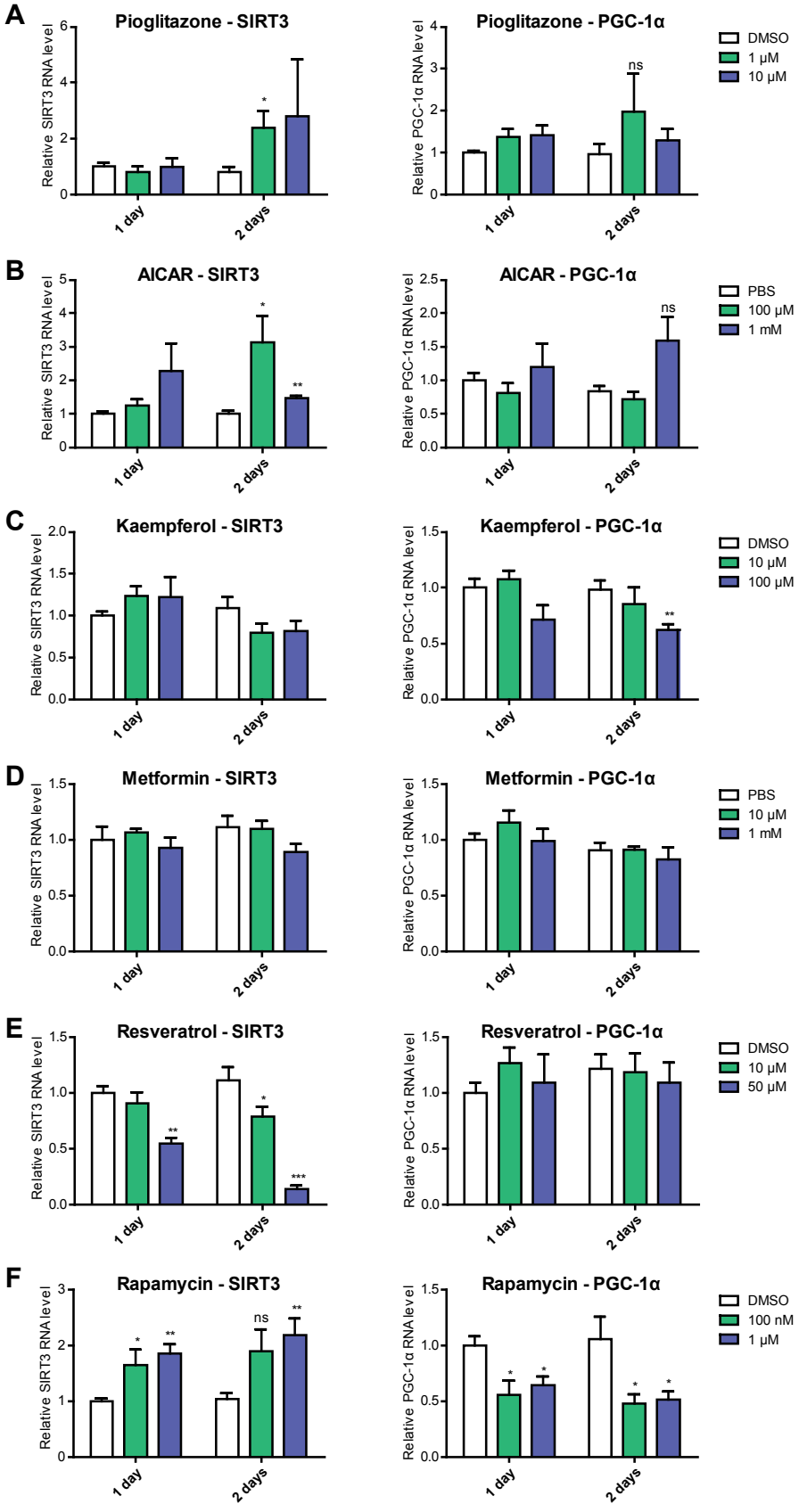

al., 2010), and in certain contexts it also has pro-apoptotic functions (Allison and Milner, 2007). Marfe et al. (2009) suggest that kaempferol treatment causes oxidative stress which leads to increased SIRT3 levels, activated SOD2, and increased apoptosis. Both Marfe et al. (2009) and Cimen et al. (2010) treated human K562 leukemia cells with 50 μM kaempferol for 48 hours and saw induction of SIRT3 protein levels. To test this effect in 293T cells, we used concentrations of 10 μM and 100 μM. However, these treatments did not lead to any significant change in SIRT3 expression. At the higher kaempferol concentration tested, PGC-1α expression was decreased after one and two days of treatment, with the decrease at two days significant (Figure A.1C, $p = 0.0042$).

Metformin is the first-line drug for treatment of type II diabetes. It has several effects, and even though it is used widely its mechanism of action continues to be a subject of research (Rena et al., 2013). Metformin decreases hyperglycemia by suppressing gluconeogenesis (Meyer et al., 1967), and it also increases PGC-1α skeletal muscle protein content and enhances mitochondrial function (Suwa et al., 2006). Anisimov et al. (2008) used metformin as a mimetic of calorie restriction and observed an increase in mean lifespan of metformin-treated female mice. It has been used in cell culture over a wide range of concentrations to achieve metabolic effects (e.g. Beeson et al., 2010, Rice et al., 2011), leading us to test concentrations of 10 μM and 1 mM. Yet these treatments had no significant effects at all, either on SIRT3 or PGC-1α (Figure A.1D). This is in line with subsequent observations (unpublished) made by our laboratory that metformin does not have an effect on 293T cells. The molecular peculiarities underlying this observation are unclear.

Resveratrol is a polyphenol found in grape skins and red wine. It activates SIRT1 (Howitz et al., 2003; Hubbard et al., 2013), the most-studied human homolog of the yeast gene

Sir2. Resveratrol activates molecular pathways similar to calorie restriction in yeast (Howitz et al., 2003), mice (Pearson et al., 2008), and humans (Timmers et al., 2011), and it has been referred to as a calorie restriction mimetic (e.g. Lam et al., 2013). Resveratrol also promotes mitochondrial biogenesis, with mice that received oral resveratrol at 20 mg/kg/day for 4 weeks exhibiting a significant increase in mitochondrial DNA content in cells from their aortas (Csiszar et al., 2009). Resveratrol has also been used in cell culture to induce mitochondrial biogenesis and increase cellular oxygen consumption (Csiszar et al., 2009; Beeson et al., 2010). We tested similar concentrations of 10 μM and 50 μM. Surprisingly, in our study resveratrol treatment led to dose- and time-dependent reductions in SIRT3 expression (Figure A.1E), with multiple decreases achieving significance. PGC-1α transcript levels were not significantly affected.

Rapamycin is a macrolide which inhibits the target of rapamycin (TOR) pathway by binding mTOR, a protein kinase. The TOR pathway is a cellular nutrient sensor. It integrates multiple nutrient and growth factor signals and, when active, drives anabolic processes like protein synthesis and inhibits catabolic processes like autophagy (Zoncu et al., 2011). In mammals, mTOR exists in one of two complexes, mTORC1 or mTORC2. Rapamycin specifically binds and inhibits mTOR when it is in mTORC1, although mTORC2 activity may also be compromised over time as mTOR molecules become sequestered in mTORC1 (reviewed in Li et al., 2014). Because rapamycin inhibits a nutrient-sensing pathway, it has been tested as a calorie restriction mimetic, and it does have calorie restriction-like effects in some organisms. Chronological lifespan in yeast was increased by rapamycin treatment (Powers et al., 2006), and rapamycin administered beginning in middle age increased lifespan in mice (Harrison et al., 2009). Concentrations used in cell culture are typically near 100 nM (e.g. Park and Chen, 2005; Chakrabarti et al., 2010). We tested concentrations of 100 nM and 1 μM and observed the most

consistent results of any molecule in our targeted screen. SIRT3 expression was increased at all times and concentrations, with all but one of the effects being significant (Figure A.1F; $p = 0.045$ for 100 nM at 1 day; $p = 0.00073$ for 1 μM at 1 day; $p = 0.060$ for 100 nM at 2 days; $p = 0.0052$ for 1 μM at 2 days). Interestingly, although SIRT3 was increased, PGC-1α transcript levels were significantly decreased at all times and concentrations tested ($p = 0.016$ for 100 nM at 1 day; $p = 0.011$ for 1 μM at 1 day; $p = 0.026$ for 100 nM at 2 days; $p = 0.031$ for 1 μM at 2 days). Nonetheless, because of the robust response of SIRT3 transcription to rapamycin, we decided to further investigate the effects of rapamycin and the TOR pathway on SIRT3 and the mitochondrial sirtuins.

Effect of small molecule TOR inhibitors on expression of mitochondrial sirtuins

Because we observed such a strong, consistent effect on SIRT3 expression with 24 and 48 hours of rapamycin treatment, we next conducted a shorter time course of mTOR inhibition and examined the transcript levels of all three mitochondrial sirtuins – SIRT3, SIRT4, and SIRT5. Eight hours of 100 nM rapamycin treatment significantly induced both SIRT3 ($p = 2.7 \times 10^{-5}$) and SIRT5 ($p = 1.3 \times 10^{-7}$) (Figure A.2A). SIRT3 was unchanged at four hours, and SIRT5 was increased slightly ($p = 0.031$). SIRT4 expression was not significantly affected by either treatment duration. To verify the results of the rapamycin treatment, we performed the same experiment using Torin1, a small molecule catalytic inhibitor of mTOR which inhibits mTORC1 more strongly than rapamycin (Thoreen et al., 2009) and also directly inhibits mTORC2. We found that 250 nM Torin1 treatment induced SIRT3 and SIRT5 levels to a greater degree than rapamycin, achieving significance for both at 4 hours ($p = 0.024$ for SIRT3; $p = 0.0053$ for SIRT5) as well as 8 hours ($p = 0.00028$ for SIRT3; $p = 2.5 \times 10^{-5}$ for SIRT5), with SIRT4 again

Figure A.2 (Next page). Effect of small molecule mTOR inhibitors on gene expression of mitochondrial sirtuins and other metabolic genes in 293T cells, MEFs, and primary murine hepatocytes. A) Relative transcript levels of SIRT3, SIRT4, and SIRT5 following treatment of 293T cells with 100 nM rapamycin for four or eight hours or DMSO control for eight hours. Data are a combination of two experiments with a total n = 8 per condition. B) Relative transcript levels of SIRT3, SIRT4, and SIRT5 following treatment of 293T cells with 250 nM of the mTOR catalytic inhibitor Torin1 for four or eight hours or DMSO control for eight hours. n = 4 per condition. C) Relative transcript levels of SIRT3, SIRT4, and SIRT5 following treatment of mouse embryonic fibroblasts with 100 nM rapamycin or DMSO control for 48 hours. n = 4 per condition. D) Western blot of MEFs following treatment with indicated concentrations of rapamycin for 48 hours. E) Relative transcript levels of SIRT3, SIRT4, and SIRT5 following treatment of primary mouse hepatocytes with 100 nM rapamycin, 250 nM Torin1, or DMSO control for 24 hours. n = 4 per condition. F) Western blot of mouse primary hepatocytes following treatment with indicated concentrations of rapamycin for 48 hours. G) Relative transcript levels of several metabolic genes following treatment of 293T cells with 250 nM Torin1 or DMSO control for eight hours. n = 4 per condition. Final concentration of DMSO in media was 0.01% for rapamycin experiments and 0.1% for Torin1 or combined experiments. For human qPCR experiments, the geometric mean of RPS16, B2M, and PPIA expression was used as the reference gene. For mouse qPCR experiments, the geometric mean of HSP90AB1, β-actin, and PPIA expression was used as the reference gene. * indicates $p < 0.05$, ** indicates $p < 0.01$, *** indicates $p < 0.001$ by two-tailed student's t-test.

Figure A.2 (Continued).

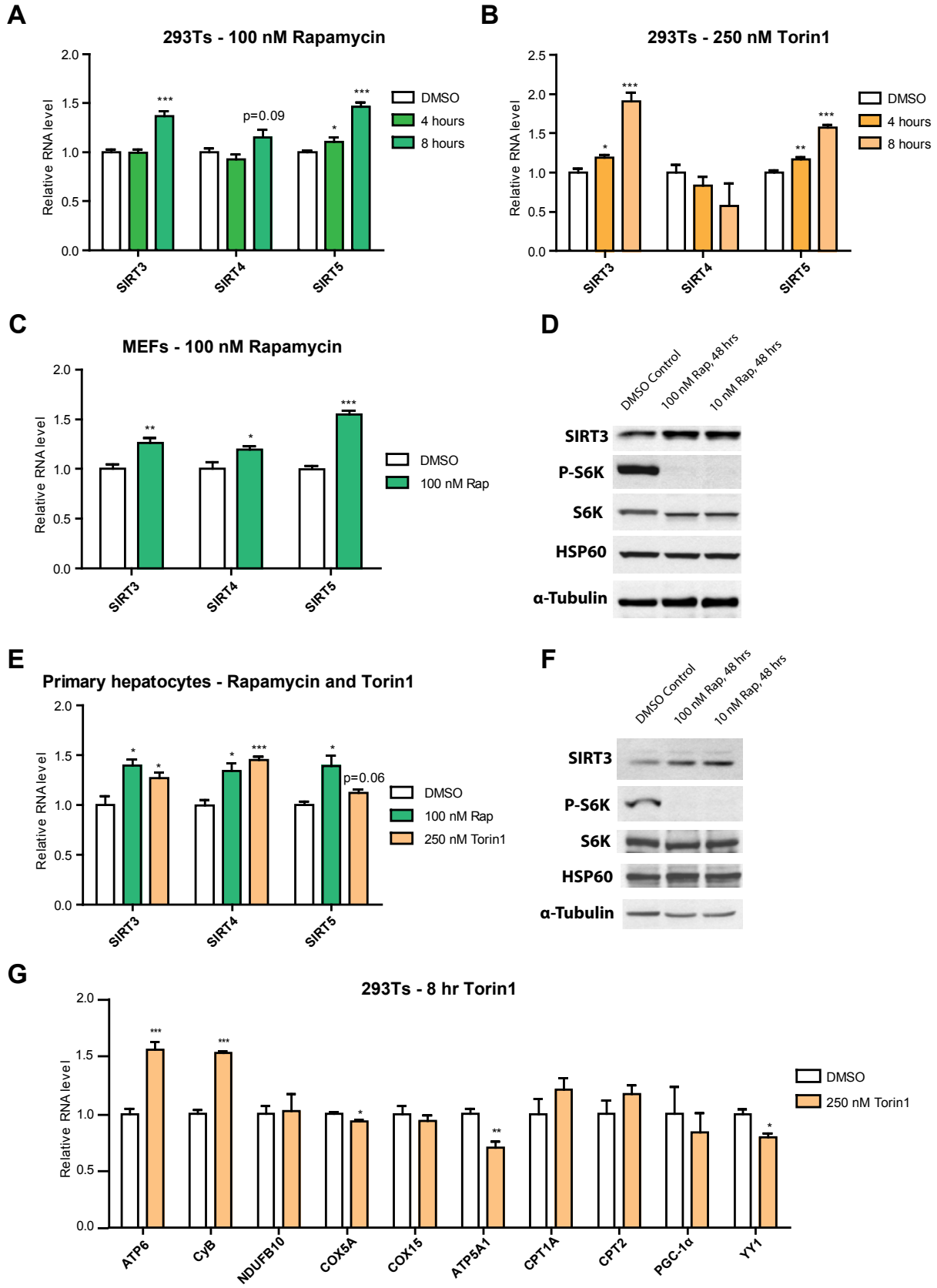

not significantly changed (Figure A.2B). As described in chapter II, we also tested the effect of mTOR inhibition on SIRT3 protein levels in 293Ts and found that 48 hour treatment with either 100 nM rapamycin or 250 nM Torin1 was sufficient to increase SIRT3 protein levels relative to the mitochondrial loading control HSP60 and the general loading control α-tubulin.

To determine if the induction of sirtuin expression by mTOR inhibition occurred in other cell lines, we tested the effects of rapamycin and Torin1 in mouse cells. Interestingly, we found that expression levels of all three mitochondrial sirtuins were induced. In immortalized mouse embryonic fibroblasts (MEFs), transcript levels of all three sirtuins were significantly increased by 48 hours of 100 nM rapamycin treatment ($p = 0.0078$ for SIRT3; $p = 0.048$ for SIRT4; $p = 2.3 \times 10^{-5}$ for SIRT5) (Figure A.2C). We tested the effect on SIRT3 protein expression and observed increased SIRT3 levels relative to loading controls HSP60 and α-tubulin (phosphorylated S6 kinase was used as a marker of mTOR activation) (Figure A.2D). Likewise, SIRT3, SIRT4, and SIRT5 transcript levels were significantly increased in murine primary hepatocytes by 24 hours of 100 nM rapamycin treatment ($p = 0.011$ for SIRT3; $p = 0.012$ for SIRT4; $p = 0.011$ for SIRT5) (Figure A.2E). SIRT3 and SIRT4 expression levels were also significantly increased by 24 hours of 250 nM Torin1 treatment ($p = 0.042$ for SIRT3; $p = 0.00037$ for SIRT4). As with the MEFs, we verified rapamycin's effect on SIRT3 at the protein level in these cells (Figure A.2F).

Having observed the induction of all three mitochondrial sirtuins by TOR pathway inhibition in mouse cells, we wanted to test whether other mitochondrial and metabolic genes were affected as well. In 293T cells, we assayed the effect of an 8-hour Torin1 treatment on several metabolic genes (Figure A.2G) and found that only the mitochondrially-encoded genes we tested, ATP6 (complex V) and CYB (complex III), were significantly induced ($p = 0.00058$

for ATP6; $p = 7.9 \times 10^{-6}$ for CyB). By contrast, nuclear-encoded mitochondrial genes such as NDUFB10 (complex I), COX5A (complex IV), and ATP5A1 (complex V) were either unchanged or decreased. This suggested that mTOR inhibition in 293Ts did not lead to a general upregulation of all mitochondrial genes but instead led to a more specific regulation.

Effect of additional TOR modulation methods on expression of mitochondrial sirtuins

We next investigated whether the mitochondrial sirtuins were induced by other means of TOR pathway inhibition. mTOR activity requires the presence of both growth factors and amino acids (reviewed in Zoncu et al., 2011), and we hypothesized that removing either one of these inputs would induce expression of SIRT3 and potentially SIRT4 and SIRT5. We therefore tested the effect of 24-hour amino acid deprivation, with or without rapamycin, on 293T cells. Interestingly, both amino acid deprivation ($p = 0.0023$) and rapamycin ($p = 0.00012$) increased SIRT3 transcript levels, and the combination of the two increased SIRT3 levels even further, suggesting that either the treatments were not individually sufficient to completely shut down the TOR pathway, or that the treatments functioned by different mechanisms (Figure A.3A). This pattern did not hold for SIRT4 or SIRT5, which were relatively unchanged by the treatments.

We also investigated the effect of amino acid deprivation in mouse cells. For this experiment we used both wildtype and tuberous sclerosis complex 2 (TSC2)-knockout MEFs; TSC2 is a negative regulator of mTOR, and we hypothesized that the constitutive activation of mTOR in $TSC2^{-/-}$ MEFs would have the opposite effect of rapamycin treatment and would depress expression levels of the mitochondrial sirtuins. Following 18 hours of amino acid deprivation, expression of all three sirtuins was significantly induced in the wildtype cells (Figure A.3B; $p = 1.2 \times 10^{-6}$ for SIRT3; $p = 0.0018$ for SIRT4; $p = 2.5 \times 10^{-8}$ for SIRT5), while

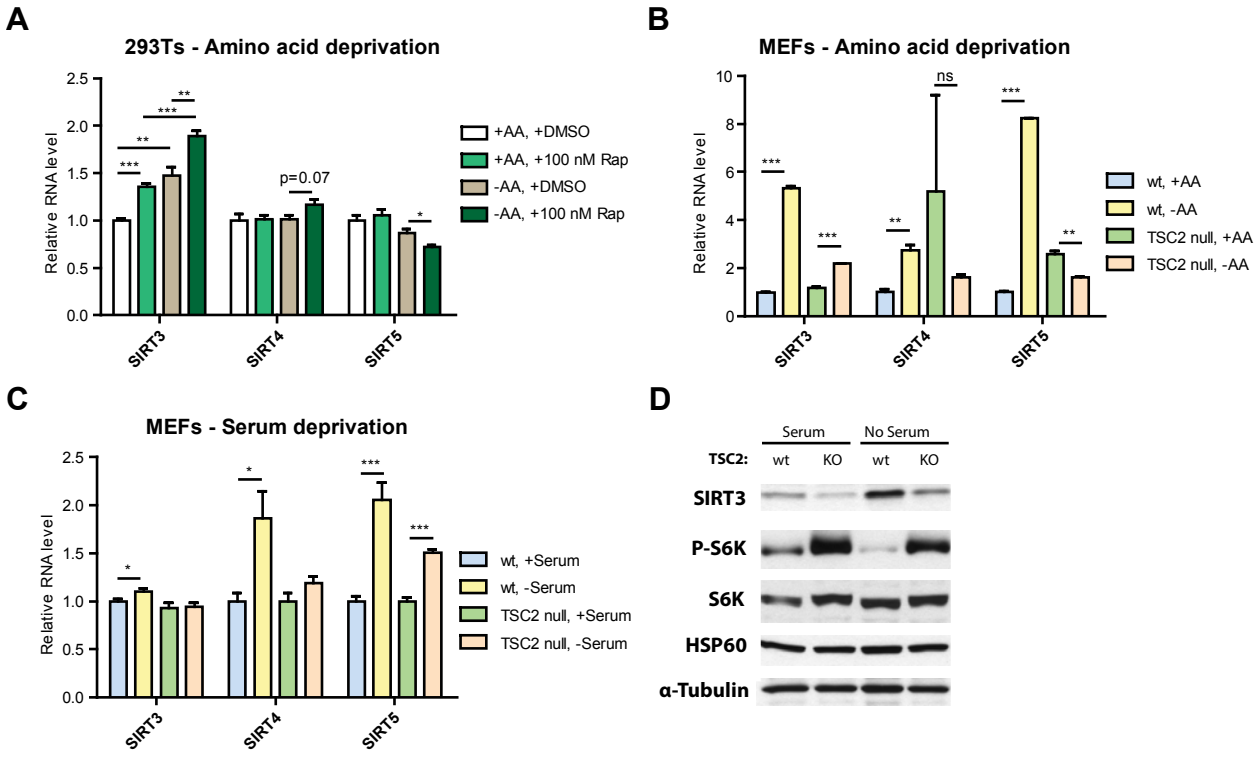

Figure A.3. Effect of mTOR inhibition on gene expression of mitochondrial sirtuins. A) Relative transcript levels of SIRT3, SIRT4, and SIRT5 following treatment of 293T cells with 100 nM rapamycin or DMSO control in the presence or absence of amino acids for 24 hours. n = 4 per condition. B) Relative transcript levels of SIRT3, SIRT4, and SIRT5 following incubation of wildtype or $TSC2^{-/-}$ MEFs in the presence or absence of amino acids for 18 hours. n = 3 per condition. C) Relative transcript levels of SIRT3, SIRT4, and SIRT5 following incubation of wildtype or $TSC2^{-/-}$ MEFs in the presence or absence of serum for 24 hours. Data are a combination of two experiments with a total n = 7 per condition. D) Western blot of wildtype or $TSC2^{-/-}$ MEFs in the presence or absence of serum for 24 hours. For A, final concentration of DMSO in media was 0.01% and the geometric mean of RPS16, B2M, and PPIA expression was used as the reference gene. For B, β-actin was used as the reference gene. For C, the geometric mean of HSP90AB1, β-actin, and PPIA expression was used as the reference gene. * indicates $p < 0.05$, ** indicates $p < 0.01$, *** indicates $p < 0.001$ by two-tailed student's t-test.

only SIRT3 was induced in the TSC2$^{-/-}$ cells ($p = 8.4 \times 10^{-5}$), and this was to a lesser degree than in the wildtype cells. Thus, contrary to our expectations, levels of the sirtuins were not lower in the TSC2$^{-/-}$ cells than in the wildtype cells; instead, the effect of TSC2 knockout seemed to be a dampened induction of the mitochondrial sirtuins with amino acid deprivation. This experiment had been planned for 24 hours but was shortened to 18 after we observed noticeably higher levels of dead and floating cells in the TSC2$^{-/-}$ amino acid-deprived cells than in the other cells and treatments (dead cells were removed prior to analysis of sirtuin transcript levels). It is possible that this effect was due to the activation of cellular protein synthesis pathways (and downregulation of autophagy pathways) by mTOR at a time when the cell did not have sufficient amino acid stores to engage in high levels of protein synthesis, leading to cell death.

As an alternative to amino acid deprivation, we tested serum deprivation in the MEFs. Serum deprivation significantly induced expression of SIRT3, SIRT4, and SIRT5 in the wildtype cells (Figure A.3C; $p = 0.048$ for SIRT3; $p = 0.012$ for SIRT4; $p = 0.00010$ for SIRT5). Again, levels of the sirtuins were not lower in the TSC2$^{-/-}$ cells than in the wildtype cells; rather, it appeared that the constitutively active mTOR lessened the impact of serum deprivation, as only SIRT5 was induced in the TSC2$^{-/-}$ cells ($p = 1.7 \times 10^{-7}$), and this induction was to a lesser degree than in the wildtype cells. At the protein level, however, our data did suggest that constitutively active mTOR led to lower SIRT3 levels (Figure A.3D). We also observed that SIRT3 protein level was induced by serum deprivation in TSC$^{-/-}$ MEFs to a lesser extent than in wildtype MEFs. Together, these studies demonstrate that TOR pathway activity regulates the expression of not just SIRT3 but the other mitochondrial sirtuins as well.

Discussion

We conducted a targeted screen of six small molecules thought to act as mimetics of calorie restriction or inducers of mitochondrial biogenesis – pioglitazone, AICAR, kaempferol, metformin, resveratrol, and rapamycin – and found that rapamycin consistently induced SIRT3 expression in 293T cells. We also saw somewhat delayed induction of SIRT3 transcript levels by pioglitazone and AICAR. Further studies in 293T cells showed that other methods of inhibiting the TOR pathway, such as treatment with Torin1 or amino acid deprivation, also induced SIRT3 levels. These findings were validated at the protein level in data presented in chapter II. Rapamycin and Torin1 treatment also induced SIRT5 and the mitochondrially-encoded electron transport chain subunits CYB and ATP6.

The effects seen on sirtuin expression with mTOR inhibition in 293Ts were validated in other cell lines. In MEFs, all three sirtuins were upregulated by mTOR-inhibiting treatments such as rapamycin, serum deprivation, and amino acid deprivation. MEFs with loss of TSC2, and therefore constitutively active mTOR, had a dampened response to amino acid deprivation or serum deprivation and did not induce the mitochondrial sirtuins as highly as did their wildtype counterparts. The induction of SIRT3 by rapamycin was also verified at the protein level in both MEFs and primary hepatocytes.

To determine whether the induction of SIRT3 levels could be validated by other studies, we turned to publicly available microarray data. In an *in vitro* study, SIRT3 expression was significantly increased by PGC-1α overexpression in TSC2-knockout MEFs, but 20 nM rapamycin treatment of these cells for 14 hours led instead to a significant decrease ($p = 0.039$) (GSE5332, Cunningham et al., 2007). The rapamycin treatment also led to a decrease in PGC-1α levels. SIRT4 was not significantly changed. SIRT5, however, was significantly induced by

both rapamycin treatment ($p = 0.0013$) and PGC-1α overexpression ($p = 0.014$). In an *in vivo* study, male mice were treated with rapamycin (14 ppm in food) or vehicle control for one year starting at 13 months of age (GSE41018, Neff et al., 2013). Although the authors found separately that rapamycin extended lifespan, SIRT3 expression was not significantly changed by rapamycin treatment in mouse kidney or brain and was in fact significantly decreased ($p = 0.043$) in heart. SIRT4 was not included in the chosen microarray platform and SIRT5 was not significantly changed in any tissue.

In a similar study, mice were treated with rapamycin (14 ppm in food) or vehicle control for 6 months beginning at 19 months of age (GSE48331, Fok et al., 2014a) or for 21 months beginning at 4 months of age (GSE48333, Fok et al., 2014a). The authors also found separately that rapamycin extended lifespan, and they analyzed liver tissue from both treatment cohorts by microarray. SIRT3 was not significantly changed by rapamycin treatment in either male or female liver with six months of rapamycin treatment, and it was in fact lowered in liver from male ($p = 0.0044$) and female ($p = 0.035$) mice treated for 21 months. SIRT4 was not included in the microarray platform for either treatment cohort. SIRT5 was increased in livers from male mice ($p = 0.046$) treated for six months, but rapamycin had no significant effect on females treated for six months or from either sex treated for 21 months.

The same group also examined the effect of rapamycin in comparison to and in combination with calorie restriction (GSE40977, Fok et al., 2014b). In a 2x2 experiment starting at 2 months of age, mice were treated with rapamycin (14 ppm in food) or vehicle control and were also allowed to eat *ad libitum* or were 40% calorie-restricted. Following six months of treatment, livers were harvested. SIRT3 levels were significantly increased in the CR group compared to the *ad libitum* control ($p = 0.00027$) but were not significantly changed by

rapamycin treatment. The two treatments did seem to have a combinatorial effect, as SIRT3 levels were highest in the combined CR+rapamycin group (though not quite significant compared to CR alone, $p = 0.056$). SIRT4 was again not included in the microarray platform. SIRT5 levels were not significantly changed by CR but were significantly induced by rapamycin, both in mice fed *ad libitum* ($p = 0.029$) and in mice on a restricted diet ($p = 0.015$). This study is consistent with an increasing body of work suggesting that lifespan extension in mice by rapamycin and by calorie restriction happen by distinct mechanisms (i.e. Miller et al., 2014). Taken into consideration with the studies above, these data suggest that perhaps rapamycin does not robustly induce SIRT3 expression *in vivo*.

We took PGC-1α expression as an indicator of mitochondrial biogenesis, and, as shown in Figure A.1F, rapamycin treatment led to lower PGC-1α expression in 293T cells. We had expected that inhibition of the nutrient-sensing TOR pathway would mimic calorie restriction, and, as noted above, PGC-1α is upregulated in CR (Anderson et al., 2008). It could be that 293T cells are not a cell line which respond to calorie restriction by upregulating PGC-1α. Or, if rapamycin and CR do in fact extend mouse lifespan by different mechanisms, then perhaps different mechanisms were also at work to induce SIRT3 levels. One mechanism thought to occur with mTOR inhibition is the regulation of translation efficiency based on a transcript's 5' untranslated region (5' UTR) – it has been suggested that transcripts with particularly long or structured 5' UTRs are dependent upon mTOR-induced inhibition of 4E-BP (and thus activation of eIF4E) for efficient translation (Hay and Sonenberg, 2004), and SIRT3 has a relatively short 5' UTR. In this model, inhibition of mTOR by rapamycin, Torin1, or other means would cause downregulation of the translation of many genes while leaving SIRT3 relatively unaffected, making it look upregulated compared to other genes used as controls. However, this would

presumably affect protein levels but not transcript levels, since the regulation is applied at the level of translation. It would thus not explain the upregulation of SIRT3 transcript levels seen with mTOR inhibition. Moreover, more recent study has called this effect into question (Thoreen et al., 2012).

In summary, we found that rapamycin consistently leads to induction of SIRT3 transcript levels in 293T cells. We verified this finding both with other methods of mTOR pathway inhibition and with MEFs and murine primary hepatocytes. We do not see this phenomenon, however, reflected in available microarray data. We studied the other mitochondrial sirtuins, SIRT4 and SIRT5, and found that SIRT4 was not induced in the human cells we studied but was induced in MEFs and primary hepatocytes. Evidence for or against SIRT4 induction by rapamycin in third-party data is lacking, as SIRT4 was not included in the microarray platform used by several of the studies. SIRT5, meanwhile, is a strong candidate to use when investigating induction of expression by rapamycin treatment. Its transcript levels were induced in most of the same experiments as SIRT3, and microarray data does agree that SIRT5 can be induced by rapamycin treatment *in vivo*. Our data would be consistent with a role for SIRT3 or SIRT5 in the extension of lifespan by calorie restriction, or rapamycin treatment, or both, and our data are a step toward understanding the regulation of these two genes and the conditions under which their expression is activated.

Methods

Reagents

Pioglitazone (Sigma, cat. # E6910), AICAR (Cell Signaling, cat. # 9944), kaempferol (Sigma, cat. # 60010), metformin (Sigma, cat. # D150959), resveratrol (Sigma, cat. # R5010),

and rapamycin (Sigma, cat. # R0395) were diluted according to suppliers' specifications. Torin1 was generously provided by Nathanael Gray.

Cell culture

Human embryonic kidney 293T cells and mouse embryonic fibroblasts were grown in Dulbecco's Modified Eagle Medium (Life Technologies, cat. # 11995) with 10% fetal bovine serum (HyClone, cat. # SH30910.03) and 1% penicillin-streptomycin-glutamine supplement (Life Technologies, cat. #10378-016) and maintained in an incubator at standard tissue culture conditions (37°C, 5% CO2). $TSC2^{-/-}$ and matched wildtype MEFs were generously provided by John Blenis. Serum deprivation experiments used growth medium with the fetal bovine serum replaced by phosphate-buffered saline (Life Technologies, cat. #14190-250). Amino acid deprivation experiments used DMEM formulated from individual ingredients, according to ATCC specifications (ATCC, cat. #30-2002). A MEM vitamin solution (Life Techologies, cat. #11120-052) was used in this process, and a MEM amino acids solution (Life Technologies, cat. #11130-051) was used for the control medium.

Murine primary hepatocytes were isolated as described (Dominy et al., 2012). Briefly, liver was perfused for 5 min with Hank's Balanced Salt Solution (CellGro, cat. #21-022) with 1.1 g/L $NaHCO_3$ and 0.2 g/L EDTA at pH 7.4, followed by perfusion with 25 mL liver digestion medium (Life Technologies, cat. #17703-034). Liver was removed and cells were manually dissociated, incubated for 5 min in digestion medium, then filtered through a 70 μM cell strainer (BD Falcon, cat. #352350). Cells were centrifuged at 40g for 4 min and the pellet was resuspended in 10 mL plating medium (DMEM with 10% FBS, 1% penicillin-streptomycin-glutamine, 1% sodium pyruvate, and final concentrations of 100 nM dexamethasone and 1 nM

insulin) and 10 mL Percoll (Percoll [Sigma, cat. #P1644] mixed 9:1 with 10x PBS [Sigma, cat. #P5493]), then centrifuged again. Cells were resuspended in plating medium and plated. Two hours later, medium was changed and replaced with maintenance medium (M199 [Gibco cat. #11150] with 1% penicillin-streptomycin-glutamine and final concentrations of 0.2% fatty acid free BSA, 100 nM dexamethasone, and 1 nM insulin).

Quantitative PCR

RNA was extracted using RNEasy Mini Kits (Qiagen) and cDNA was synthesized using iScript cDNA Synthesis Kits (Bio-Rad). Quantitative PCR was performed with 2x LightCycler 480 SYBR Green I Master mix (Roche, cat. #04707516001) on a LightCycler 480 thermal cycler (Roche). Sequences of primers used are given in Table A.2. Primers for human 40S ribosomal protein S16 (RPS16), β2 microglobulin (B2M), and peptidyl-prolyl cis-trans isomerase A (PPIA) were tested in 293Ts for each chemical used in the targeted screen, and the primer set which had the least variation in amplification between treatment groups was selected as the reference gene to use with that chemical. The geometric mean of all three was used in most subsequent experiments with human cells to give a baseline reference that was more stable than one gene alone. The geometric mean of β-actin, heat shock protein 90kDa α, class B member 1 (HSP90AB1), and PPIA was used as a reference in most experiments with mouse cells after HSP90AB1 and PPIA were found to be most representative of a panel of 14 different reference genes in wildtype and $TSC2^{-/-}$ MEFs grown with and without serum.

Table A.2. Sequences of qPCR primers used in this study.

Gene	Organism	Direction	Sequence
SIRT3	Human	Forward	5'-AGCCCTCTTCATGTTCCGAAGTGT-3'
		Reverse	5'-TCATGTCAACACCTGCAGTCCCTT-3'
SIRT4	Human	Forward	5'-ATGTGGATGCTTTGCACACCAAGG-3'
		Reverse	5'-TTCAGGACTTGGAAACGCTCTTGC-3'
SIRT5	Human	Forward	5'-AGAGAGCTCGCCCACTGTGATTTA-3'
		Reverse	5'-AGGGTCCCTGGAAATGAAACCTGA-3'
PGC-1α	Human	Forward	5'-GCGCAGGTCAAACGAAACTGACTT-3'
		Reverse	5'-GCGCAAGCTTCTCTGAGCTTCTTT-3'
ATP5A1	Human	Forward	5'-TGCTATTGGTCAAAAGAGATCCA-3'
		Reverse	5'-GTAGCCGACACCACAATGG-3'
ATP6	Human	Forward	5'-CCTCTACCTGCACGACAACA-3'
		Reverse	5'-GGTCATTAGGAGGGCTGAGAG-3'
COX5A	Human	Forward	5'-TCATCCAGGAACTTAGACCAACT-3'
		Reverse	5'-TCAATAAATCCTTGGGGAAGC-3'
COX15	Human	Forward	5'-CTGCTGGCTTTGGCGTAT-3'
		Reverse	5'-GAGCCTGACTGGTGAGTGG-3'
CPT1A	Human	Forward	5'-GACAATACCTCGGAGCCTCA-3'
		Reverse	5'-AATAGGCCTGACGACACCTG-3'
CPT2	Human	Forward	5'-TGACCAAAGAAGCAGCAATG-3'
		Reverse	5'-GAGCTCAGGCAAGATGATCC-3'
CYB	Human	Forward	5'-CAATGGCGCCTCAATATTCT-3'
		Reverse	5'-GCCGATGTTTCAGGTTTCTG-3'
NDUFB10	Human	Forward	5'-GCCAAGGCCTACCAGGAC-3'
		Reverse	5'-GCTTTTCTCTCTTGCAGCATC-3'
YY1	Human	Forward	5'-TGGAGAGAACTCACCTCCTGA-3'
		Reverse	5'-TCTTTAATTTTTCTTGGCTTCATTC-3'
B2M	Human	Forward	5'-AGATGAGTATGCCTGCCGTGTGAA-3'
		Reverse	5'-TGCTGCTTACATGTCTCGATCCCA-3'
RPS16	Human	Forward	5'-AGATCAAAGACATCCTCATCCAG-3'
		Reverse	5'-TGAGTTTTGAGTCACGATGGG-3'
PPIA	Human/Mouse	Forward	5'-AGCATACAGGTCCTGGCATCTTGT-3'
		Reverse	5'-CAAAGACCACATGCTTGCCATCCA-3'
SIRT3	Mouse	Forward	5'-TACACAGAACATCGACGGGCTTGA-3'
		Reverse	5'-ACACAATGTCGGGTTTCACAACGC-3'
SIRT4	Mouse	Forward	5'-GAATTGAGGCCAGCCCACAAAGTT-3'
		Reverse	5'-ATCCAGCACATTGATTTCGTCCGC-3'
SIRT5	Mouse	Forward	5'-AAACCTGGATCCTGCCATTCTGGA-3'
		Reverse	5'-TGGTCTCCATGTTAAACTCGGCCA-3'
β-actin	Mouse	Forward	5'-AGCCATGTACGTAGCCATCC-3'
		Reverse	5'-CTCTCAGCTGTGGTGGTGAA-3'
HSP90AB1	Mouse	Forward	5'-TTTCAGGCAGAAATTGCCCAGCTC-3'
		Reverse	5'-TCTTGTCCAGGGCATCTGAAGCAT-3'

Western blots

As described in more detail in chapter II, whole cell lysates were obtained by applying 1% NP40 buffer (1% NP40 detergent with 150 mM NaCl, 50 mM Tris [pH 8], 1 mM TSA, 1 mM DTT, 10 mM nicotinamide, plus 1x Roche cOmplete Mini protease inhibitor tablets [cat. #11836170001] and 1% each of Sigma phosphatase inhibitor cocktail #s 2 [cat. #P5726] and 3 [cat. #P0044]) to a pellet of collected cells. Lysates were run on a polyacrylamide gel (Bio-Rad, cat. #345-0043), transferred to nitrocellulose membrane (Bio-Rad, cat. #162-0112), and blotted for the proteins of interest using standard molecular biology techniques. Antibodies used included SIRT3 (Cell Signaling D22A3, cat. #5490, 1:1000), phospho-S6K (Cell Signaling, cat. #9234, 1:1000), total S6K (Cell Signaling, cat. #9202, 1:1000), HSP60 (Abcam, cat. #ab3080, 1:5000), and α-tubulin (Santa Cruz Biotechnology, cat. #TU-02, 1:5000).

References

Allison SJ, Milner J (2007) SIRT3 is pro-apoptotic and participates in distinct basal apoptotic pathways. *Cell Cycle* **6**, 2669-2677.

Anderson RM, Barger JL, Edwards MG, Braun KH, O'Connor CE, Prolla TA, Weindruch R (2008) Dynamic regulation of PGC-1alpha localization and turnover implicates mitochondrial adaptation in calorie restriction and the stress response. *Aging Cell* **7**, 101-111.

Anderson RM, Weindruch R (2010) Metabolic reprogramming, caloric restriction and aging. *Trends Endocrinol. Metab*. **21**, 134-141.

Anisimov VN, Berstein LM, Egormin PA, Piskunova TS, Popovich IG, Zabezhinski MA, Tyndyk ML, Yurova MV, Kovalenko IG, Poroshina TE, Semenchenko AV (2008) Metformin slows down aging and extends life span of female SHR mice. *Cell Cycle* **7**, 2769-73.

Beeson CC, Beeson GC, Schnellmann RG (2010) A high-throughput respirometric assay for mitochondrial biogenesis and toxicity. *Anal. Biochem*. **404**, 75-81.

Bergeron R, Ren JM, Cadman KS, Moore IK, Perret P, Pypaert M, Young LH, Semenkovich CF, Shulman GI (2001) Chronic activation of AMP kinase results in NRF-1 activation and mitochondrial biogenesis. *Am. J. Physiol. Endocrinol. Metab*. **281**, E1340-1346.

Chakrabarti P, English T, Shi J, Smas CM, Kandror KV (2010) Mammalian target of rapamycin complex 1 suppresses lipolysis, stimulates lipogenesis, and promotes fat storage. *Diabetes* **59**, 775-781.

Cimen H, Han MJ, Yang Y, Tong Q, Koc H, Koc EC (2010) Regulation of succinate dehydrogenase activity by SIRT3 in mammalian mitochondria. *Biochemistry* **49**, 304-311.

Csiszar A, Labinskyy N, Pinto JT, Ballabh P, Zhang H, Losonczy G, Pearson K, de Cabo R, Pacher P, Zhang C, Ungvari Z (2009) Resveratrol induces mitochondrial biogenesis in endothelial cells. *Am. J. Physiol. Heart Circ. Physiol*. **297**, H13-20.

Cui Y, Morgenstern H, Greenland S, Tashkin DP, Mao JT, Cai L, Cozen W, Mack TM, Lu QY, Zhang ZF (2008) Dietary flavonoid intake and lung cancer--a population-based case-control study. *Cancer* **112**, 2241-2248.

Cunningham JT, Rodgers JT, Arlow DH, Vazquez F, Mootha VK, Puigserver P (2007) mTOR controls mitochondrial oxidative function through a YY1-PGC-1alpha transcriptional complex. *Nature* **450**, 736-740.

Dominy JE Jr, Lee Y, Jedrychowski MP, Chim H, Jurczak MJ, Camporez JP, Ruan HB, Feldman J, Pierce K, Mostoslavsky R, Denu JM, Clish CB, Yang X, Shulman GI, Gygi SP, Puigserver P (2012) The deacetylase Sirt6 activates the acetyltransferase GCN5 and suppresses hepatic gluconeogenesis. *Mol. Cell* **48**, 900-913.

Fok WC, Chen Y, Bokov A, Zhang Y, Salmon AB, Diaz V, Javors M, Wood WH 3rd, Zhang Y, Becker KG, Pérez VI, Richardson A (2014a) Mice fed rapamycin have an increase in lifespan associated with major changes in the liver transcriptome. *PLoS One* **9**, e83988.

Fok WC, Bokov A, Gelfond J, Yu Z, Zhang Y, Doderer M, Chen Y, Javors M, Wood WH 3rd, Zhang Y, Becker KG, Richardson A, Pérez VI (2014b) Combined treatment of rapamycin and dietary restriction has a larger effect on the transcriptome and metabolome of liver. *Aging Cell* **13**, 311-319.

Fujisawa K, Nishikawa T, Kukidome D, Imoto K, Yamashiro T, Motoshima H, Matsumura T, Araki E (2009) TZDs reduce mitochondrial ROS production and enhance mitochondrial biogenesis. *Biochem. Biophys. Res. Commun*. **379**, 43-48.

Ghosh S, Patel N, Rahn D, McAllister J, Sadeghi S, Horwitz G, Berry D, Wang KX, Swerdlow RH (2007) The thiazolidinedione pioglitazone alters mitochondrial function in human neuron-like cells. *Mol. Pharmacol*. **71**, 1695-1702.

Hallows WC, Yu W, Smith BC, Devries MK, Ellinger JJ, Someya S, Shortreed MR, Prolla T, Markley JL, Smith LM, Zhao S, Guan KL, Denu JM (2011) Sirt3 promotes the urea cycle and fatty acid oxidation during dietary restriction. *Mol. Cell* **41**, 139-149.

Hardie DG, Ross FA, Hawley SA (2012) AMPK: a nutrient and energy sensor that maintains energy homeostasis. *Nat. Rev. Mol. Cell. Biol*. **13**, 251-62.

Harrison DE, Strong R, Sharp ZD, Nelson JF, Astle CM, Flurkey K, Nadon NL, Wilkinson JE, Frenkel K, Carter CS, Pahor M, Javors MA, Fernandez E, Miller RA (2009) Rapamycin fed late in life extends lifespan in genetically heterogeneous mice. *Nature* **460**, 392-395.

Hay N, Sonenberg N (2004) Upstream and downstream of mTOR. *Genes Dev*. **18**, 1926-45.

Hirschey MD, Shimazu T, Goetzman E, Jing E, Schwer B, Lombard DB, Grueter CA, Harris C, Biddinger S, Ilkayeva OR, Stevens RD, Li Y, Saha AK, Ruderman NB, Bain JR, Newgard CB, Farese RV Jr, Alt FW, Kahn CR, Verdin E (2010) SIRT3 regulates mitochondrial fatty-acid oxidation by reversible enzyme deacetylation. *Nature* **464**, 121-125.

Howitz KT, Bitterman KJ, Cohen HY, Lamming DW, Lavu S, Wood JG, Zipkin RE, Chung P, Kisielewski A, Zhang LL, Scherer B, Sinclair DA (2003) Small molecule activators of sirtuins extend Saccharomyces cerevisiae lifespan. *Nature* **425**, 191-196.

Hubbard BP, Gomes AP, Dai H, Li J, Case AW, Considine T, Riera TV, Lee JE, E SY, Lamming DW, Pentelute BL, Schuman ER, Stevens LA, Ling AJ, Armour SM, Michan S, Zhao H, Jiang Y, Sweitzer SM, Blum CA, Disch JS, Ng PY, Howitz KT, Rolo AP, Hamuro Y, Moss J, Perni RB, Ellis JL, Vlasuk GP, Sinclair DA (2013) Evidence for a common mechanism of SIRT1 regulation by allosteric activators. *Science* **339**, 1216-1219.

Jose C, Hébert-Chatelain E, Bellance N, Larendra A, Su M, Nouette-Gaulain K, Rossignol R (2011) AICAR inhibits cancer cell growth and triggers cell-type distinct effects on OXPHOS biogenesis, oxidative stress and Akt activation. *Biochim. Biophys. Acta* **1807**, 707-718.

Lam YY, Peterson CM, Ravussin E (2013) Resveratrol vs. calorie restriction: data from rodents to humans. *Exp. Gerontol*. **48**, 1018-1024.

Leung HW, Lin CJ, Hour MJ, Yang WH, Wang MY, Lee HZ (2007) Kaempferol induces apoptosis in human lung non-small carcinoma cells accompanied by an induction of antioxidant enzymes. *Food Chem. Toxicol*. **45**, 2005-2013.

Li J, Kim SG, Blenis J (2014) Rapamycin: one drug, many effects. *Cell Metab*. **19**, 373-379.

Marfe G, Tafani M, Indelicato M, Sinibaldi-Salimei P, Reali V, Pucci B, Fini M, Russo MA (2009) Kaempferol induces apoptosis in two different cell lines via Akt inactivation, Bax and SIRT3 activation, and mitochondrial dysfunction. *J. Cell. Biochem*. **106**, 643-650.

Merrill GF, Kurth EJ, Hardie DG, Winder WW. AICA riboside increases AMP-activated protein kinase, fatty acid oxidation, and glucose uptake in rat muscle (1997) *Am. J. Physiol*. **273**, E1107-1112.

Meyer F, Ipaktchi M, Clauser H (1967) Specific inhibition of gluconeogenesis by biguanides. *Nature* **213**, 203-204.

Miller RA, Harrison DE, Astle CM, Fernandez E, Flurkey K, Han M, Javors MA, Li X, Nadon NL, Nelson JF, Pletcher S, Salmon AB, Sharp ZD, Van Roekel S, Winkleman L, Strong R (2014) Rapamycin-mediated lifespan increase in mice is dose and sex dependent and metabolically distinct from dietary restriction. *Aging Cell* **13**, 468-477.

Neff F, Flores-Dominguez D, Ryan DP, Horsch M, Schröder S, Adler T, Afonso LC, Aguilar-Pimentel JA, Becker L, Garrett L, Hans W, Hettich MM, Holtmeier R, Hölter SM, Moreth K, Prehn C, Puk O, Rácz I, Rathkolb B, Rozman J, Naton B, Ordemann R, Adamski J, Beckers J, Bekeredjian R, Busch DH, Ehninger G, Graw J, Höfler H, Klingenspor M, Klopstock T, Ollert M, Stypmann J, Wolf E, Wurst W, Zimmer A, Fuchs H, Gailus-Durner V, Hrabe de Angelis M, Ehninger D (2013) Rapamycin extends murine lifespan but has limited effects on aging. *J. Clin. Invest*. **123**, 3272-3291.

Qiu X, Brown K, Hirschey MD, Verdin E, Chen D (2010) Calorie restriction reduces oxidative stress by SIRT3-mediated SOD2 activation. *Cell Metab*. **12**, 662-667.

Park IH, Chen J (2005) Mammalian target of rapamycin (mTOR) signaling is required for a late-stage fusion process during skeletal myotube maturation. *J. Biol. Chem*. **280**, 32009-32017.

Pearson KJ, Baur JA, Lewis KN, Peshkin L, Price NL, Labinskyy N, Swindell WR, Kamara D, Minor RK, Perez E, Jamieson HA, Zhang Y, Dunn SR, Sharma K, Pleshko N, Woollett LA, Csiszar A, Ikeno Y, Le Couteur D, Elliott PJ, Becker KG, Navas P, Ingram DK, Wolf NS,

Ungvari Z, Sinclair DA, de Cabo R (2008) Resveratrol delays age-related deterioration and mimics transcriptional aspects of dietary restriction without extending life span. *Cell Metab*. **8**, 157-168.

Phielix E, Szendroedi J, Roden M (2011). The role of metformin and thiazolidinediones in the regulation of hepatic glucose metabolism and its clinical impact. *Trends Pharmacol. Sci*. **32**, 607-616.

Powers RW 3rd, Kaeberlein M, Caldwell SD, Kennedy BK, Fields S (2006) Extension of chronological life span in yeast by decreased TOR pathway signaling. *Genes Dev*. **20**, 174-184.

Rena G, Pearson ER, Sakamoto K (2013) Molecular mechanism of action of metformin: old or new insights? *Diabetologia* **56**, 1898-1906.

Reznick RM, Shulman GI (2006) The role of AMP-activated protein kinase in mitochondrial biogenesis. *J. Physiol*. **574**, 33-39.

Rice S, Pellatt LJ, Bryan SJ, Whitehead SA, Mason HD (2011) Action of metformin on the insulin-signaling pathway and on glucose transport in human granulosa cells. *J. Clin. Endocrinol. Metab*. **96**, E427-435.

Scarpulla RC (2011) Metabolic control of mitochondrial biogenesis through the PGC-1 family regulatory network. *Biochim. Biophys. Acta* **1813**, 1269-1278.

Shi T, Wang F, Stieren E, Tong Q (2005) SIRT3, a mitochondrial sirtuin deacetylase, regulates mitochondrial function and thermogenesis in brown adipocytes. *J. Biol. Chem*. **280**, 13560-13567.

Shimazu T, Hirschey MD, Hua L, Dittenhafer-Reed KE, Schwer B, Lombard DB, Li Y, Bunkenborg J, Alt FW, Denu JM, Jacobson MP, Verdin E (2010) SIRT3 deacetylates mitochondrial 3-hydroxy-3-methylglutaryl CoA synthase 2 and regulates ketone body production. *Cell Metab*. **12**, 654-661.

Someya S, Yu W, Hallows WC, Xu J, Vann JM, Leeuwenburgh C, Tanokura M, Denu JM, Prolla TA (2010) Sirt3 mediates reduction of oxidative damage and prevention of age-related hearing loss under caloric restriction. *Cell* **143**, 802-812.

Suwa M, Egashira T, Nakano H, Sasaki H, Kumagai S (2006) Metformin increases the PGC-1alpha protein and oxidative enzyme activities possibly via AMPK phosphorylation in skeletal muscle in vivo. *J. Appl. Physiol. (1985)* **101**, 1685-1692.

Tao R, Coleman MC, Pennington JD, Ozden O, Park SH, Jiang H, Kim HS, Flynn CR, Hill S, Hayes McDonald W, Olivier AK, Spitz DR, Gius D (2010) Sirt3-mediated deacetylation of evolutionarily conserved lysine 122 regulates MnSOD activity in response to stress. *Mol. Cell* **40**, 893-904.

Thoreen CC, Kang SA, Chang JW, Liu Q, Zhang J, Gao Y, Reichling LJ, Sim T, Sabatini DM, Gray NS (2009) An ATP-competitive mammalian target of rapamycin inhibitor reveals rapamycin-resistant functions of mTORC1. *J. Biol. Chem*. **284**, 8023-8032.

Thoreen CC, Chantranupong L, Keys HR, Wang T, Gray NS, Sabatini DM (2012) A unifying model for mTORC1-mediated regulation of mRNA translation. *Nature* **485**, 109-113.

Timmers S, Konings E, Bilet L, Houtkooper RH, van de Weijer T, Goossens GH, Hoeks J, van der Krieken S, Ryu D, Kersten S, Moonen-Kornips E, Hesselink MK, Kunz I, Schrauwen-Hinderling VB, Blaak EE, Auwerx J, Schrauwen P (2011) Calorie restriction-like effects of 30 days of resveratrol supplementation on energy metabolism and metabolic profile in obese humans. *Cell Metab*. **14**, 612-622.

Zoncu R, Efeyan A, Sabatini DM (2011) mTOR: from growth signal integration to cancer, diabetes and ageing. *Nat. Rev. Mol. Cell Biol*. **12**, 21-35.

APPENDIX B

Supplemental file listing

The files listed below are provided on separate media. All are Excel files in *.xlsx format.

Supplementary File 3.1. Complete correlations with SIRT3 expression for each gene in each of four datasets analyzed.

Supplementary File 3.2. Gene ontology term enrichment in top 50 SIRT3-correlated genes for each analyzed dataset.

Supplementary File 3.3. All input gene groups used in PhylCRM-Lever DNA sequence analysis algorithm.

Supplementary File 3.4. Complete PhylCRM-Lever results for each analyzed dataset.

Supplementary File 4.1. Complete raw read values, normalized gene expression values, and isoform scores from RNA-seq data.